

Three Velocity Modulated Myoelectric A/K Prosthesis Controllers;
Initial Subject Evaluation

By
Ronny N. Galloway
B.S., University of Missouri, Rolla 1980

Submitted in Partial Fulfillment of the
Requirements for the Degree of
Master of Science at the
Massachusetts Institute of Technology
February 1982

Signature of Author
Department of Mechanical Engineering

Certified by
Thesis Supervisor

Accepted by
Chairman, Department Committee on Graduate Students

Archives
MASSACHUSETTS INSTITUTE
OF TECHNOLOGY
JUN 7 1982
LIBRARIES

Three Velocity Modulated Myoelectric A/K Prosthesis Controllers;
Initial Subject Evaluation

By Ronny N. Galloway

Submitted to the Department of Mechanical Engineering
on January 14, 1982 in Partial Fulfillment of the
Requirements for the Degree of Master of Science.

ABSTRACT

The research described herein investigated methods of passive above-knee prosthesis control using myoelectric signals acquired from the remnant above-knee stump musculature. Initial feasibility studies were conducted using four above-knee amputees walking with a prosthesis simulator controlled to emulate a friction prosthesis. Results from these studies indicated that practical myoelectric controllers, which improve amputee gait cosmesis and energy consumption, could be designed if a suitable modulator of the myoelectric activity from hamstrings and quadriceps muscle groups could be found. This modulator would allow the controller to recognize amputee intent. Velocity modulation of the myoelectric signals was postulated as a practical method of selecting the appropriate muscle group activity for controller input. Since the preliminary studies indicated that a strong correlation did not exist between simulator friction level and the activity of the muscle groups studied, three velocity modulated, myoelectric controllers were developed and tested off-line using data taken during the initial investigations. Further human experimentation was warranted and results from real time testing of the controllers are included. The controllers were not developed fully and further work is necessary.

Thesis Supervisor: Woodie C. Flowers
Title: Associate Professor of Mechanical Engineering

CONTENTS

ABSTRACT.....	2
ACKNOWLEDGEMENTS.....	6
LIST OF FIGURES.....	7
1.1 PROBLEM DESCRIPTION.....	10
1.2 Myoelectric Data Acquisition and Processing.....	12
1.3 Comments About the Task.....	14
1.4 Scope and Relevance.....	16
2.1 INTRODUCTION.....	18
2.2 Hardware.....	18
2.2.1 Lampe Prosthesis Simulator.....	18
2.2.2 Simulator Instrumentation.....	21
2.2.3 Interface Hardware.....	25
2.2.4 Other Hardware.....	29
2.3 Liveware.....	29
2.3.1 Subject 1.....	32
2.3.2 Subject 2.....	32
2.3.3 Subject 3.....	32
2.3.4 Subject 4.....	33
2.4 Software.....	33
3.1 INTRODUCTION.....	34

3.2	Procedure.....	34
3.3	Observations.....	37
3.4	Results.....	38
4.1	INTRODUCTION.....	61
4.2	Velocity, a Possible ME Signal Modulator.....	62
4.3	Velocity Modulation of the Rectified ME Activity; a Simple Approach.....	64
4.4	Velocity Modulated Pulse Width Modulation; First Cut Noise Rejection.....	64
4.5	Velocity Modulation of the Threshold Count; a More Elaborate Approach.....	71
5.1	INTRODUCTION.....	82
5.2	Procedure.....	82
5.3	Observations.....	83
5.4	Results.....	83
	5.4.1 Subject 1 Results.....	84
	5.4.2 Subject 2 Results.....	84
	5.4.3 Subject 3 Results.....	92
6.1	INTRODUCTION.....	100
6.2	Discussion and Conclusions.....	100
6.3	Recommendations for Further Research.....	102
	APPENDIX 1: Selected Circuit Diagrams.....	104

APPENDIX 2: Selected Source Listings..... 110
BIBLIOGRAPHY..... 133

ACKNOWLEDGEMENTS

First, I would like to thank my employer, Bell Telephone Laboratories, Inc., and particularly my direct supervision for making this possible. Also, my colleagues in the gait lab, by their comments and criticism, helped form the work herein. Will Durfee, Bill Murray and Ralph Burgess were helpful when the electronics misbehaved. Erik Antonsson, Tom Macirowski and Dan Ottenheimer, thanks for the help with programming. I am especially indebted to Woodie Flowers for the opportunity to do this particular research, the numerous suggestions, and for working to help me make deadlines. Most of all, I want to thank Teresa, Melissa and Erin, my wife and family for making the sacrifices necessary to accommodate a workaholic graduate student. This work took place in the Eric E. and Evelyn P. Newman Laboratory for Biomechanics and Human Rehabilitation and was funded in part by NSF Grant Number ECS-8023193.

LIST OF FIGURES

NUMBER	TITLE
Figure 1.	Hardware Configuration Schematic
Figure 2.	Lampe Prosthesis Simulator
Figure 3.	Simulator Instrumentation
Figure 4.	Ideal Behavior of Differentiator Circuit
Figure 5.	Ideal Behavior of Myoamps
Figure 6.	Interface Hardware
Figure 7.	Ideal Behavior of Interface Filters
Figure 8.	PDP 11/60 Computer
Figure 9.	Kepeco Bipolar Operational Amplifier and ANDS 5400
Figure 10.	Preamp Mounting Procedure for Suction Sockets
Figure 11.	Subject 1: Zero Friction Simulation
Figure 12.	Subject 1: Comfortable Friction Simulation
Figure 13.	Subject 2: Zero Friction Simulation
Figure 14.	Subject 2: Extreme Friction Simulation
Figure 15.	Subject 3: Zero Friction Simulation
Figure 16.	Subject 3: Comfortable Friction Simulation
Figure 17.	Filtered Version of Figure 16
Figure 18.	Subject 4: Zero Friction Simulation
Figure 19.	Subject 4: Comfortable Friction Simulation
Figure 20.	Subject 1: Quadriceps Correlated with Damping
Figure 21.	Subject 1: Hamstrings Correlated with Damping

- Figure 22. Subject 2: Quadriceps Correlated with Damping
- Figure 23. Subject 2: Hamstrings Correlated with Damping
- Figure 24. Subject 3: Quadriceps Correlated with Damping
- Figure 25. Subject 3: Hamstrings Correlated with Damping
- Figure 26. Subject 4: Quadriceps Correlated with Damping
- Figure 27. Subject 4: Hamstrings Correlated with Damping
- Figure 28. Lower Limb Musculature
- Figure 29. Flowchart of Simple Rectification Scheme
- Figure 30. Subject 1: Simple Rectification Scheme
- Figure 31. Subject 2: Simple Rectification Scheme
- Figure 32. Subject 3: Simple Rectification Scheme
- Figure 33. Subject 4: Simple Rectification Scheme
- Figure 34. Flowchart of Modulated Pulse Width Controller
- Figure 35. Subject 1: Modulated Pulse Width Controller
- Figure 36. Subject 2: Modulated Pulse Width Controller
- Figure 37. Subject 3: Modulated Pulse Width Controller
- Figure 38. Subject 4: Modulated Pulse Width Controller
- Figure 39. Flowchart of Threshold Counting Controller
- Figure 40. Subject 1: Threshold Counting Controller
- Figure 41. Subject 2: Threshold Counting Controller
- Figure 42. Subject 3: Threshold Counting Controller
- Figure 43. Subject 4: Threshold Counting Controller
- Figure 44. Subject 1: Comfortable Friction Simulation
- Figure 45. Subject 1: Comfortable Hydraulic Simulation
- Figure 46. Subject 1: Simple Rectifying Controller
- Figure 47. Subject 1: Modulated Pulse Width Controller

- Figure 48. Subject 1: Threshold Counting Controller
- Figure 49. Subject 2: Comfortable Friction Simulation
- Figure 50. Subject 2: Comfortable Velocity Simulation
- Figure 51. Subject 2: Modulated Pulse Width Controller
- Figure 52. Subject 2: Threshold Counting Controller
- Figure 53. Subject 3: Comfortable Friction Simulation
- Figure 54. Subject 3: Comfortable Velocity Simulation
- Figure 55. Subject 3: Modulated Pulse Width Controller
- Figure 56. Subject 3: Threshold Counting Controller
- Figure 57. Interface Filters
- Figure 58. Myo-Amps
- Figure 59. Foot Switch Instrumentation
- Figure 60. Torque Instrumentation
- Figure 61. Motion Instrumentation

CHAPTER 1 INTRODUCTION

1.1 PROBLEM DESCRIPTION

Commercially available prosthesis use various methods of providing resistive torque (damping) at the knee. A plethora of these devices is available to the physician for prescription to the above-knee (A/K) population. A general classification is provided by the Veterans Administration (1). However, most common prostheses provide preprogrammed control of knee damping with a limited range of adjustment. Thus, the amputee must learn to adapt his gait to accommodate the innate behavior of the prosthesis at a cost of inferior gait cosmesis and increased energy consumption. Therefore, it seems reasonable to try to improve the cybernetic link between man and machine in order that the machine may respond to the man in a symbiotic fashion.

One way to improve the efferent channel is to make use of information contained in the myoelectric (ME) activity of remnant stump musculature. There seems to be little available data taken from A/K amputees. Perhaps this is due to technical difficulties encountered because the subject traverses large distances during data acquisition. Nevertheless, Dyck et. al. (2), propose volitional control of swing phase damping using the semimembranosis ME activity

to select one of three possible damping coefficients of a hydraulic cylinder. Their results provide a good approximation of normal knee trajectory. Horn (3), has developed a flexion lock designed to assist the amputee in stair climbing. The lock is activated voluntarily with a remnant stump muscle not "active" in gait. Saxena and Mukhopadhyay (4) also use ME activity from a control muscle along with the output of a heel-mounted pressure transducer to lock the knee during stance phase.

It is the opinion of the author that the above controllers, although significant technical achievements, require a great deal of conscious effort on the part of the amputee. While the human may be trained to walk with such a device, amputee acceptance may not be universal, especially among amputees very accustomed to conventional prostheses. Above-knee ME controllers which interact more symbiotically with the amputee have been developed by Kato et. al. (5) and Donath (6). The former group has found a relationship between cadence and the rectified, smoothed amplitude of ilio-psoas ME activity. This result was used to design a controller which would change knee damping according to gait speed. Donath implemented a controller in which knee damping was proportionally controlled by filtered ME activity from muscles in the area of the gracilis.

1.2 Myoelectric Data Acquisition and Processing

Generally, there are two types of myoelectrodes. Subcutaneous needle electrodes give the best electromyograms but have limited practical use in prosthesis control. Surface electrodes, on the other hand, are feasible for this purpose but high frequency components of the ME signal are attenuated by tissue between the muscle and electrode. Electrodes may be monopolar (one electrode and ground), bipolar or configured in an array of three or more. However, to minimize electromagnetic interference and other artifacts the recording electrode is generally bipolar. It is common practice to differentially amplify the ME signal at the recording site. This, in fact, is the only practical way to avoid the ubiquitous 60 Hz power line noise.

The ME signal is manifest in an electric field as a result of depolarization of the postsynaptic membrane in striated muscles. Saxena (4) states a bandwidth of 1000 Hz for the signal but notes that tissue effects and motion artifact (i.e., electrode - skin polarization) probably limit the useful range of the signal to frequencies between 10 and 500 Hz. Hogan (7), shows frequency spectra for ME activity taken from biceps on the upper arm. These results indicate that the power spectral density has a maximum between 50 and 80 Hz for most contraction levels. The peak should be at a lower frequency for larger muscles and vice

versa for smaller muscles.

By far the most common myoelectric processing technique consists of the following steps. First, the signal is high pass filtered to remove low frequency artifact. The ME signal is then rectified or passed through a nonlinear device to regain a D. C. level. Finally, the signal as passed through an envelope detector, usually an RC integrated, to obtain a control input. Hogan (8) points out various problems with this approach and suggests alternative processing methods. The basic point is that unless the envelope detector is very high order, the control input will contain relatively large low frequency oscillations. On the other hand, if it is high order, excessive phase lag may become a problem.

An interesting processing method suggested by Childress (9) uses the ME signal to modulate a pulse which is the input to a servo-motor which controls the opening and closing of a hand prosthesis. In particular, if and only if the magnitude of the ME activity is above a preset threshold, a constant current is supplied to the actuator. Advantages of this technique are simplicity of hardware implementation and rejection of spurious peaks in the ME signal since such a pulse would have a very short duration. On the other hand, sufficient signal processing is necessary to insure that low frequency artifact will not generate a

long pulse inconsistent with the amputee's control strategy.

Another interesting technique was demonstrated by Close et. al. (10). This method used a high speed digital counter to count action potentials per unit time of a normally contracting muscle. The result of applying this technique will give a number which reflects both the frequency and amplitude of a ME signal.

Yet another method, applied by Myers and Moskowitz (11), is spatial pattern recognition. An array of electrodes was used to record ME activity from the thigh of normal subjects. Pattern recognition algorithms were then employed to classify spatial patterns correlating with knee flexion, knee extension or hip action involving no knee activity.

1.3 Comments About the Task

It is not obvious why A/K ME control has not been more successful. Perhaps it is helpful to enumerate some reasonable goals for the A/K controller. The lower extremity basically provides suspension and propulsion. The actuator requirements are extremely stringent for the prosthesis designed to functionally replace the limb. In fact, current actuator technology does not permit design of an active, self-contained A/K prosthesis which meets power requirements for all gait modes (level walking, stair

climbing, etc.). However, Grimes (12) shows that the normal knee acts as an energy dissipator during level walking. Hence, the following goals can be set forth for a practical A/K prosthesis.

1. The prosthesis should provide stability during stance phase.
2. The prosthesis should provide enough damping during swing phase to insure against excessive heel rise and abrupt deceleration at hyperextension.
3. The prosthesis should provide minimal damping during swing to conserve energy.
4. The prosthesis should adapt itself to different modes.

There is more than one way to resolve the conflict in two and three above. Chow and Jacobsen (13) use optimal programming techniques to analytically make the compromise. Another approach involves observation of ME signals trying to infer how this task is accomplished by the normal human. Observations by Brandell and Williams (14) indicate that maximum ME of a select set of muscles levels correspond to instances in time when the knee is changing direction. These observations are verified by Carlsoo (15).

1.4 Scope and Relevance

The above considerations led the author to the following hypothesis.

Myoelectric signals from remnant stump musculature can be used to control the swing-phase damping profile of a passive above-knee prosthesis and the gait resulting from such a control scheme should yield an acceptable compromise between gait cosmesis and energy consumption.

The following goals were set forth to ascertain its validity.

1. Develop the appropriate instrumentation to measure ME signals.
2. Select subjects from the A/K population.
3. Propose and perform experiments to determine if the signal is consistent with results from normals.
4. If so, propose ME controllers and conduct experiments to evaluate them.

This project should contribute to general knowledge in the area by increasing the data base describing ME activity in A/K amputees and suggesting swing-phase myoelectric controllers which are simple to implement but

consistent with the amputee's intent.

CHAPTER 2 GETTING STARTED

2.1 INTRODUCTION

This project made use of a prosthesis simulator developed at M.I.T. by Lampe (16). In addition, an instrumentation package was developed to acquire necessary data. Software was developed in order that the experiments could be computer controlled to expedite data acquisition and storage. Subjects were solicited, screened and fitted with the necessary equipment to walk with the simulator.

2.2 Hardware

The diagram of the hardware configuration, shown in Figure 1, gives a good synopsis of the hardware details. First, data is collected from the man-machine system and transmitted through an umbilical to be stored and processed. Before the data can be stored, it is filtered and converted into digital data. Then, an appropriate control signal is generated and sent out to the prosthesis. This involves proportional control of a current source to achieve the desired torque level at the prosthesis.

2.2.1 Lampe Prosthesis Simulator

Figure 2 shows the simulator along with a socket, Sach (solid ankle cushioned heel) foot, and the umbilical.

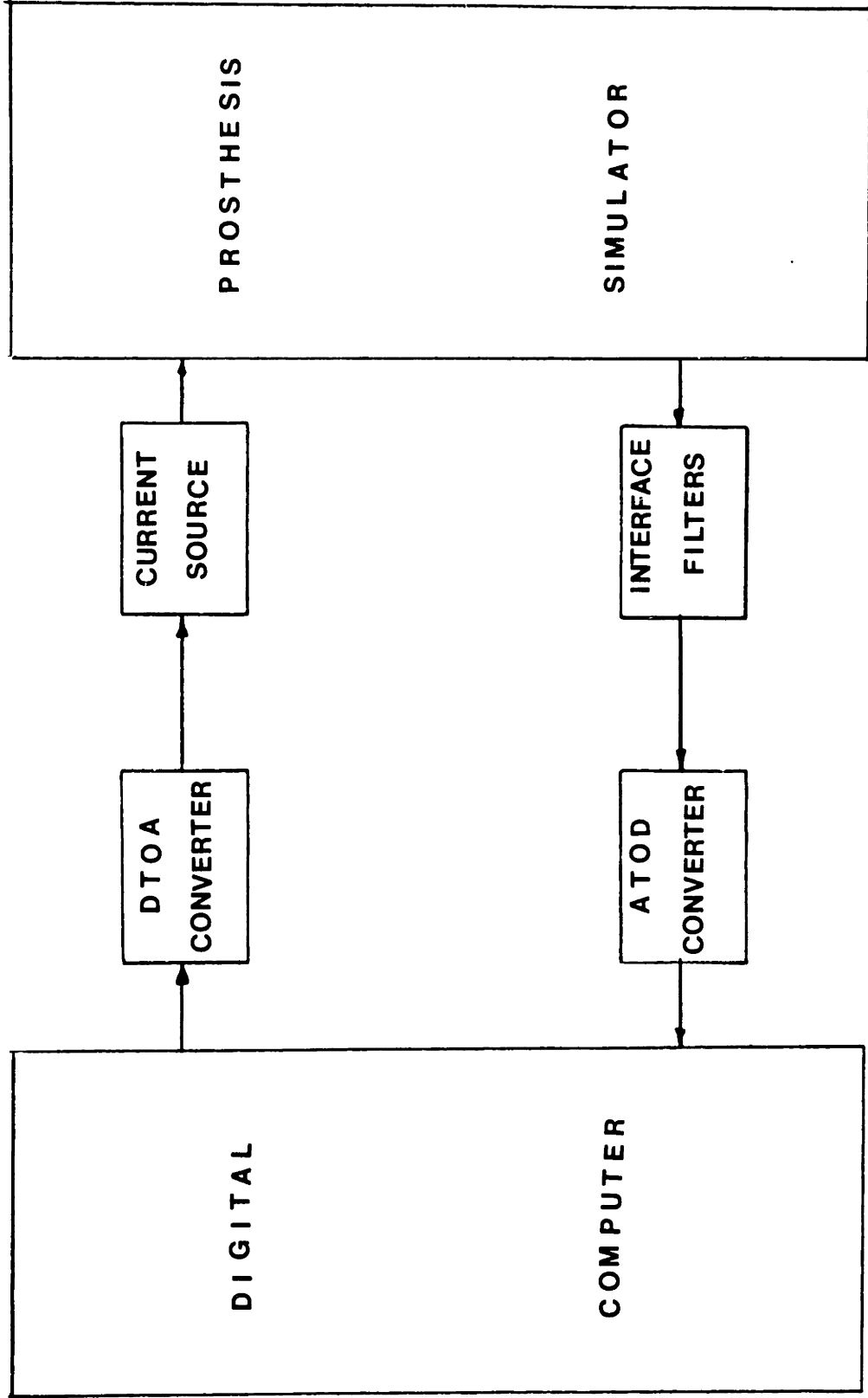
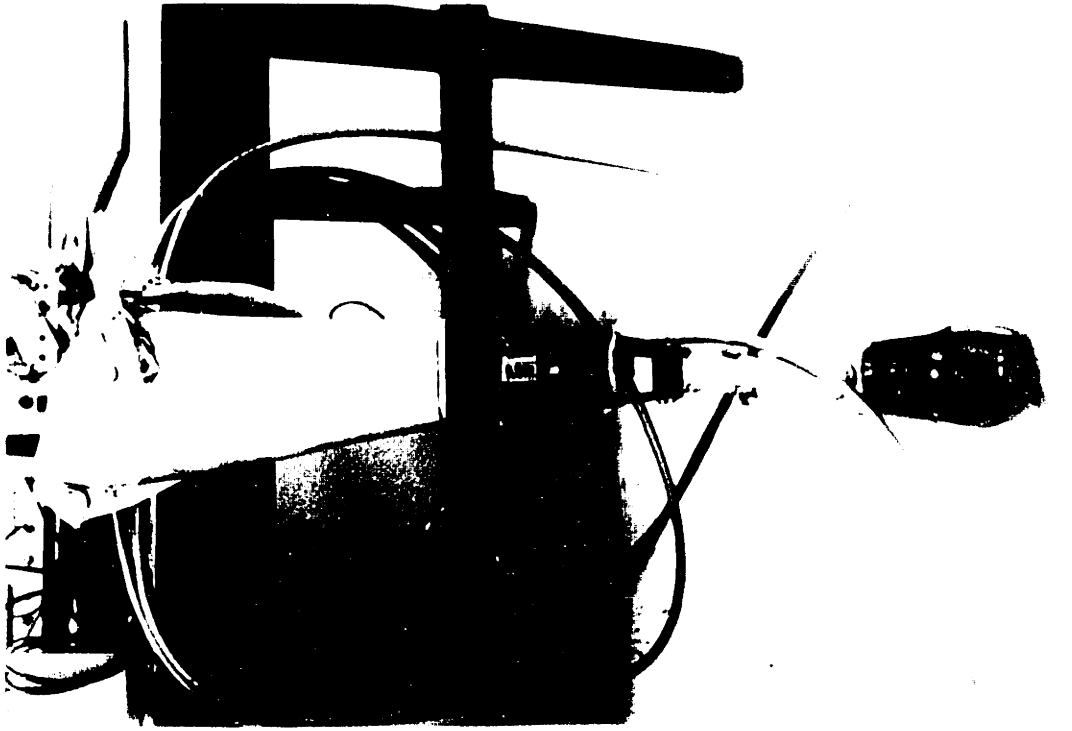
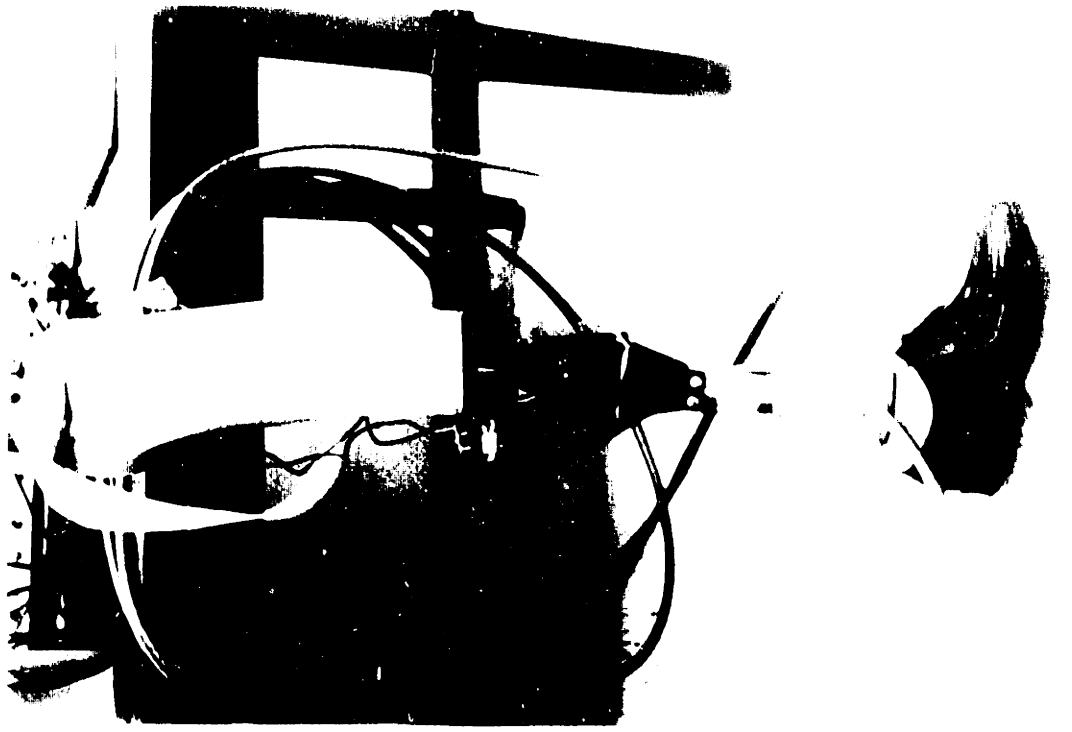


Figure 1. Hardware Configuration Schematic



It is a passive device, not capable of supplying knee moment, which can produce virtually arbitrary knee resistive torques. The simulator, in its present configuration, is computer controlled allowing experimentation with novel control schemes limited only by simulator instrumentation and software speed.

2.2.2 Simulator Instrumentation

Several new types of instrumentation were added to the prosthesis simulator for the purposes of this study. This package, shown in Figure 3, contains the necessary components to process kinematic, kinetic, ME and timing data. Instrumentation circuit diagrams are included in Appendix (1) and relevant details are discussed in the following. Angular position information was obtained from a potentiometer. In order to avoid nonlinearities due to input impedance loading, the potentiometer was isolated from further instrumentation with a voltage follower circuit. This signal was amplified to insure an acceptable signal to noise ratio for transmission to the digital to analog converter via the umbilical cable. The angular velocity was obtained by differentiating the position signal. The differentiator was actually a 2nd order band pass filter with a 15 Hz break frequency. Figure 4 shows the theoretical bode plot of this filter. The actual filter was tested with known sinusoidal inputs and found to

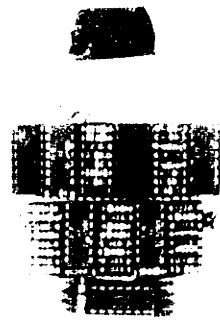
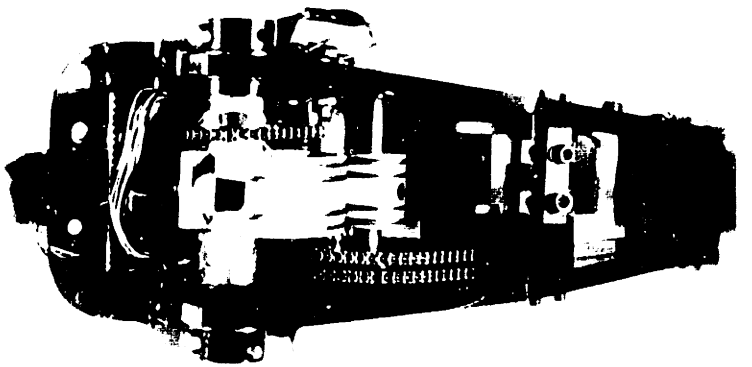
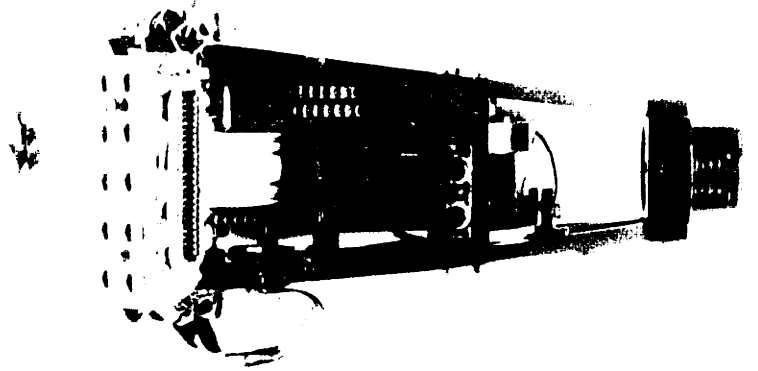
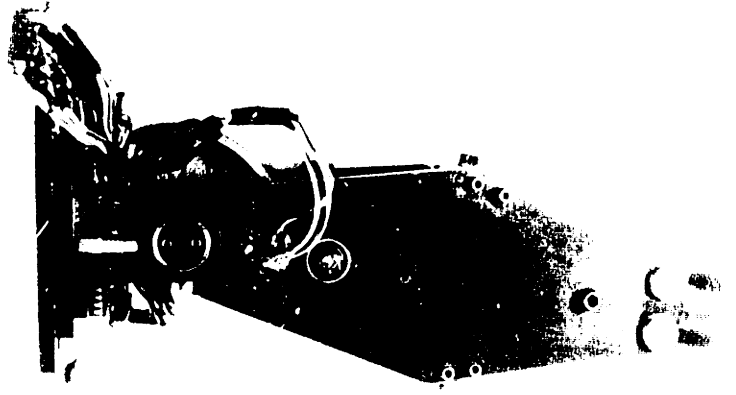
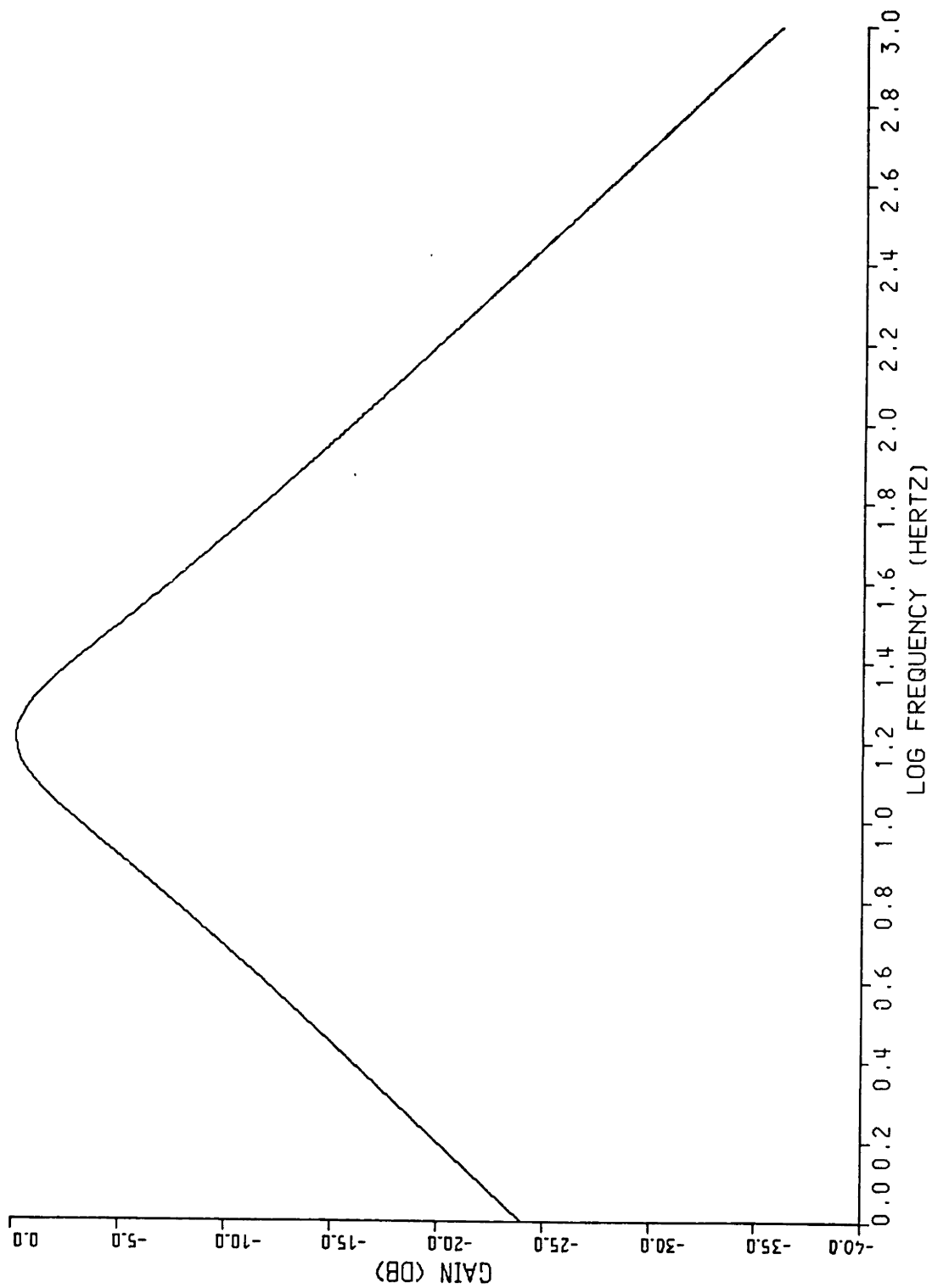


FIGURE 4 . IDEAL RESPONSE OF DIFFERENTIATORS



behave in the manner predicted by theory. Research by Antonsson (17) verifies that the break frequency is reasonable for normal level walking position data. Angular acceleration was obtained by differentiating the angular velocity with a similar filter. Double differentiation, although not generally practicable, was possible here due to the limited bandwidth of the data. Since the Lampe prosthesis simulator was previously equipped with a torsional strain gage bridge, it was only necessary to balance the bridge and amplify its output.

Gait timing information, generated by foot switches mounted inside both the subject's shoes, measured the heel contact, foot flat and toe-off for both feet. Summing amplifiers gave an output which indicated the status of the foot. These switches worked well for the normal foot, but did not perform well on the prosthetic side due to the tight fit of the Sach foot in the subjects shoe.

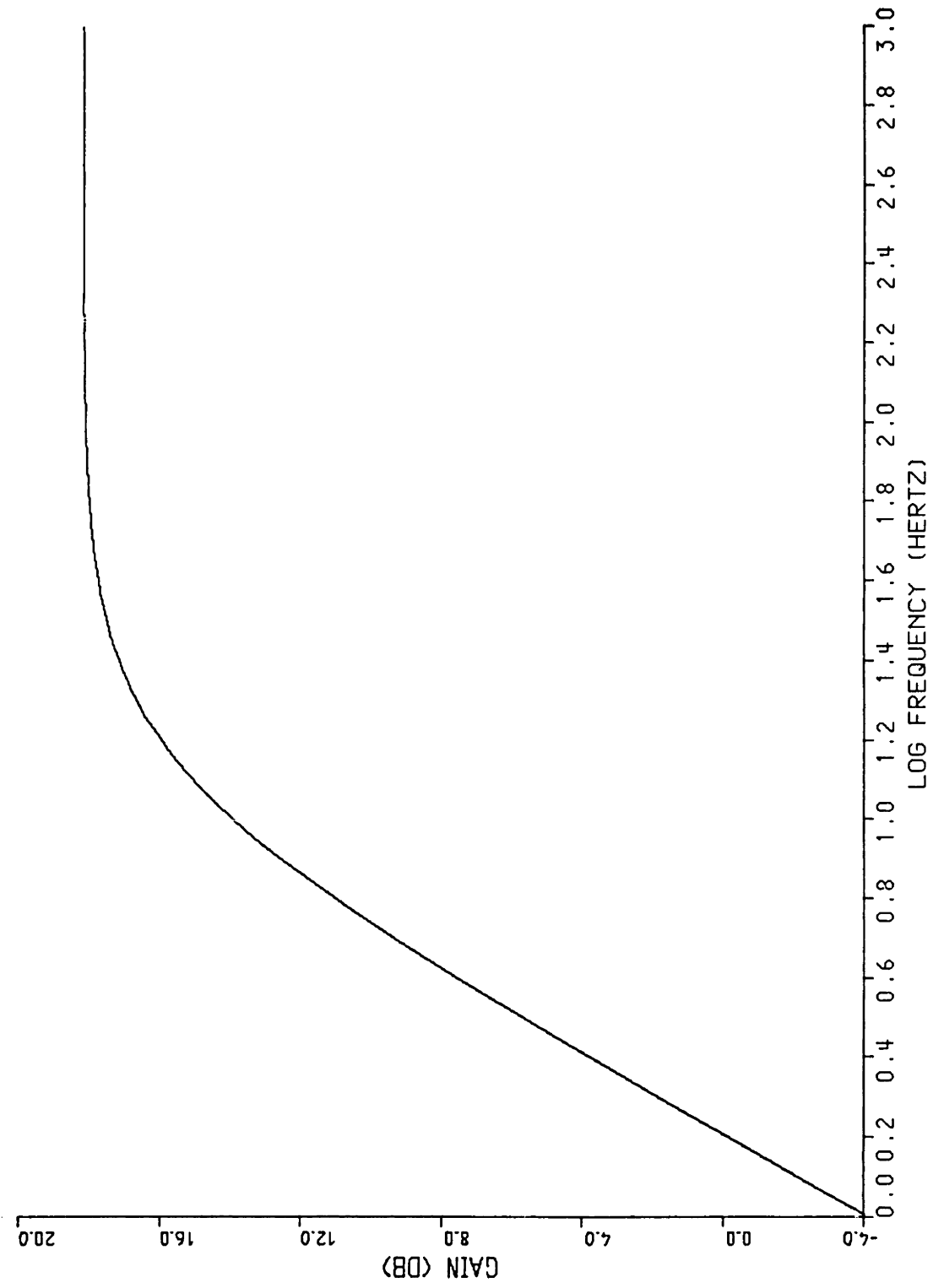
Circuitry to amplify 10 channels of myoelectric data was also designed and mounted on the prosthesis simulator. Although it was important to acquire most of the frequency content of the ME signal, low frequency artifact (an order of magnitude larger than the signal) and the extreme gain (necessary because of the umbilical) required that the signal be high pass filtered and amplified simultaneously at the simulator. Thus, a first order high

pass filter was designed which has the theoretical bode plot shown in Figure 5. The myoamps were tested with known inputs and they were found to closely approximate the ideal. Bipolar myoelectric preamps, manufactured by Motion Control, Inc., were used for myoelectric data acquisition. These electrodes feature a differential input with high common mode rejection ratio. Since the differential amplification takes place at the surface of the skin, these electrodes produce electromyograms which are relatively free from electromagnetic interference.

2.2.3 Interface Hardware

It is common practice to filter the data before sampling to limit frequency content (Stearns 18). The interface hardware, shown in Figure 6 performed this function and provided connections to the simulator via the umbilical cable. Filter design involved a compromise between adequate information rate and reasonable sampling frequency. The final design specifications required an active 3rd order, 3 dB, Chebychev filter with 100 Hz break frequency. Stout (19) provided the equations necessary for selection of the components used in the circuit shown in Appendix (1). This particular design was chosen because greater attenuation of high frequency was deemed more important than unity gain throughout the pass band. Ideal behavior for these filters is shown in Figure 7.

FIGURE 5. IDEAL BEHAVIOR OF MYOAMPS



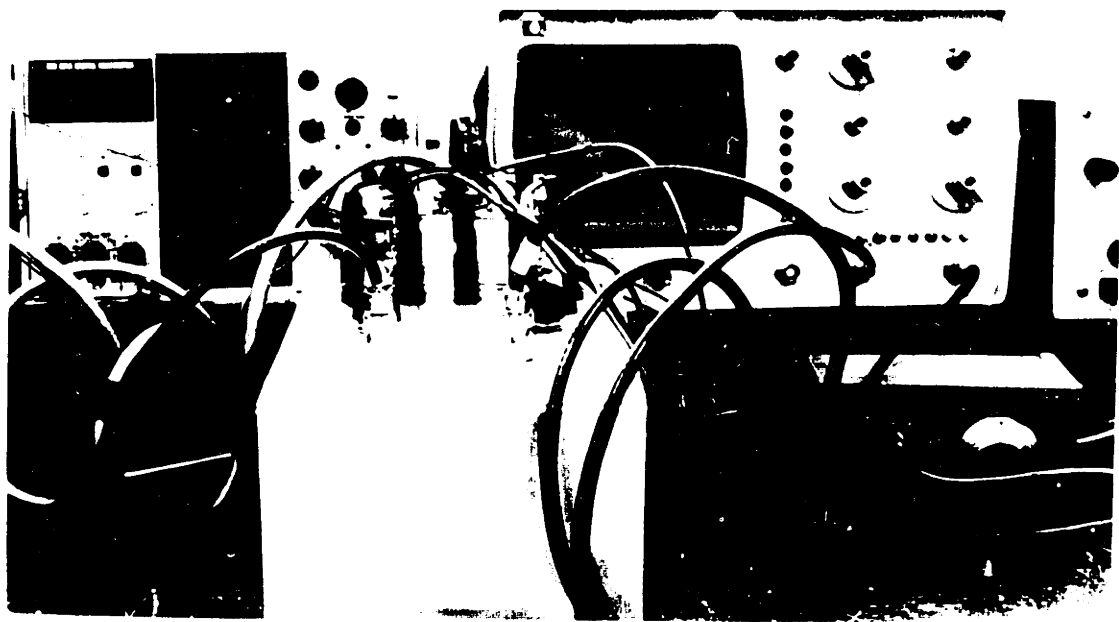
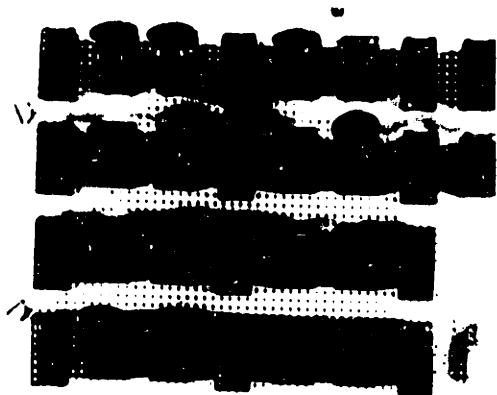
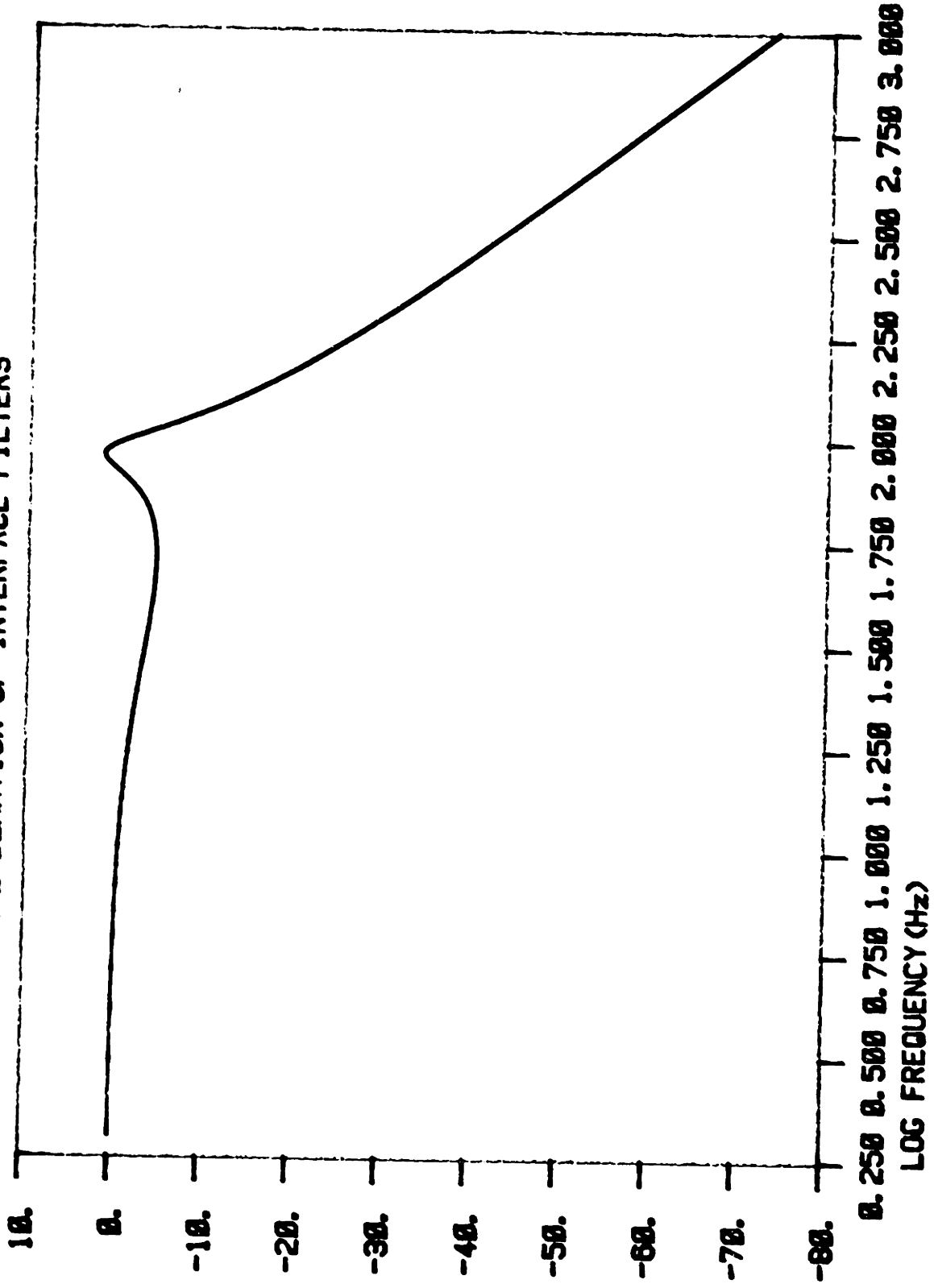


FIGURE 7. IDEAL BEHAVIOR OF INTERFACE FILTERS



GAIN (dB)

Once again, performance of all filters was checked with a known input and judged satisfactory.

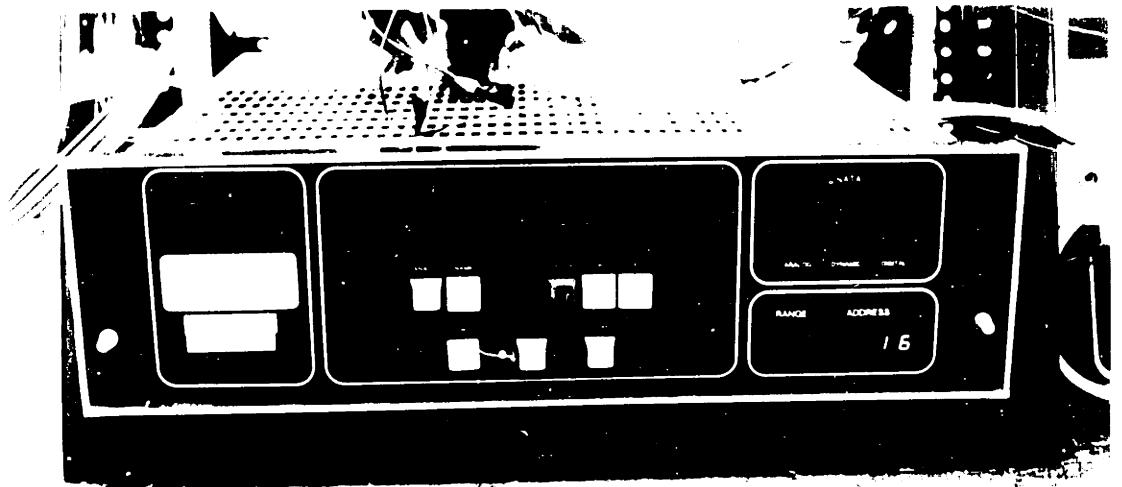
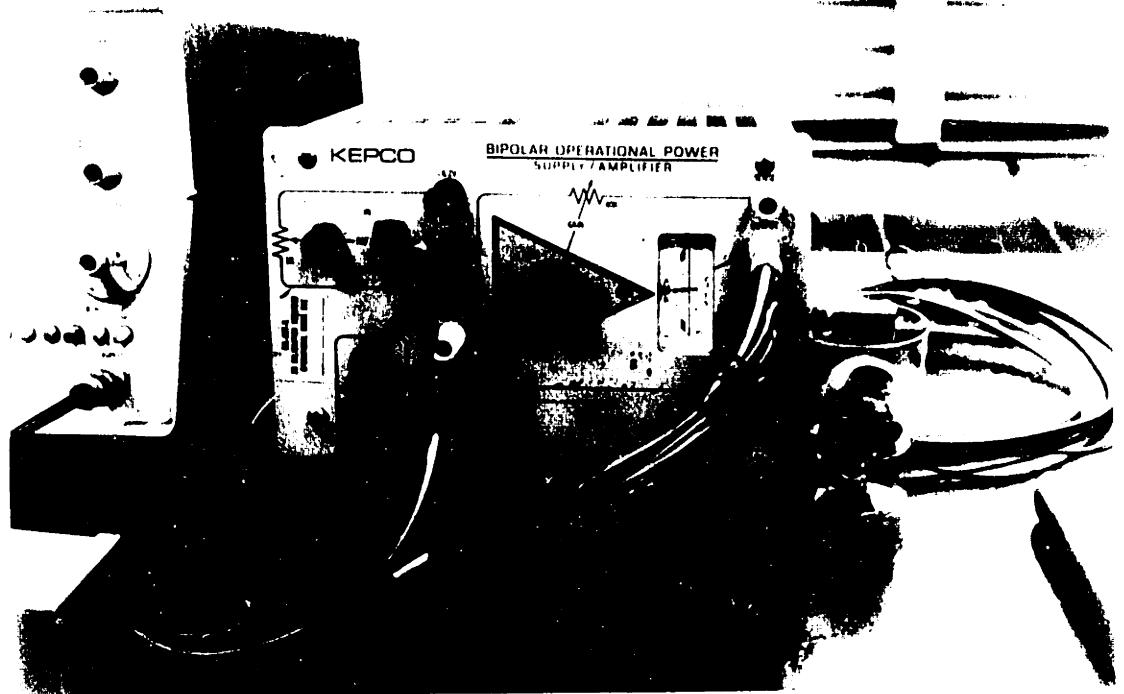
2.2.4 Other Hardware

Other hardware used in the experiments included a PDP 11/60 computer, Figure (8), for data processing and simulator control. Also, a Tektronix voltage supply powered electronics in both the interface module and prosthesis simulator. A Hewlett Packard oscilloscope was available for visual review of the data. A Kepco bipolar operational amplifier, shown in Figure 9, in conjunction with a proportional current controller designed by Lampe (16) acted as a voltage controlled current source to generate the desired torque at the knee.

2.3 Liveware

Four subjects were screened from the group solicited from the A/K population in the area. They were selected on the basis of attitude, physical condition, and walking ability. Thus, they represented the best available characteristics in the population for a study of this type.





Each subject was fitted with a socket and Sach foot similar to that worn everyday. Brief case histories are given below.

2.3.1 Subject 1

Subject 1 is a 36 year old male who underwent above-knee amputation in 1976 as a result of injuries suffered in a pedestrian accident. His current prosthesis is equipped with a suction socket, a Dupaco hydraulic cylinder and a Sach foot.

2.3.2 Subject 2

Subject 2, a 25 year old male, is in good physical condition. He contracted osteogenic sarcoma in his early teens and, as a result, had a right knee disarticulation in 1969. He presently uses a quadrilateral socket and a Mauche "Stance-N-Swing" knee cylinder with an articulated ankle. His hobbies include skiing and horse back riding.

2.3.3 Subject 3

Subject 3, a student at M.I.T., possesses a unique conventional prosthesis in that the suction socket and calf segment are fabricated from aluminum sheet metal. The resistive knee moment is provided by friction alone. He underwent right leg, above knee amputation in 1969 after a fibroma tumor was diagnosed in the knee joint. Subject 3

reports that his conventional prosthesis is lighter than the simulator used in this study.

2.3.4 Subject 4

Subject 4 is currently wearing a prosthesis equipped with a quadrilateral socket, Dupaco hydraulic cylinder and Sach foot. Like most amputees wearing a socket not held in place with suction, he wears a belt to keep the prosthesis securely fastened to his body. He is 45 years old and in good physical condition. His above-knee amputation resulted from injuries incurred in an automobile accident in 1961.

2.4 Software

Since the experiments were computer controlled, some Fortran programming was necessary. Also, machine language programs were developed to operate a programmable real time clock, included as option with the PDP 11/60, and the ANDS 5400 Data Acquisition System. Also, Fortran software was developed to allow graphical presentation of the data. The software mentioned above is included in Appendix B. Digital filter algorithms used in these programs were taken from Stearns (18).

CHAPTER 3 INITIAL EXPERIMENTS

3.1 INTRODUCTION

This chapter describes experiments conducted with the simulator emulating prostheses which control motion by mechanical friction. This particular simulation was chosen because it was easy to implement and did not require a large software overhead. Since changing the friction coefficient of the knee joint was easy to understand physically, one could gain qualitative and quantitative knowledge about the sensitivity of A/K amputee gait to prosthesis characteristics. Also, a large amount of data could be collected and processed off-line to determine the feasibility of ME control. Procedures are discussed in Section 3.2, observations in Section 3.3, and results in Section 3.4.

3.2 Procedure

With exception of electrode placement, procedural details were the same for all subjects. Since two of the subjects were fitted with suction sockets, electrodes were fabricated which could be placed inside the socket and threaded into the myoelectric preamps resting on the outside surface of the socket Figure 10. Thus, once promising recording sites had been found, consistent placement was insured by this mounting technique.

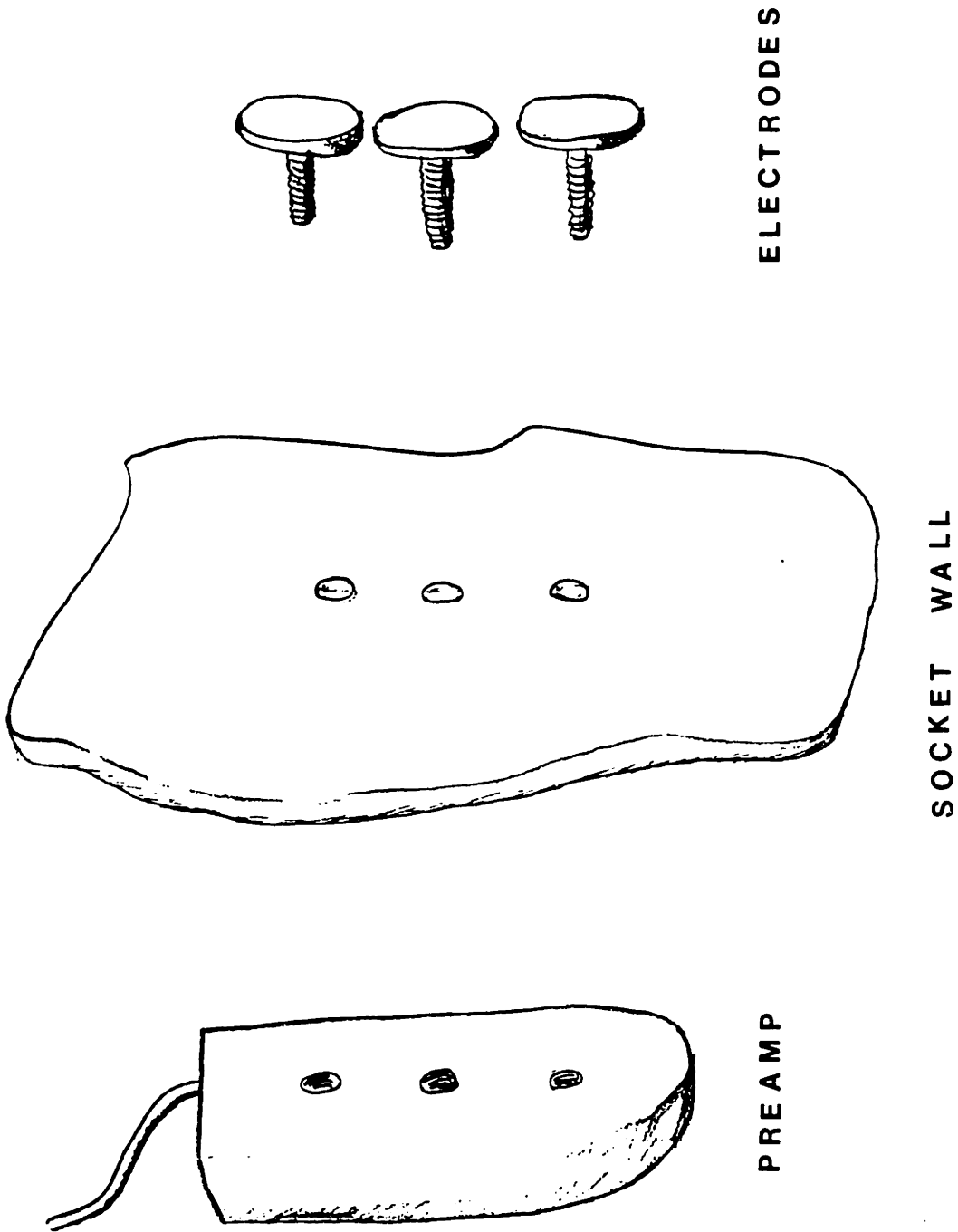


Figure 10. Preamp Mounting Procedure for Suction Sockets

The remaining subjects had the electrodes placed between the socket and stump. The second method required testing electrode placement at the beginning of each experimental session.

A typical experimental session consisted of a number of walking trials. After the subjects had put on the prosthesis simulator and proper alignment (overall length, etc.) had been checked, they were asked to walk in an oval pattern at an even cadence. They were also informed of the relative simulator friction level before each trial. After they were accustomed to a given level of friction, five representative data sets were sampled. Each set consisted of 2048 samples which, at the 1000 Hz sampling rate, represented about 2 seconds. Sampling was started near the end of swing and in general, lasted longer than a complete gait cycle. In general, the sessions started with very low dissipative torque and finished with the highest level of damping for which a subject could ambulate. Data was taken to describe the angular position and velocity of the knee axis and myoelectric activity of the quadriceps and hamstrings muscle groups on the above knee stump. Comments were solicited from the subjects to help gain an understanding of the consequences of varying the damping level.

3.3 Observations

In a qualitative way, observing the walking trials added to the authors knowledge and tuned intuition about A/K gait and the way A/K amputees control their conventional prostheses. In general, the lower segment of the simulator impacted at high speed against the hyperextension stops for all subjects at low friction levels. On the other hand, subjects had to expend a lot of energy to throw the shank into full extension at very high levels. Also, there seemed to be a range of levels at which the subjects could ambulate very well. For example, out of five levels representing the range of friction levels, discussed in 3.2, the subjects were generally quite good at controlling two with little observable gait deterioration.

Observable differences between subjects included the fact that some subjects were able to walk with higher friction than others. This seemed to be related to the physical condition and age of the subject and to the length of the simulator shank. In particular, subject two, having only an average shank length was able to walk with the simulator at the same maximum level as subject four who had the longest lower segment length. Conversely, subject one and subject three, while having approximately the same shank length as subject two, effectively could not at high energy dissipation.

All of the subjects noted that the task required constant attention at higher levels. Subject four, using a friction type prosthesis everyday, did not notice this problem as much as the others. Also, all subjects found walking at high friction levels very tiring.

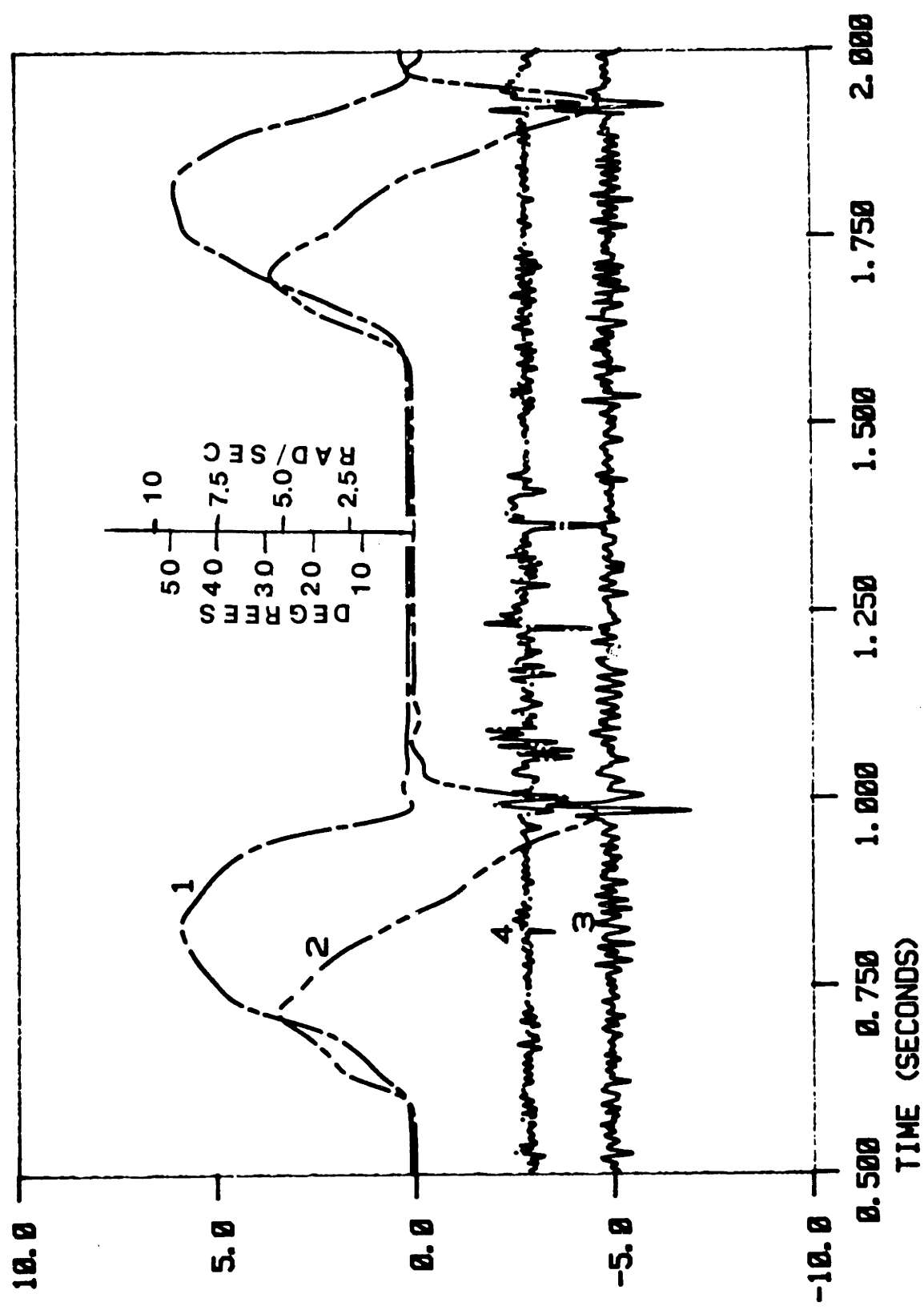
3.4 Results

Representative sample sets are presented in the following figures. Also, an indicator of the relationship between ME activity and friction level of the simulator is explained and results of its implementation are included. These results indicated that further development of ME control schemes was a reasonable course of action.

Figure 11 shows a sample set from the data acquired during the walking trial in which the simulator damping for subject 1 was zero. Curve 1, the position trajectory, shows that the subject was not yet accustomed to the simulator damping. This can be seen by noting that the curve was not very smooth during swing phase. Toe off occurs shortly after the knee begins to buckle. This correlates to the times 0.62 and 1.62 on the abscissa. Another thing to note is the oscillatory behavior as the knee goes into full extension. This is due to compliance of transmission components in the simulator and is

POSITION (1) VELOCITY (2) QUADRICEPS (3) HAMSTRINGS (4)

FIGURE 11. SUBJECT 1 FRICTION SIMULATION (0)

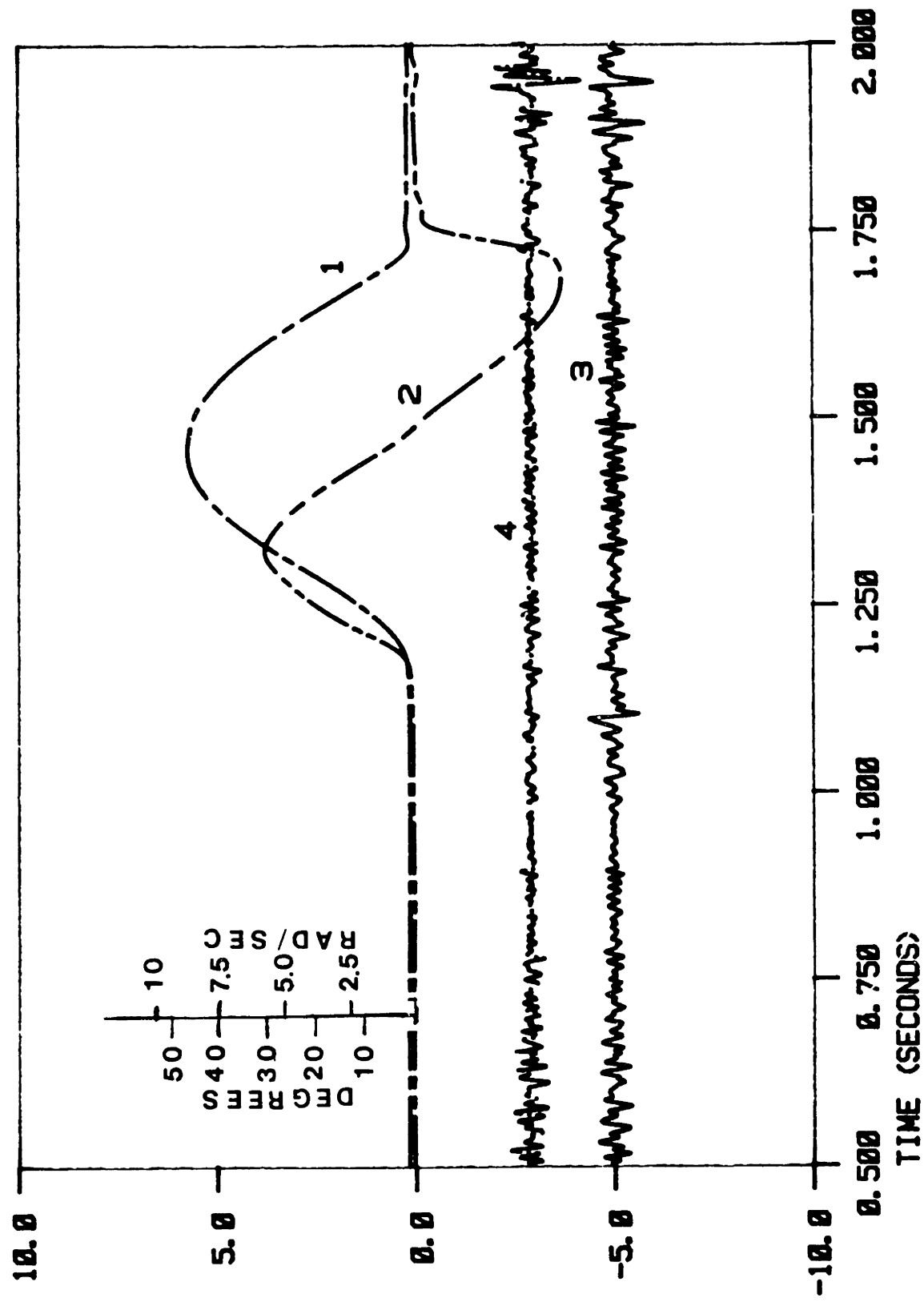


an indication of how hard the lower segment collides with the hyperextension stops. Another indication of this impact is curve 2 the velocity trajectory. The velocity trajectory seems reasonable given curve 1. Curve 3 shows the ME activity from the quadriceps muscle group. This electromyogram is presented in "raw" form, meaning it has only been filtered at the prosthesis (in the manner discussed above), low pass filtered at the interface module, sampled and plotted. Hence, A 5 volt D.C. offset is inherent in the data as it comes from the simulator. Significant quadriceps activity is apparent during swing and the first part of stance. The hamstrings ME activity is shown by curve 4. The offset in this data has been adjusted in order to clarify graphical presentation. Note that significant activity occurs during the first part of stance and the first part of swing.

Figure 12 shows a sample set from a more comfortable level for subject 1. Apparently, the subject was in better control of the simulator since the position trace is very smooth. Also, the impact at full extension is less as noted from the behavior at the end of swing. The shape of the velocity trace at the end of swing is of interest since the shape is quite consistent among trials using the friction controller. Again, significant quadriceps activity is noticeable starting

POSITION (1) VELOCITY (2) QUADRICEPS (3) HAMSTRINGS (4)

FIGURE 12. SUBJECT 1 FRICTION SIMULATION (8)

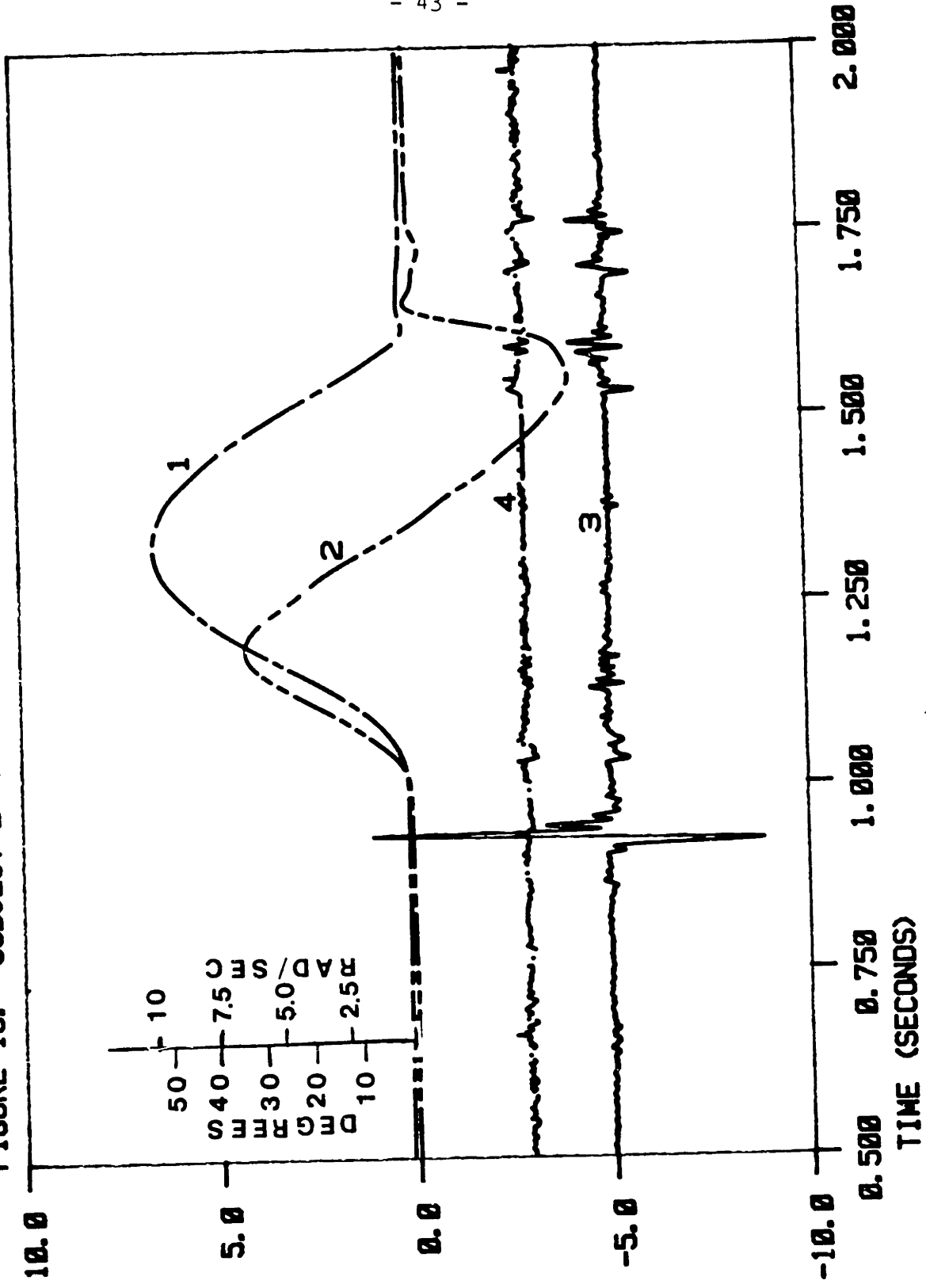


before the beginning and continuing until just before the end of swing. This activity is also apparent at the beginning of stance phase. Significant hamstrings activity occurs during the beginning of stance phase and, to a lesser extent, during swing.

Figure 13 shows data acquired during the zero damping trial for subject 2. This subject was able to control the simulator at this level almost immediately, and could keep the hyperextension impact to a minimum. A couple of differences between this subject and the former can be noted. First, the duration of the ME activity for this subject is less of the overall cycle. The magnitude of the hamstrings activity is significantly less than for the former subject. Also, a large amplitude artifact can be noted before the beginning of swing. This artifact is probably due to electrode-skin separation. Similarities between the two subjects can be seen in the temporal pattern of the ME curves.

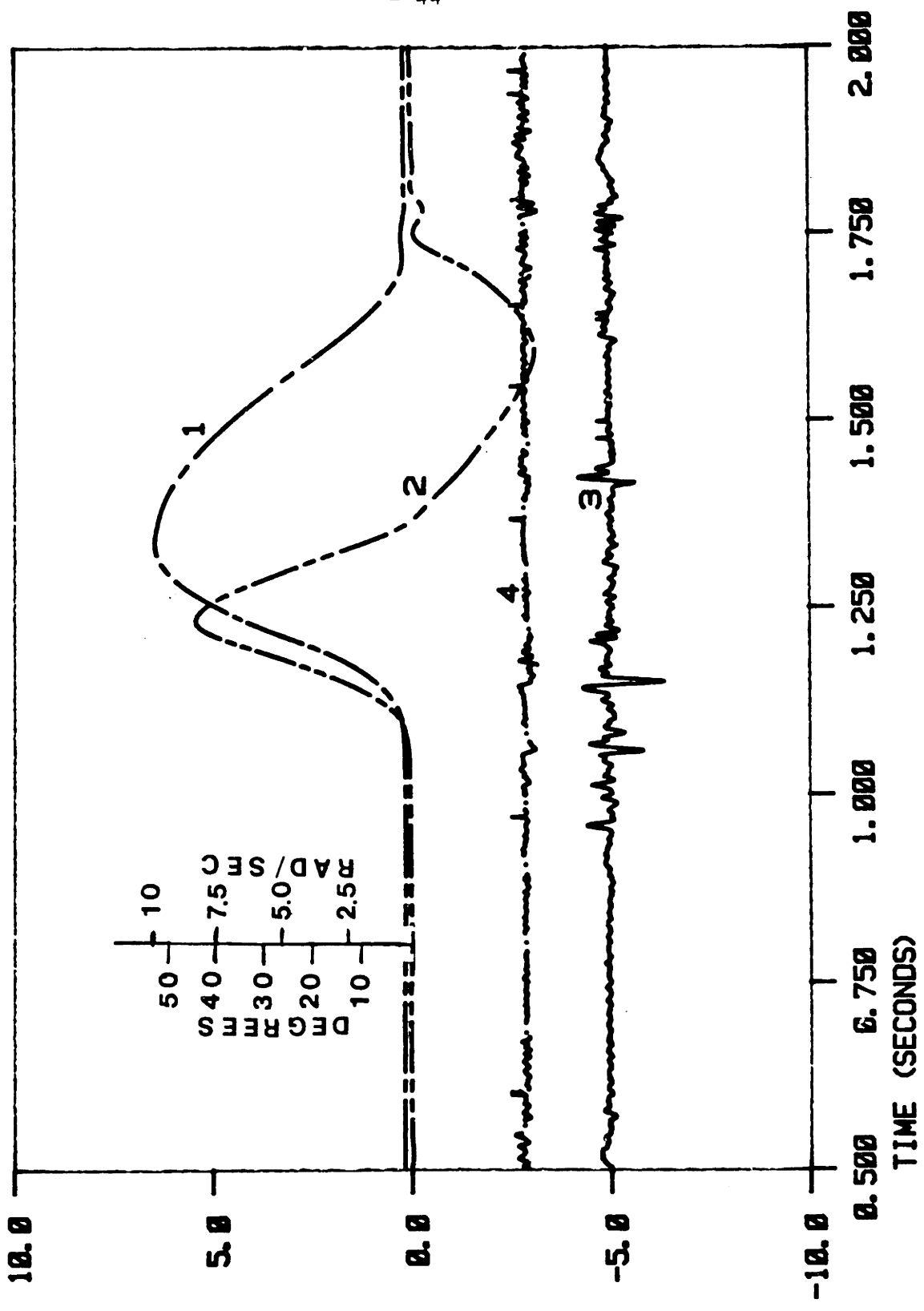
Figure 14 shows data from the trial for which damping was set to the highest level in the session. Note the asymmetry in the kinematic data introduced by this extreme friction level. This data implies that the subject increased acceleration during the first part of swing to insure full extension at the end of swing phase. Also, poor gait cosmesis is inherent in this method of control by the

FIGURE 13. SUBJECT 2 FRICTION SIMULATION (0)



POSITION (1) VELOCITY (2) QUADRICEPS (3) HAMSTRINGS (4)

FIGURE 14. SUBJECT 2 FRICTION SIMULATION (30)



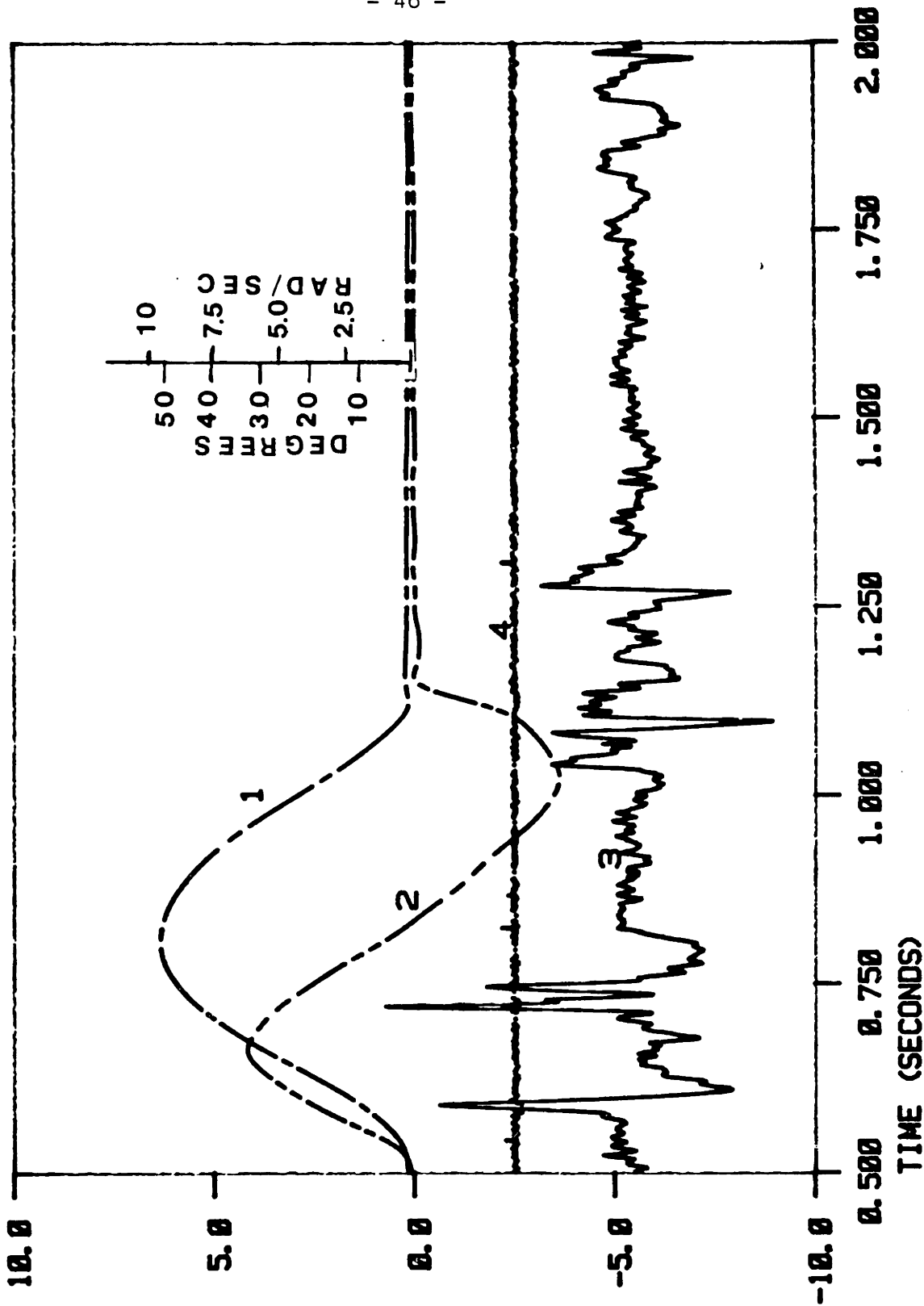
POSITION (1) VELOCITY (2) QUADRICEPS (3) HAMSTRINGS (4)

subject. Again, the temporal pattern of the ME data is consistent with previous results.

Figure 15 is a zero damping sample set for subject 3. This subject was also able to control the prosthesis simulator at this low damping level. Again, note the characteristic shape of the velocity trace. The quadriceps activity is masked by artifact from electrode-skin interaction. The hamstrings activity is of very low magnitude. This is consistent with electrode placement difficulties encountered with this subject.

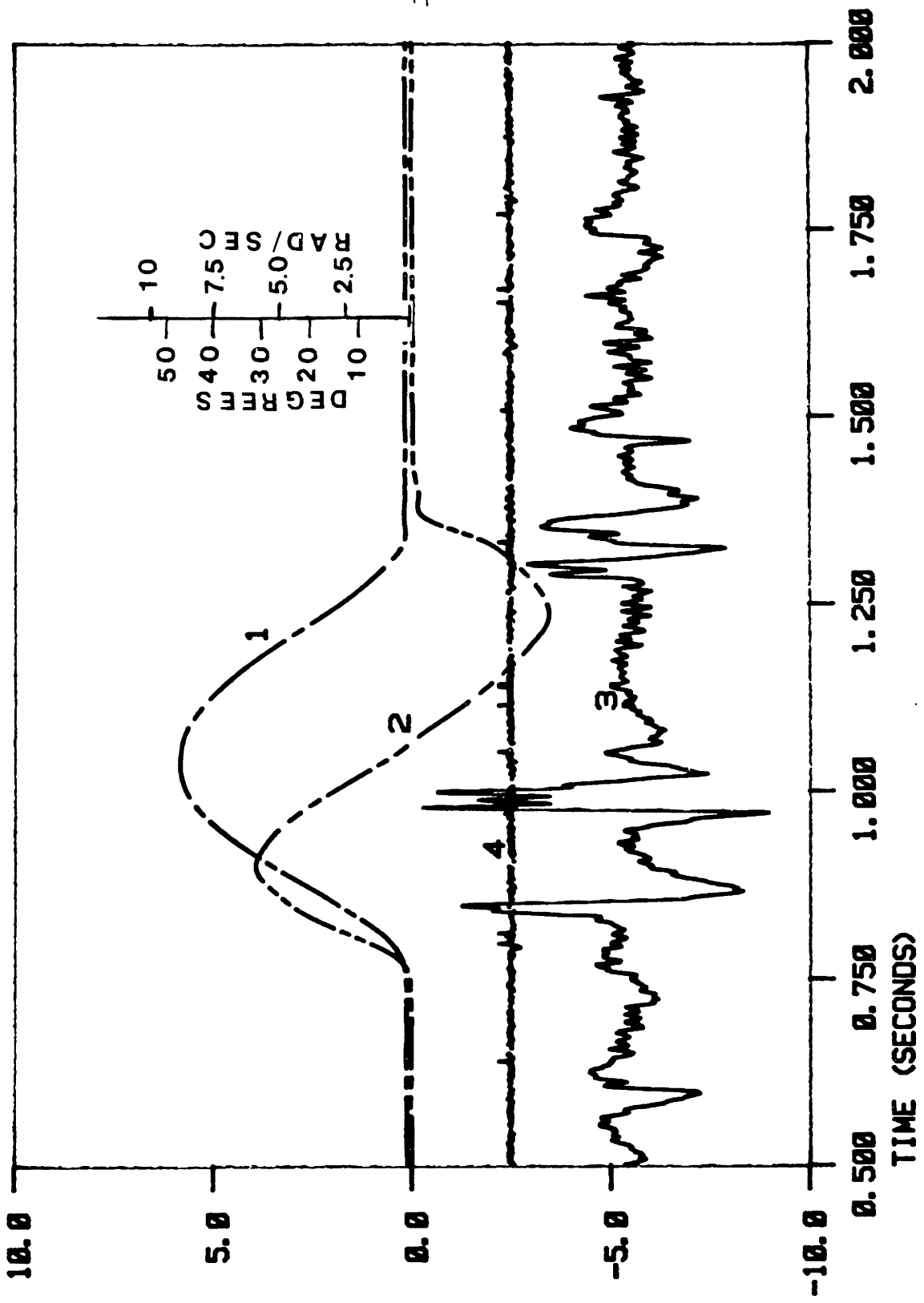
Figure 16 shows results from a simulation more like the subject's conventional prosthesis. It can be seen that electrode-skin interaction is the prominent effect in the quadriceps trace. Figure 17 shows this plot after digital filtering of the ME data. A third order Butterworth filter algorithm was used for this purpose. Noticeable effects of the filtering include elimination of the D.C. offset and attenuation of low frequency artifact in the signal. The break frequency selected for this filter was 20 Hz. This plot indicates that a higher break frequency was probably reasonable to enable better presentation of the data. It also indicates that a large majority of the undesirable artifacts can be removed by suitable filtering.

FIGURE 15. SUBJECT 3 FRICTION SIMULATION (Ø)



POSITION (1) VELOCITY (2) QUADRICEPS (3) HAMSTRINGS (4)

FIGURE 16. SUBJECT 3 FRICTION SIMULATION (8)



POSITION (1) VELOCITY (2) QUADRICEPS (3) HAMSTRINGS (4)

POSITION (1) VELOCITY (2) QUADRICEPS (3) HAMSTRINGS (4)

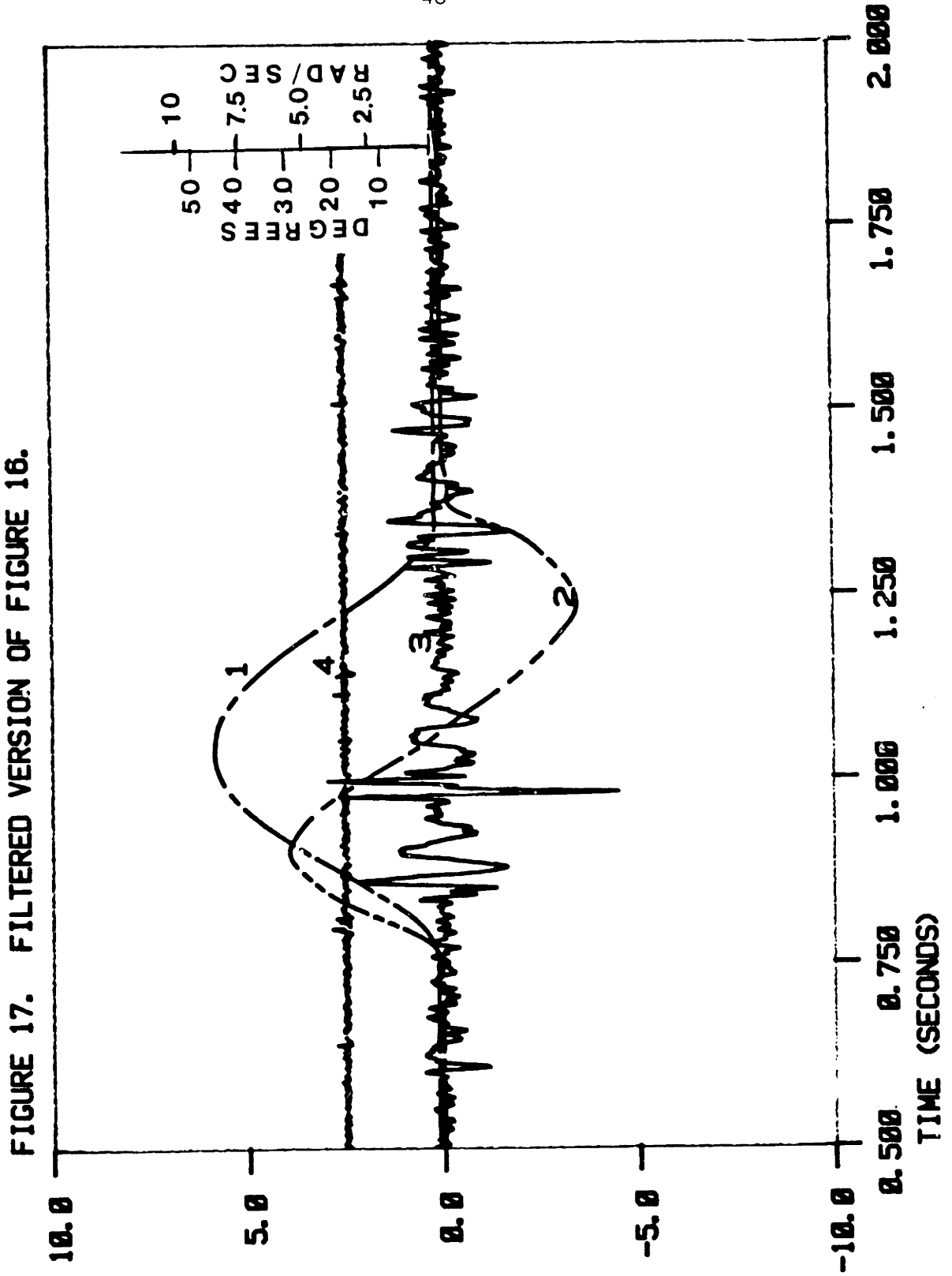


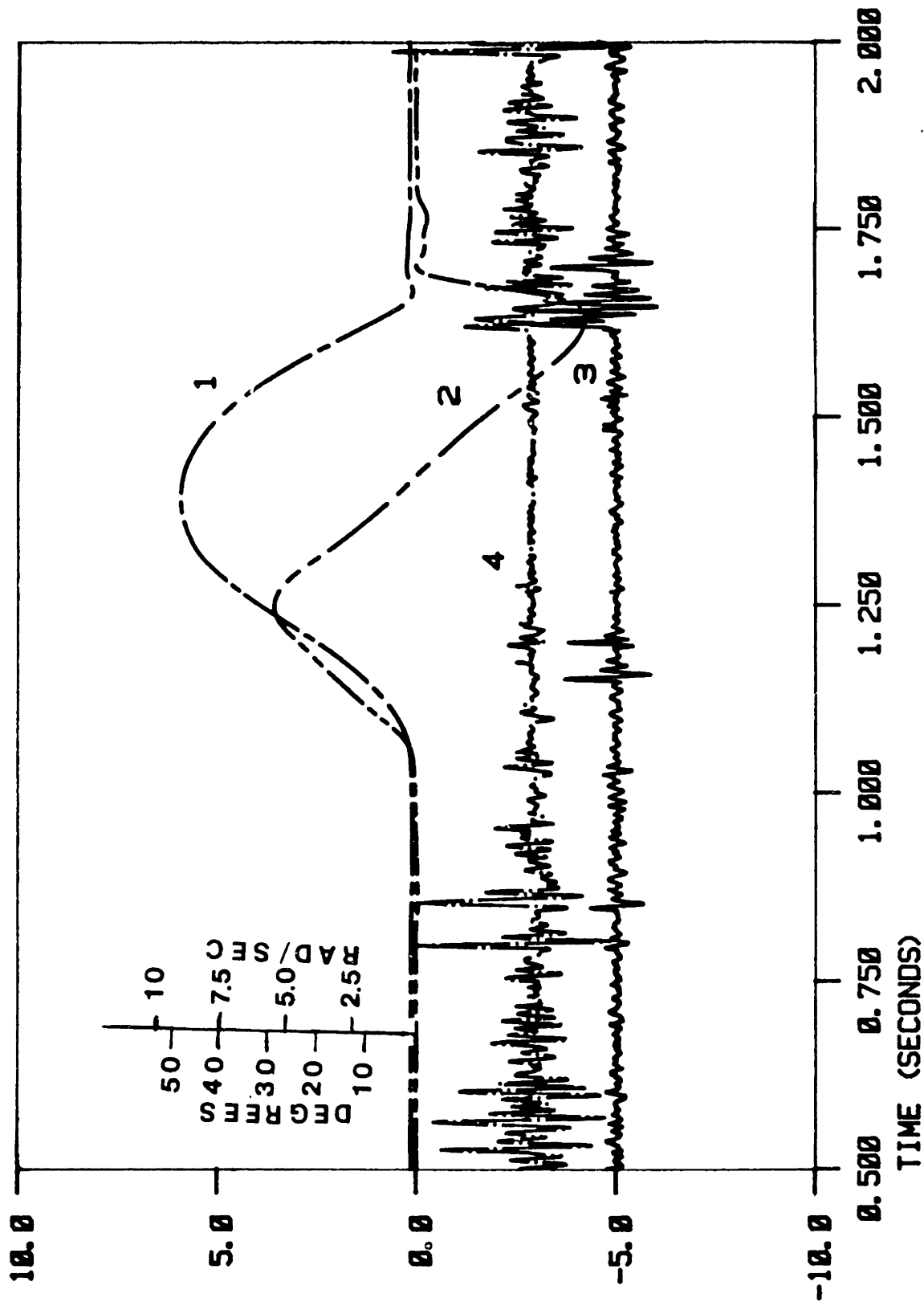
FIGURE 17. FILTERED VERSION OF FIGURE 16.

The results from the zero friction simulation for subject 4 are presented in Figure 18. Note that this subject could not control the hyperextension impact at this level. In addition, the temporal pattern of the ME data seems consistent with previous results. It can also be seen that hamstrings data was easily acquired. The electrode for this muscle group was mounted with tape on scar tissue resulting from surgery after the amputation.

Figure 19 shows the results from a more comfortable friction simulation. Again, the temporal pattern of the ME data is quite consistent with earlier results, except that very little ME activity is apparent during swing phase. The transition between swing and stance phase is accomplished smoothly and the shape of the velocity profile is consistent with others obtained with this type of simulation.

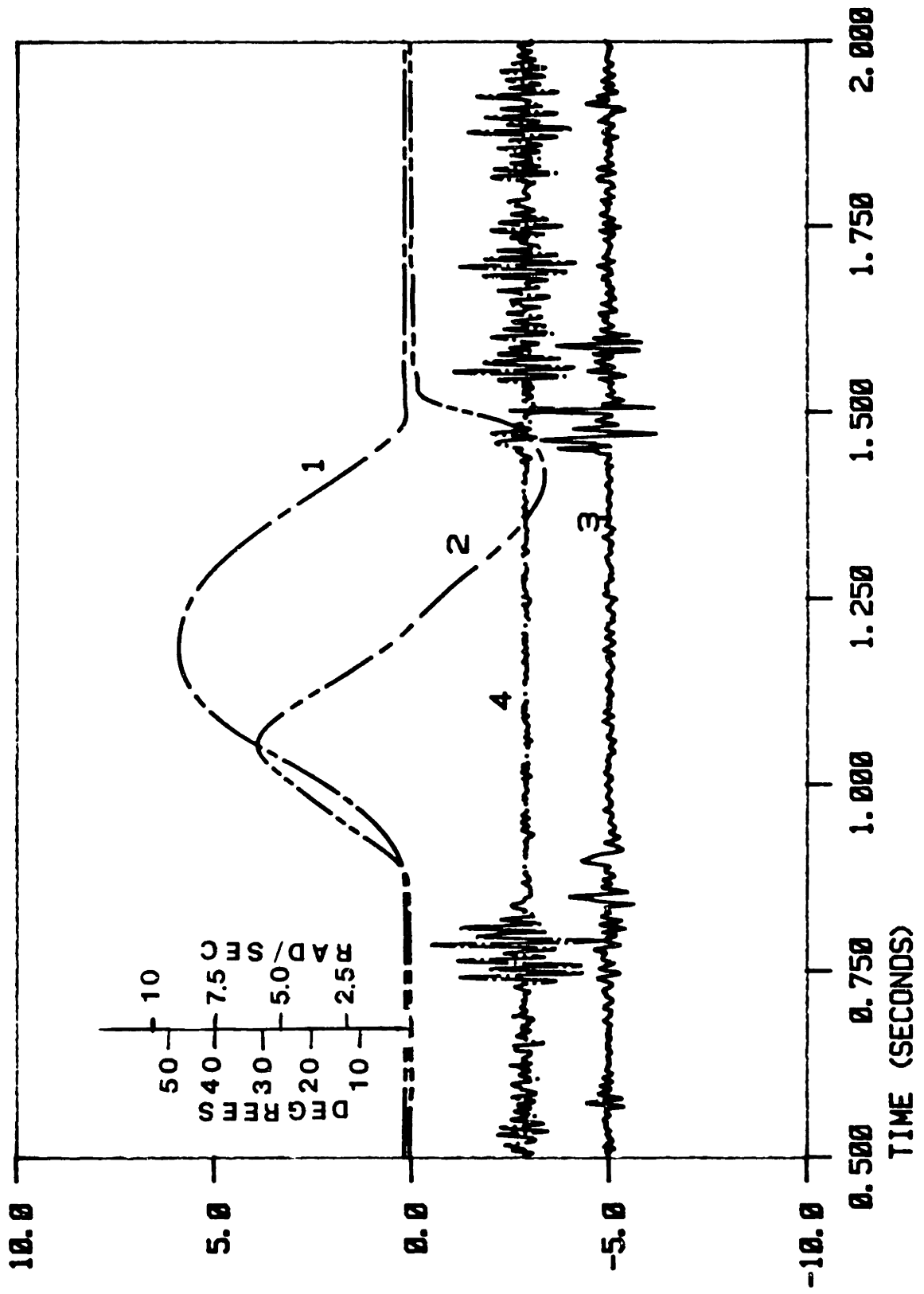
These results indicated that, although a relationship between ME activity and damping probably exists, the effect of such a relationship was masked by other factors. A study of this relationship during swing phase was performed using the area under the smoothed electromyogram as an indicator of the ME activity. The data processing consisted of high pass filtering, rectification, low pass filtering, and Simpson's rule (Kreysig 20) numerical integration of the particular electromyogram.

FIGURE 18. SUBJECT 4 FRICTION SIMULATION (Ø)



POSITION (1) VELOCITY (2) QUADRICEPS (3) HAMSTRINGS (4)

FIGURE 19. SUBJECT 4 FRICTION SIMULATION (8)



POSITION (1) VELOCITY (2) QUADRICEPS (3) HAMSTRINGS (4)

The data was smoothed because the error in the above integration method depends upon the highest derivative in the interval of interest. Swing phase was detected from the position data. In the following plots, a damping level of zero represents negligible friction while 30 corresponds to a very stiff knee. Figure 20 shows the results from the quadriceps ME data of subject 1. The data points, denoted by X, represent the number obtained by applying the above processing to a data set of a particular sample set at a particular damping level. Figure 21 shows the corresponding results for the hamstrings data. Note from both of these graphs that the indicator remains constant within 2 percent of the signal level. Also note that the indicator seems to be decreasing over the course of the session indicating that fatigue and electrode-skin impedance changes may have influenced the results. Figure 22 shows results for quadriceps data taken from subject 2. Figure 23 presents the corresponding results for the hamstrings group. Similar comments about the magnitude of the indicator change apply here. However, the indicator for this subject seems to be a minimum at a damping level of 16 for both muscle groups. A similar effect can be seen in the next two graphs for subject 3 at a damping level of 24. The next two graphs show the same sort of behavior, although not as dramatically, for subject 4 at a damping level 16.

FIGURE 20. SUBJECT 1: QUADRICEPS CORRELATED WITH DAMPING

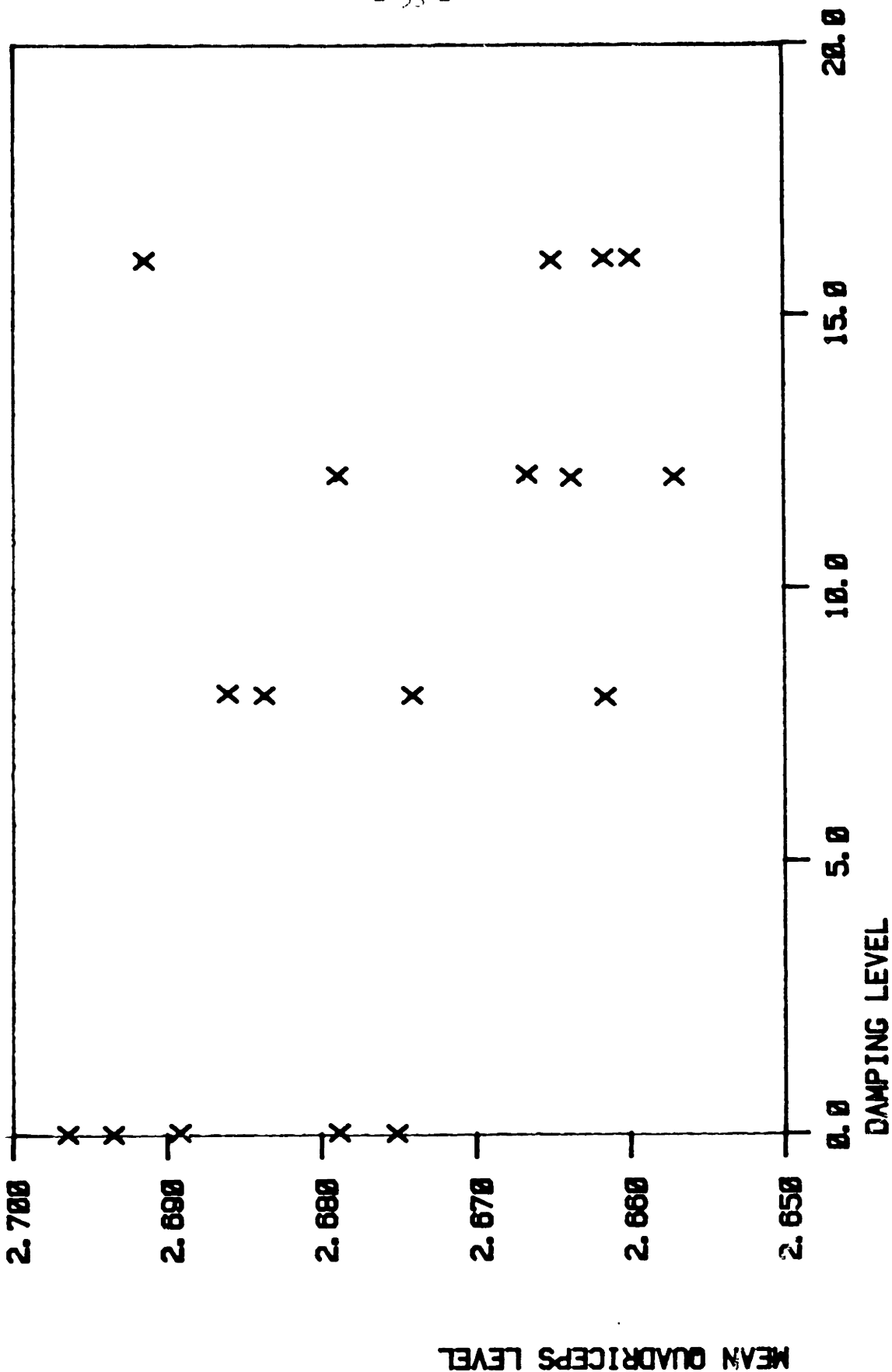


FIGURE 21. SUBJECT 1: HAMSTRINGS CORRELATED WITH DAMPING

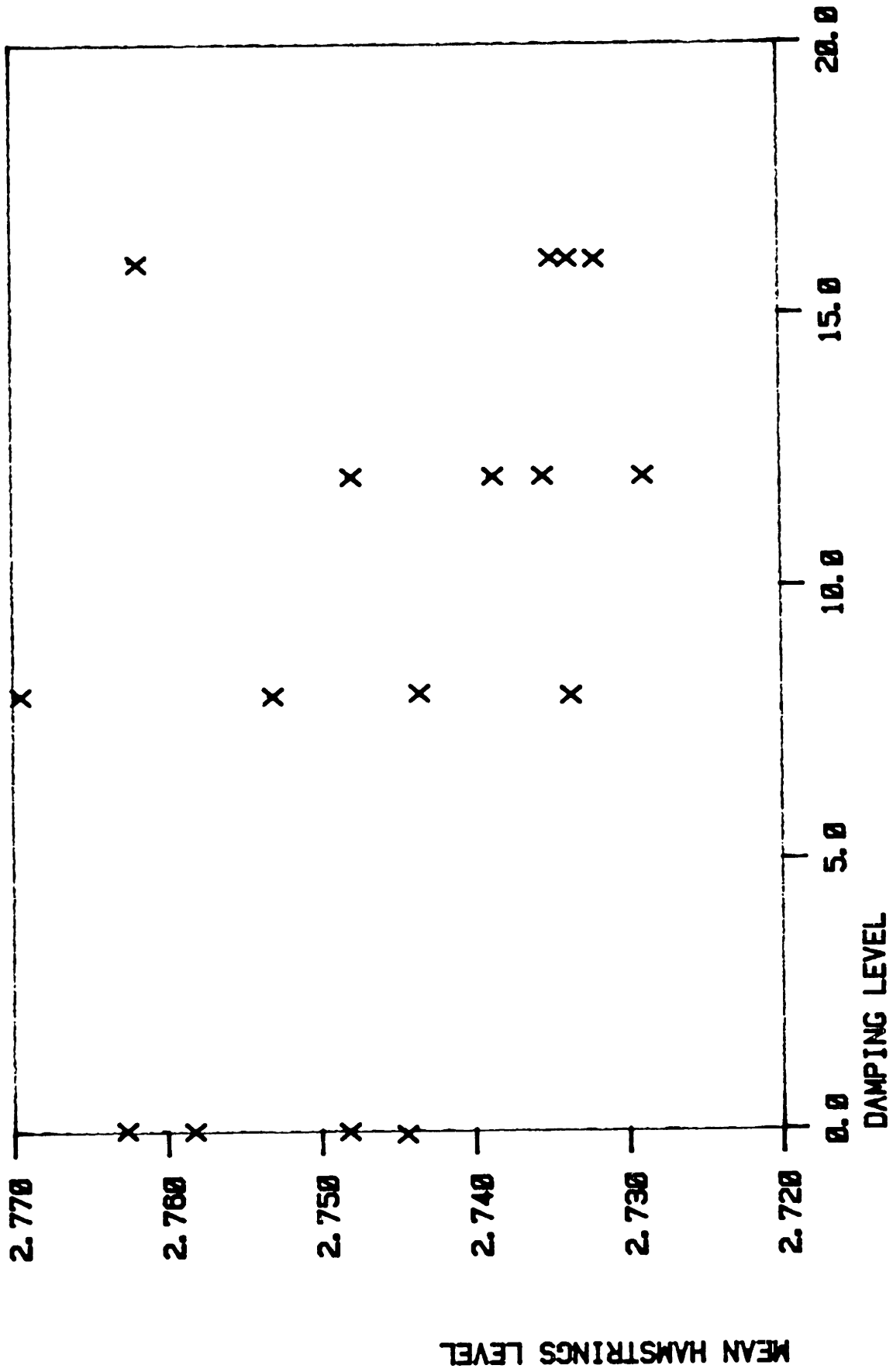


FIGURE 22. SUBJECT 2: QUADRICEPS CORRELATED WITH DAMPING

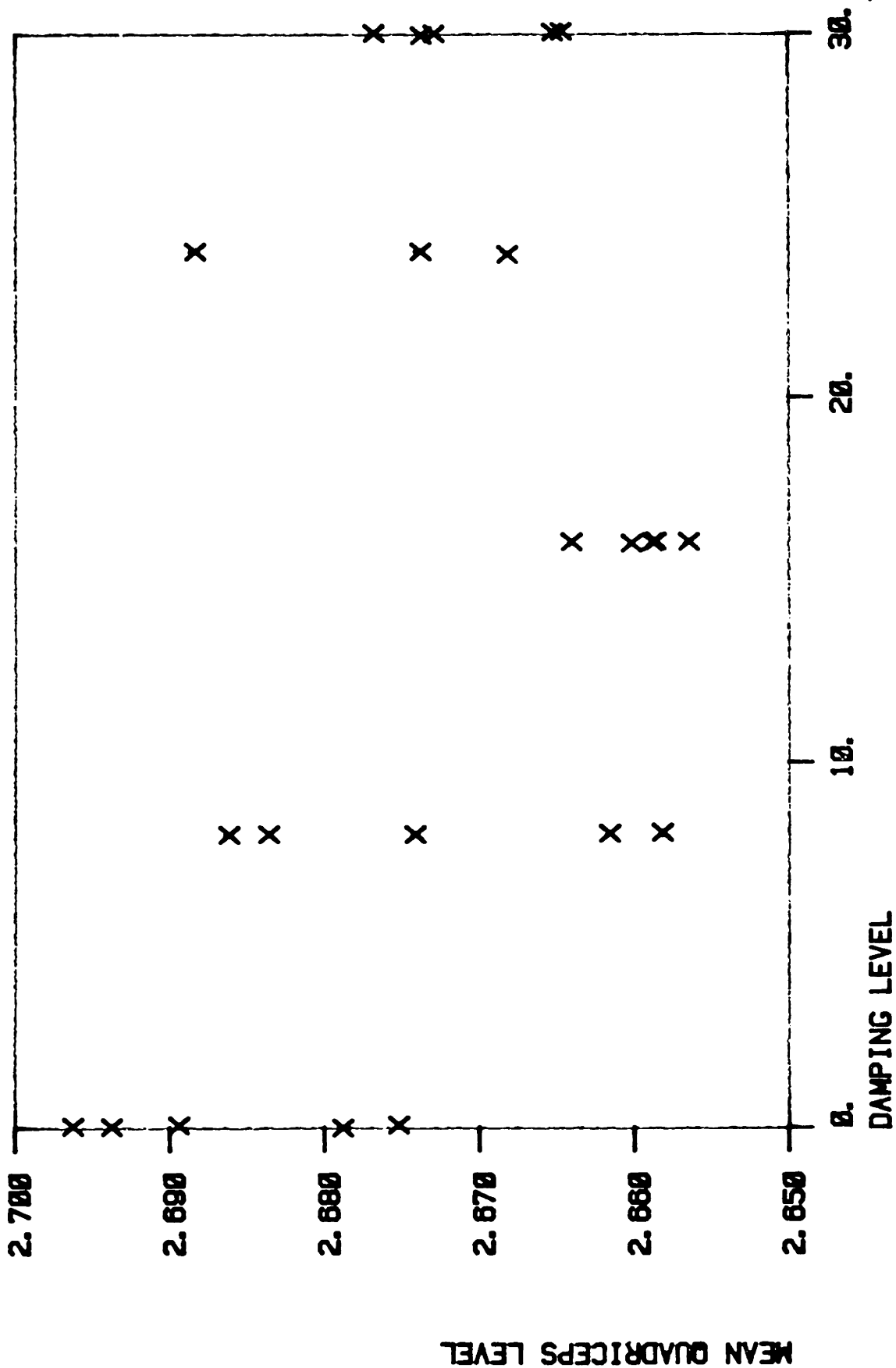
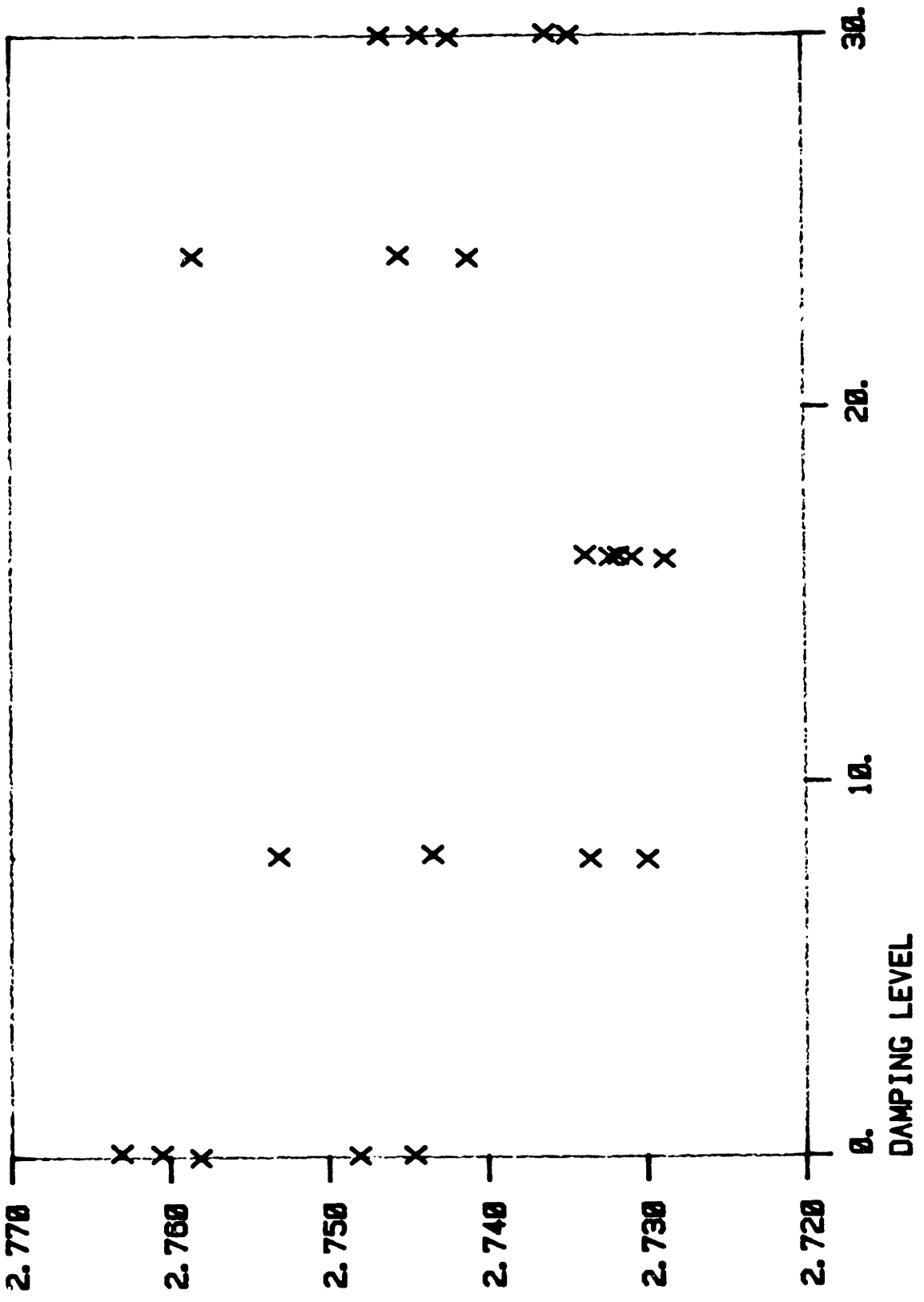


FIGURE 23. SUBJECT 2: HAMSTRINGS CORRELATED WITH DAMPING



MEAN HAMSTRINGS LEVEL

FIGURE 24. SUBJECT 3: QUADRICEPS CORRELATED WITH DAMPING

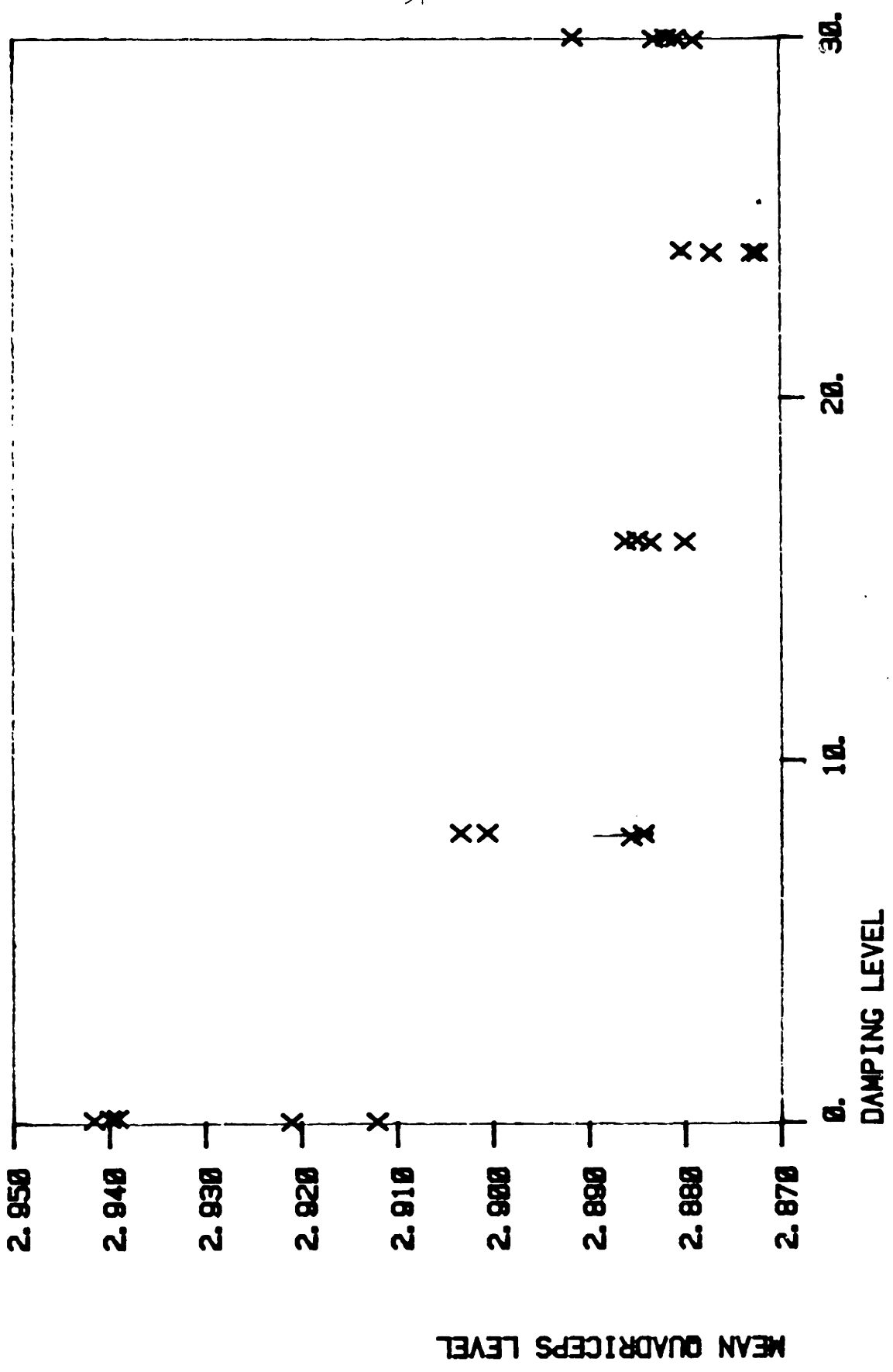


FIGURE 25. SUBJECT 3: HAMSTRINGS CORRELATED WITH DAMPING

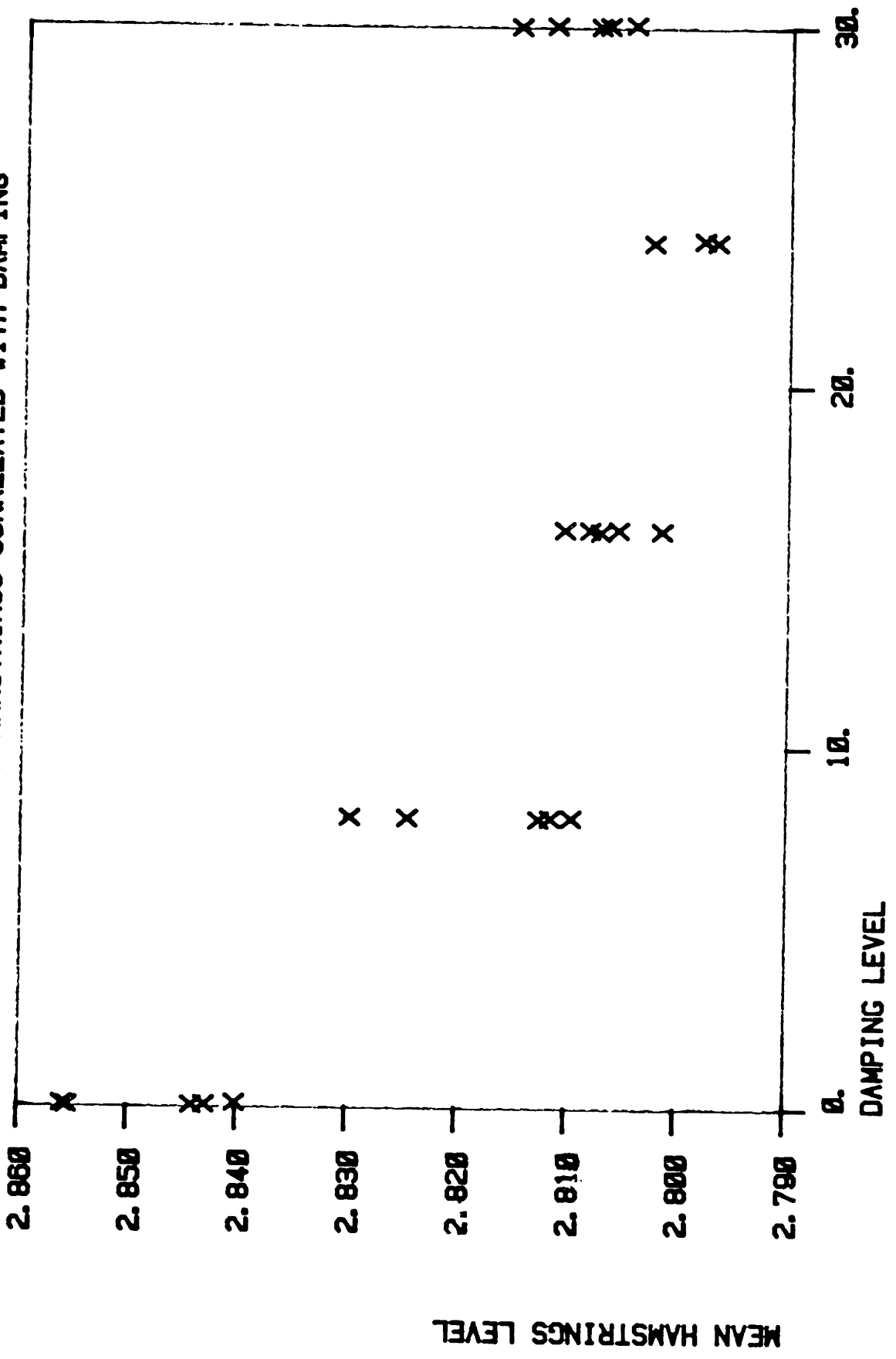


FIGURE 26. SUBJECT 4: QUADRICEPS CORRELATED WITH DAMPING

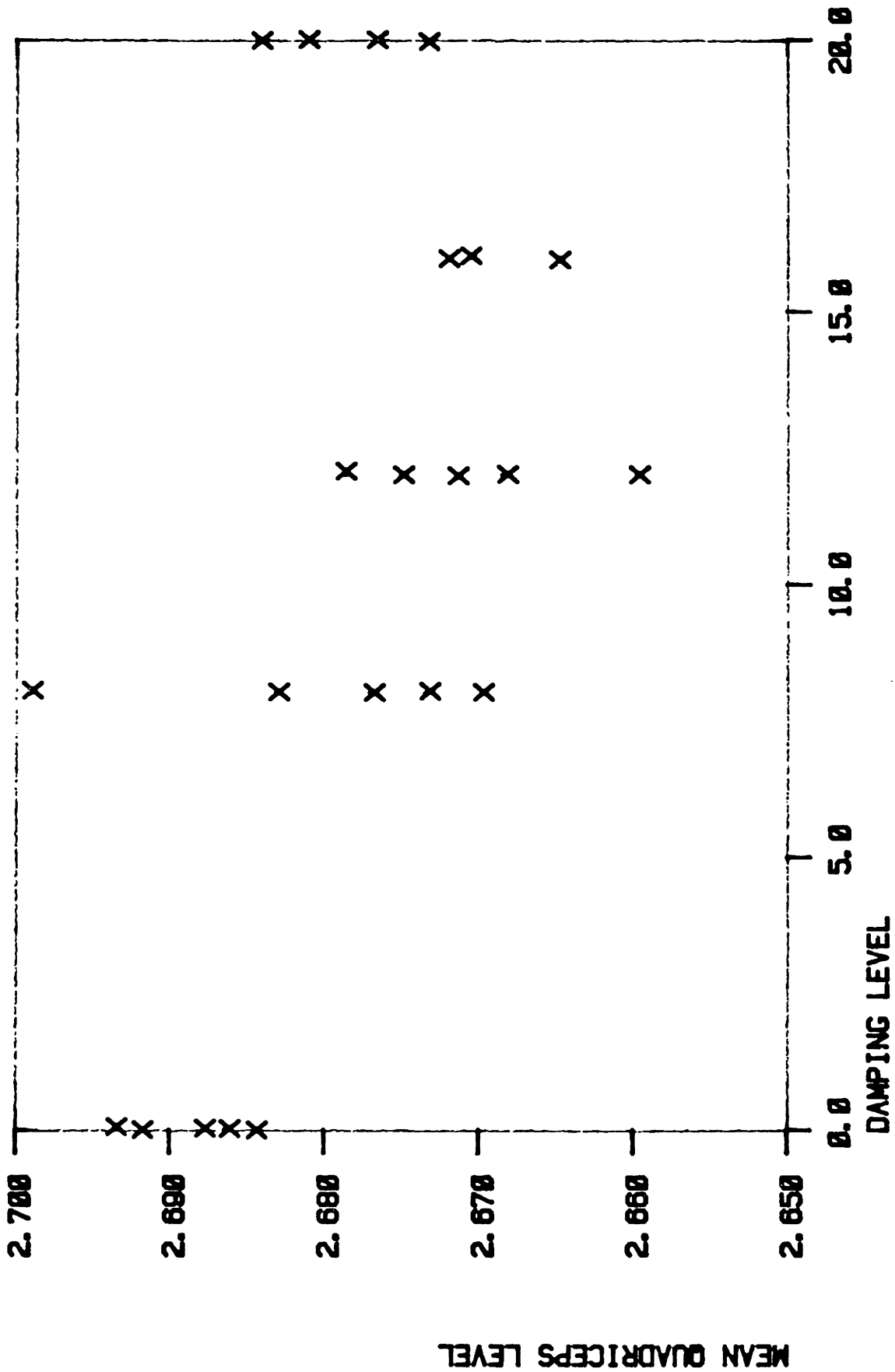
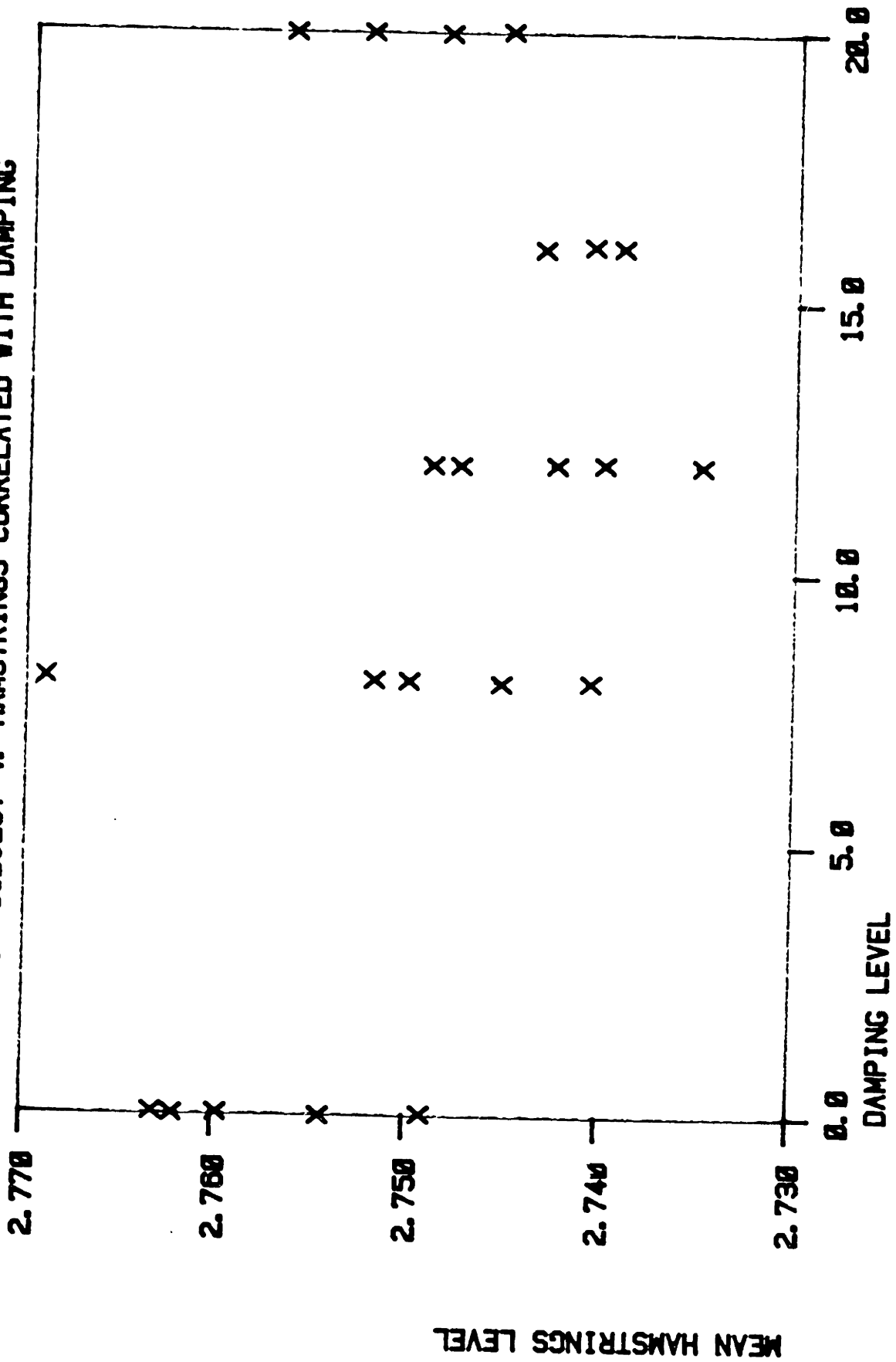


FIGURE 27. SUBJECT 4: HAMSTRINGS CORRELATED WITH DAMPING



MEAN HAMSTRINGS LEVEL

DAMPING LEVEL

CHAPTER 4 CONTROLLER RATIONALE AND DESCRIPTION

4.1 INTRODUCTION

The results presented in Chapter 3 indicated that, if used as a control input, the ME data would have to be used selectively. Consider, as an example, the case in which significant quadriceps activity becomes apparent during swing phase after maximum heel rise. It is necessary for the amputee to extend the lower segment into full extension in preparation for the initiation of stance. Any quadriceps activity during this part of the cycle is probably acting to accelerate the lower segment. Thus, if the quadriceps activity implies damping, the simulator acts to oppose this muscle. Hence, it becomes necessary to find a way to modulate the signal to prevent such action while taking advantage of information contained in the signal about the amputee's intent. Also, it is important to reiterate the limitation of a passive prosthesis which can only act as an energy sink. The following paragraph discusses the ME signal modulator used in all of the controllers discussed in later sections of this chapter. Following sections also present results of off-line implementations of the controllers using the data acquired during the friction simulations.

4.2 Velocity, a Possible ME Signal Modulator

The sign of the angular velocity, positive when the knee is flexing and negative when it is extending, provides a convenient indication of the relative direction of travel of the below-knee segment. To see how this can be used, consider the normal population in which the quadriceps and hamstrings muscle groups are attached below the knee (Figure 28). One of the quadriceps, the rectus femoris, is attached above the hip and contributes to hip flexion. So, it can be seen, in general, that quadriceps activity imparts an extensive torque about the knee while hamstrings activity ultimately generates a flexural torque. Bearing in mind the limited function of a passive prosthesis, consider the following. Quadriceps activity when the knee is flexing (positive velocity) implies deceleration of the knee. When the knee is extending (negative velocity), quadriceps activity acts to accelerate the knee. The two totally opposite statements are true for the hamstrings group. Since the simulator is inherently dissipative, the velocity signal can be used to allow use of only quadriceps activity when the knee is flexing and hamstrings activity when the knee is extending. Thus, the ME activity is modulated by the velocity signal. This was the basic idea behind the development of the controllers that follow.

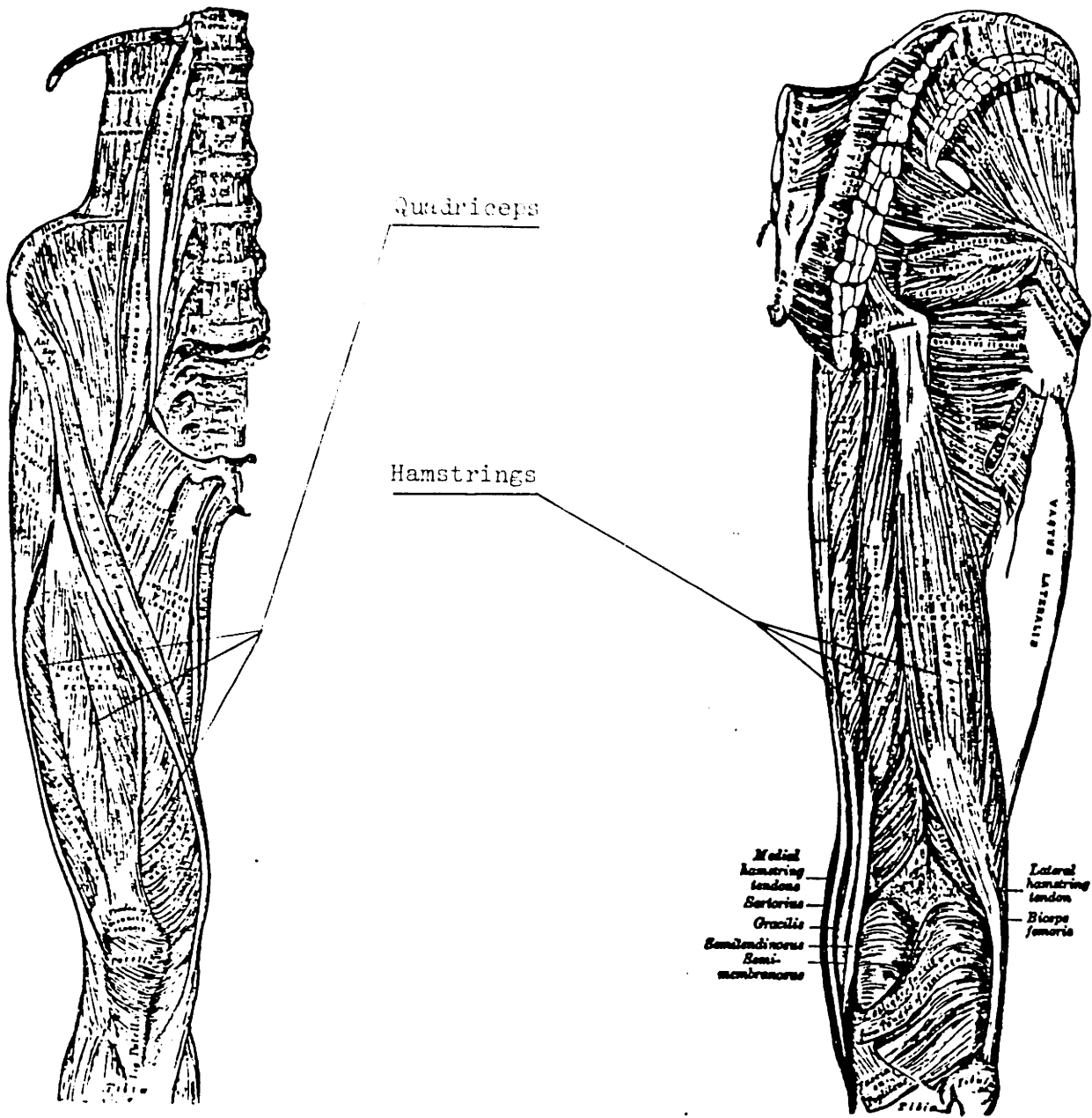


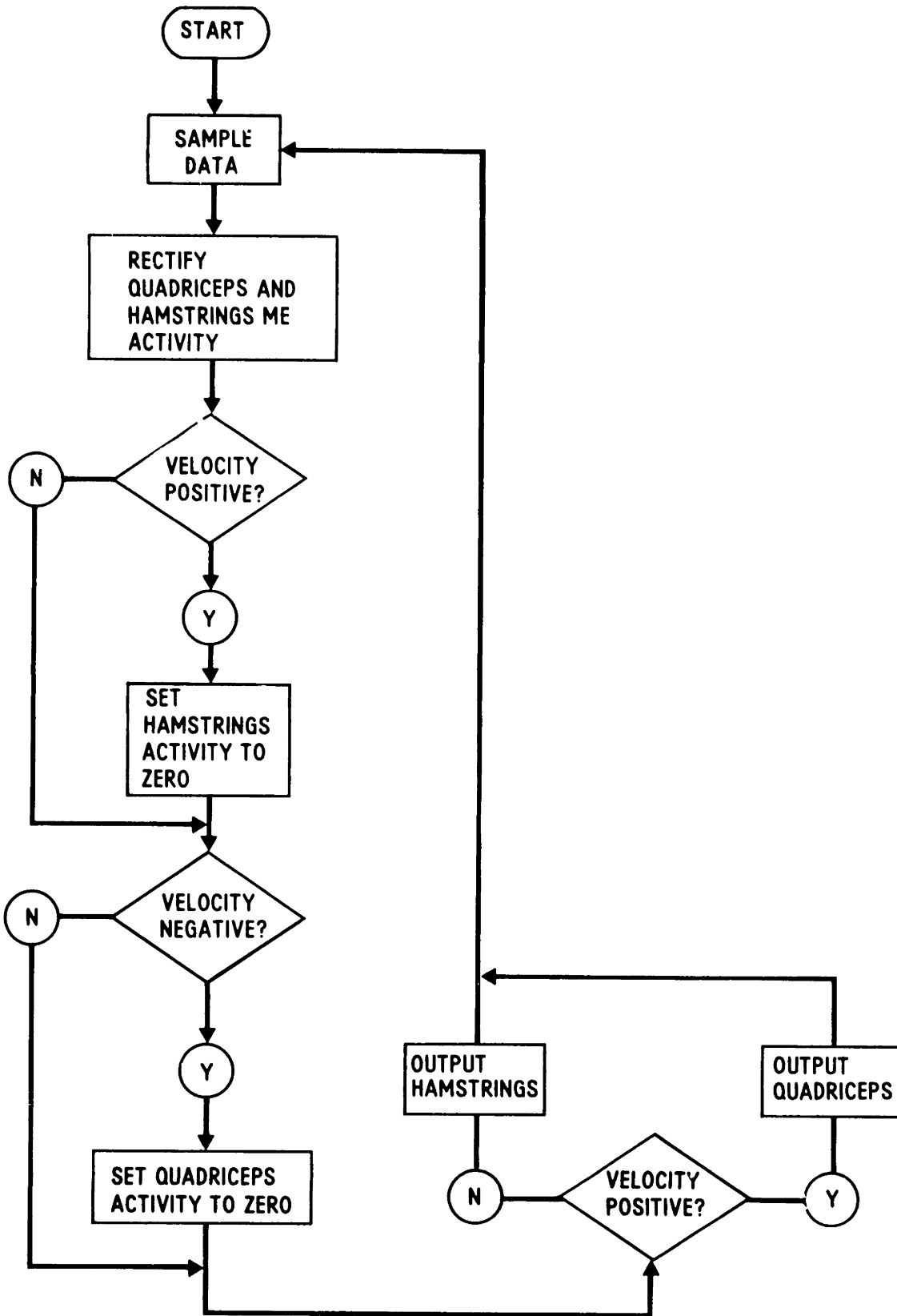
Figure 28. Lower Limb Musculature (From Gray (21))

4.3 Velocity Modulation of the Rectified ME Activity; a Simple Approach

A very simple controller was devised using the velocity modulated, rectified, amplified ME data. Figure 29 shows a flow diagram of the processing sequence. In detail, the ME data was first high pass filtered at a break frequency of 70 Hz then, both channels were rectified and amplified by an empirically developed gain factor. Next, the velocity was checked to determine if the ME data for a particular muscle group was to be used. Advantages of this scheme include simplicity and quick response. On the other hand, artifact can easily produce an unwanted effect. Figure 30 shows the results of an off-line implementation of this scheme for subject 1. Figure 31 shows the same result for subject 2, Figure 32 for subject 3, and Figure 33 for subject 4.

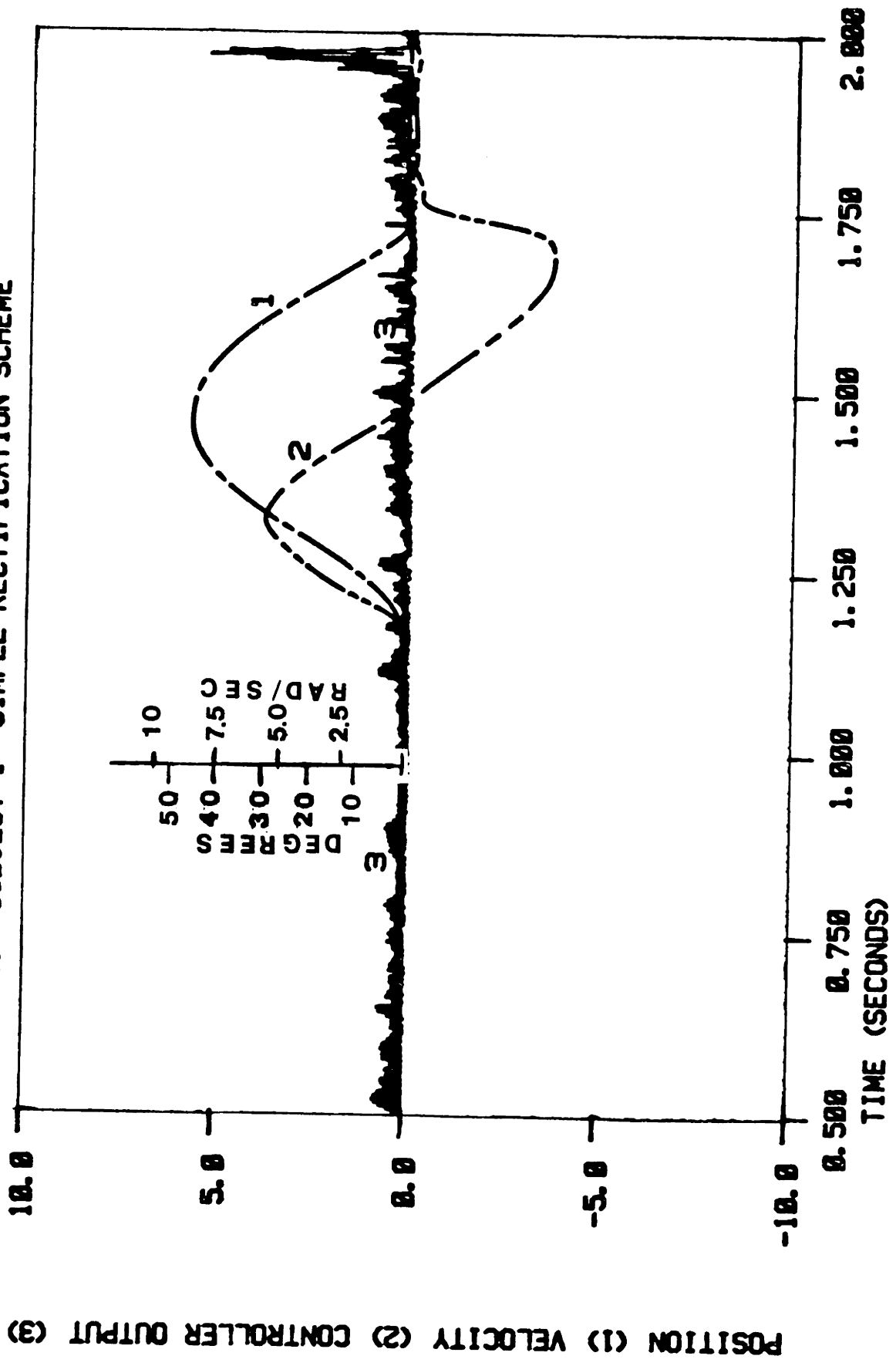
4.4 Velocity Modulated Pulse Width Modulation; First Cut Noise Rejection

A second controller was designed to allow the ME signal to modulate the width of a pulse of current to the magnetic particle brake on the prosthesis simulator. Figure 34 shows a flow diagram of the sequence of operations of this control scheme. This figure shows that both ME signals are high pass filtered at a break



FLOW DIAGRAM FOR SIMPLE RECTIFICATION
 FIGURE 29

FIGURE 30. SUBJECT 1 SIMPLE RECTIFICATION SCHEME



POSITION (1) VELOCITY (2) CONTROLLER OUTPUT (3)

FIGURE 31. SUBJECT 2 SIMPLE RECTIFICATION SCHEME

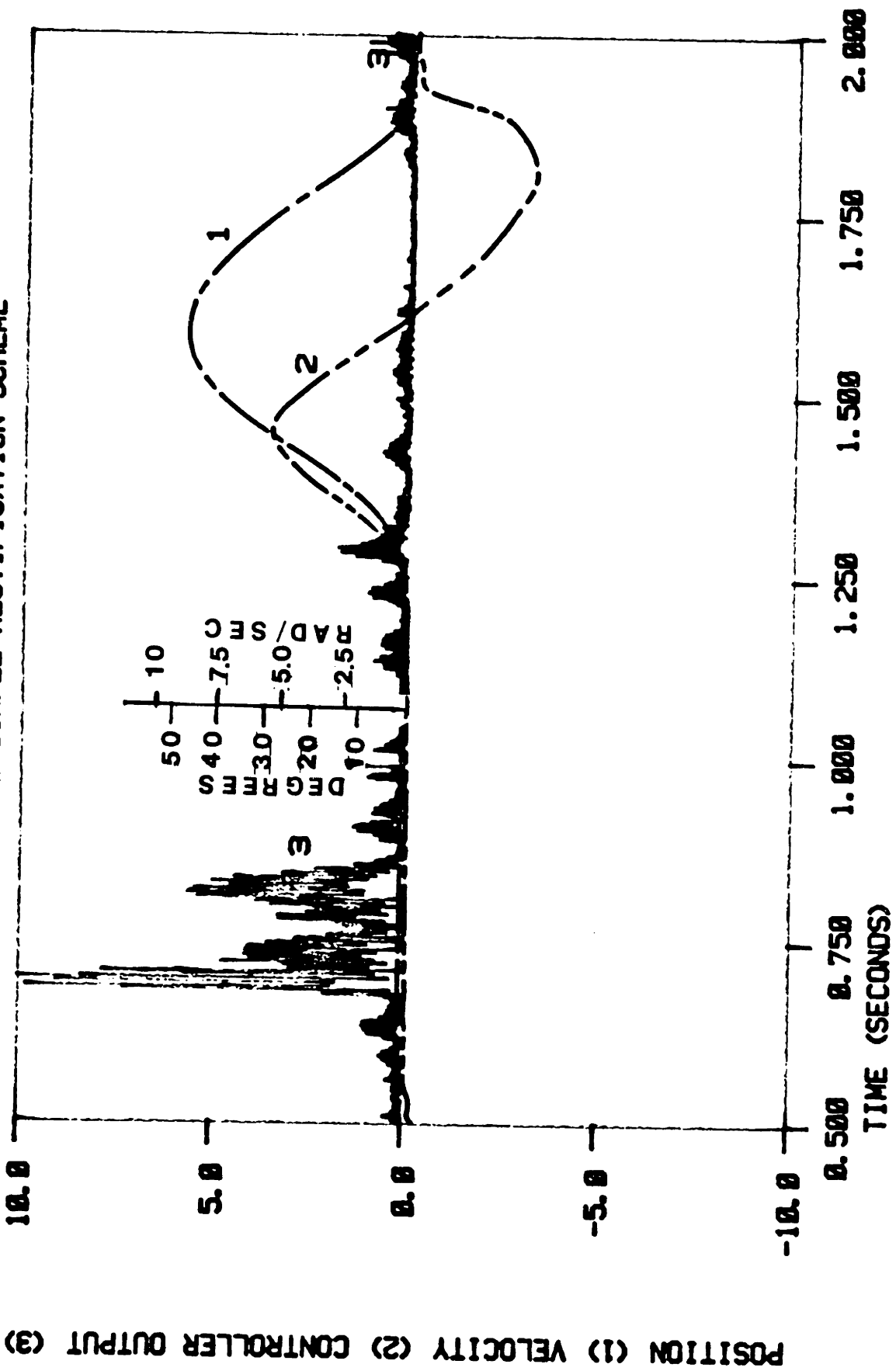


FIGURE 32. SUBJECT 3 SIMPLE RECTIFICATION SCHEME

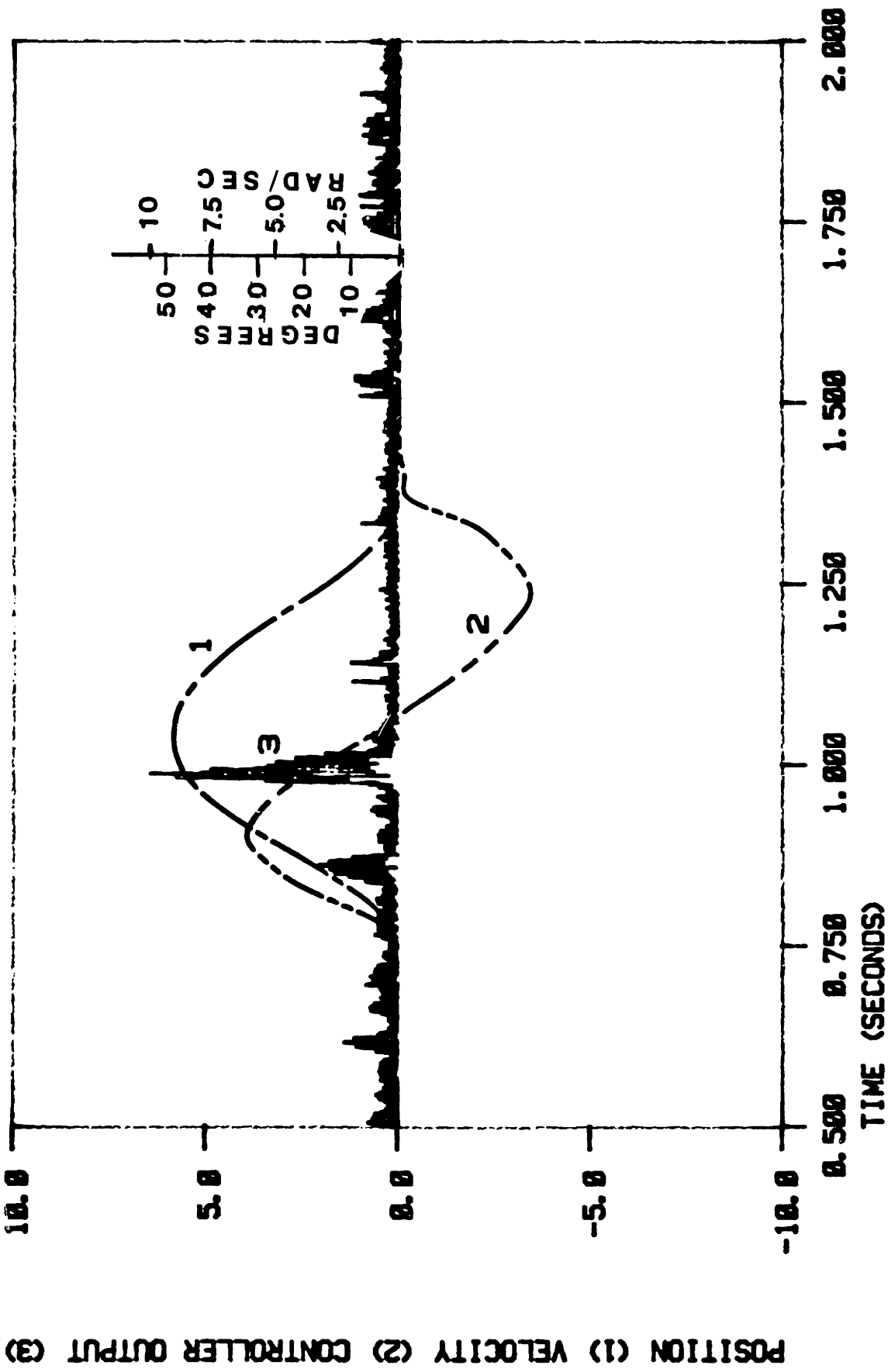
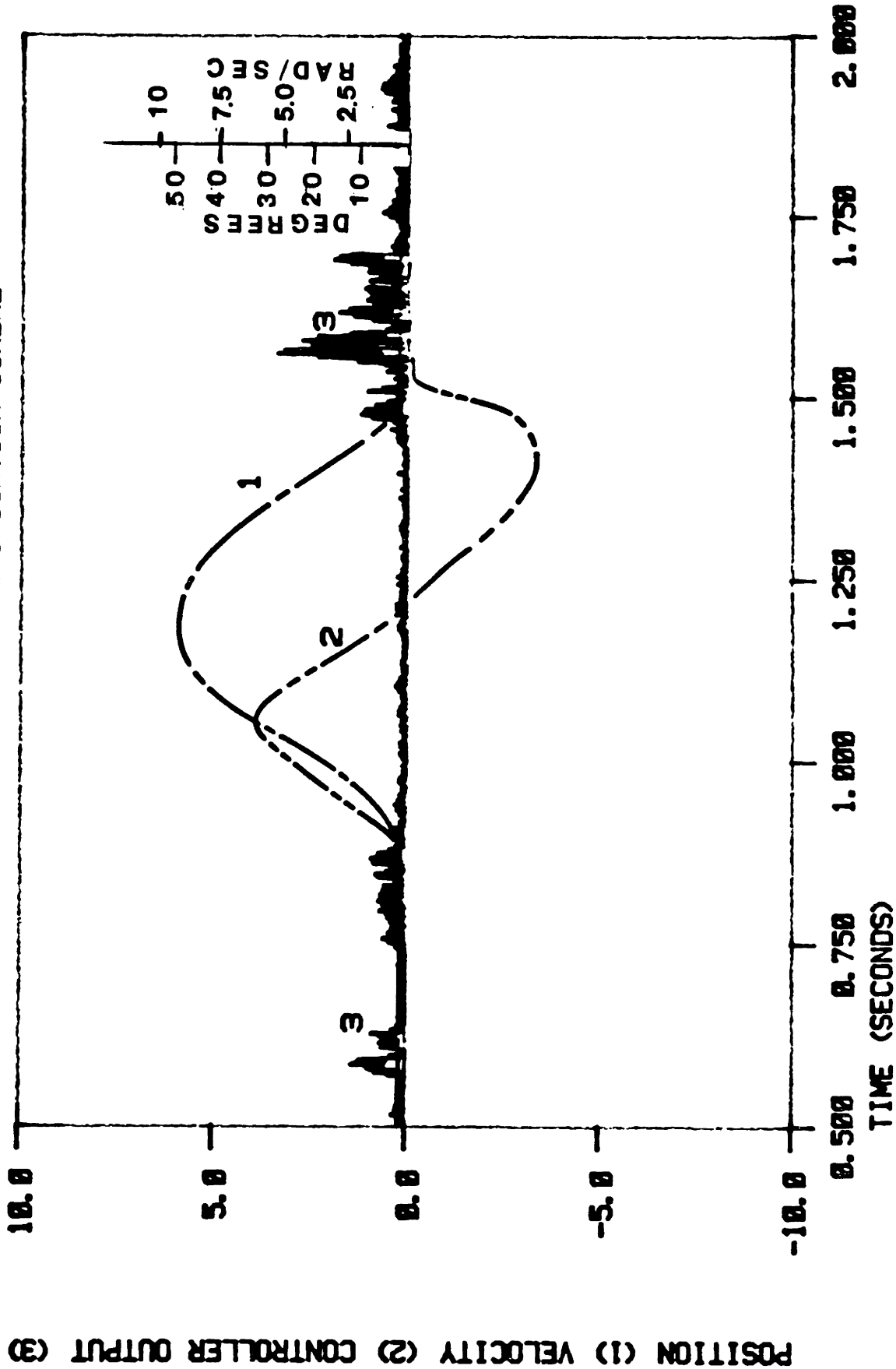
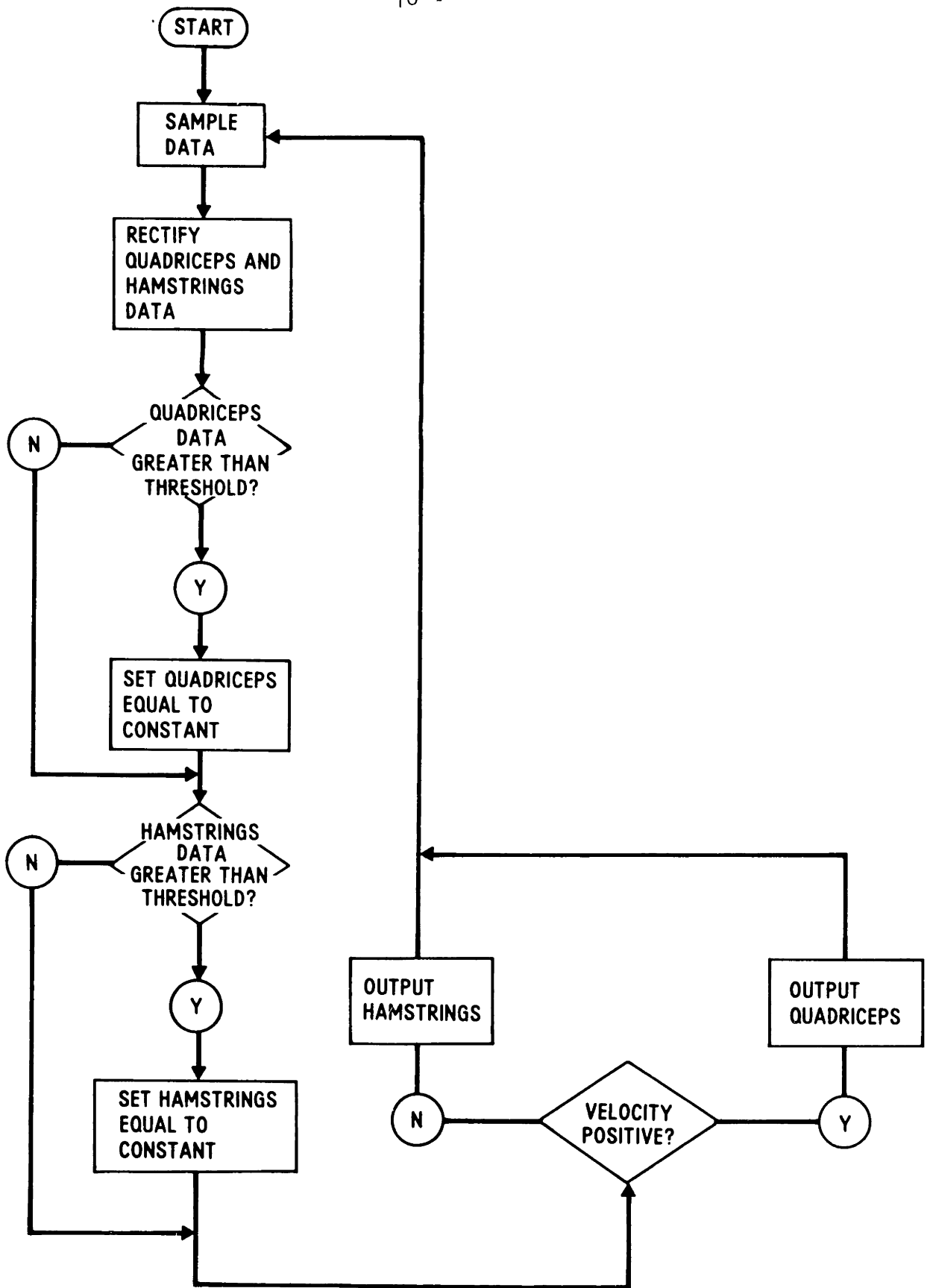


FIGURE 33. SUBJECT 4 SIMPLE RECTIFICATION SCHEME



POSITION (1) VELOCITY (2) CONTROLLER OUTPUT (3)



FLOW DIAGRAM FOR MODULATED PULSE WIDTH

FIGURE 34

frequency of 70 Hz with a digital filter algorithm similar to those discussed previously. Then, each channel is tested against preset thresholds which are found with Program THFIND included in Appendix 2. If a particular channel is greater than its threshold, an output is generated. Both channels are then modulated by the velocity signal and the resulting output is amplified by an empirically determined gain factor. The results of off-line implementation of this scheme are shown in the next four figures. Figure 35 shows the results for subject 1, Figure 36 for subject 2, Figure 37 for subject 3 and Figure 38 for subject 4.

4.5 Velocity Modulation of the Threshold Count; a More Elaborate Approach

This controller counts the number of times the ME activity exceeds the threshold selected for the given ME channel by Program THFIND. The count is accumulated for a time period of 4 milliseconds and then reset. Figure 39 shows the flow chart for this controller. The figure shows that the controller output consists of the amplified, velocity modulated threshold count of the input ME data. This controller was expected to take advantage of a large amount of the information contained in the ME signal while rejecting spurious electrode-skin artifact. Figure 40 shows the off-line implementation results for subject 1. The three following figures show the respective results for the

remaining subjects.

FIGURE 35. SUBJECT 1 MODULATED PULSE WIDTH CONTROLLER

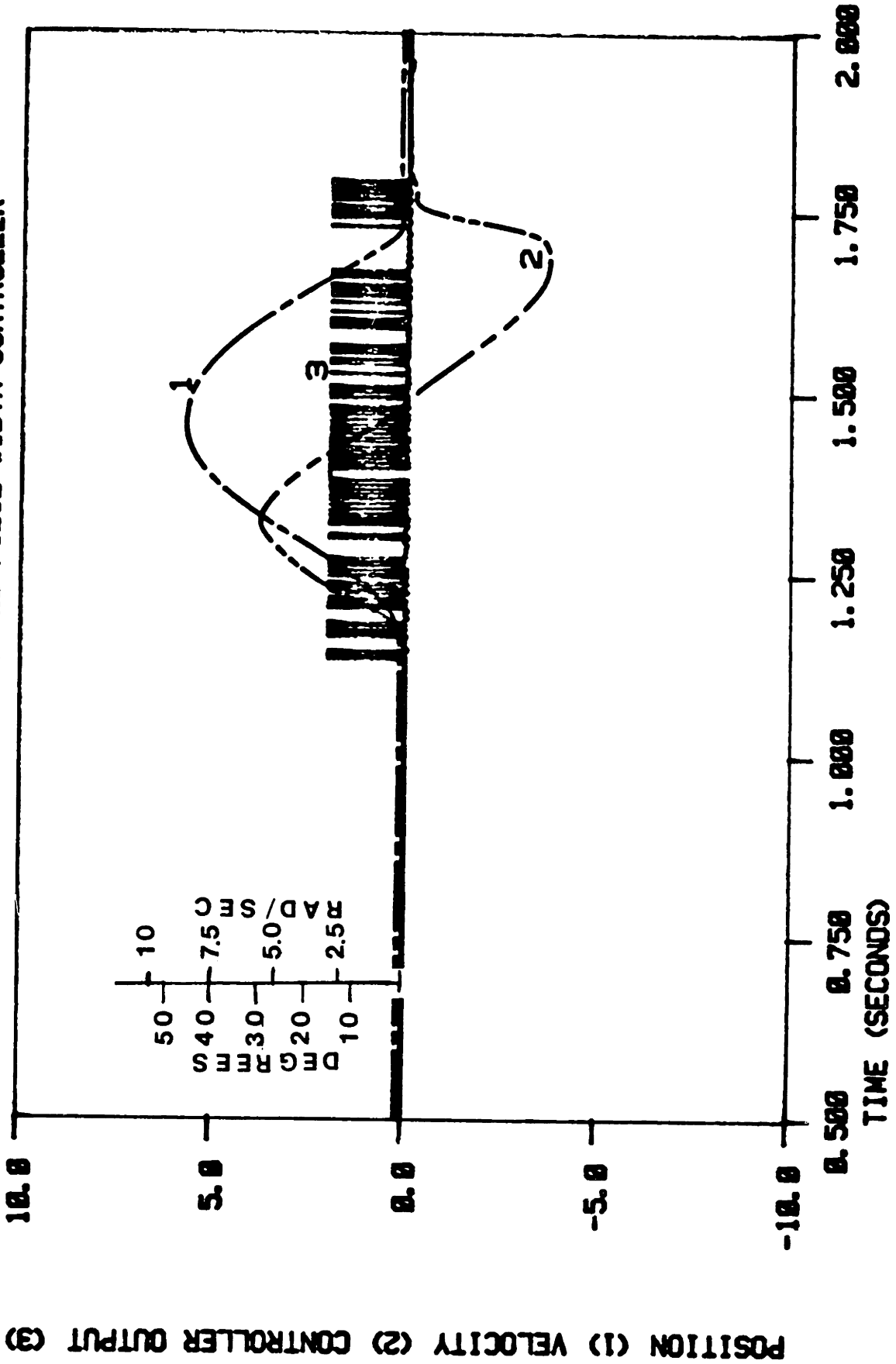
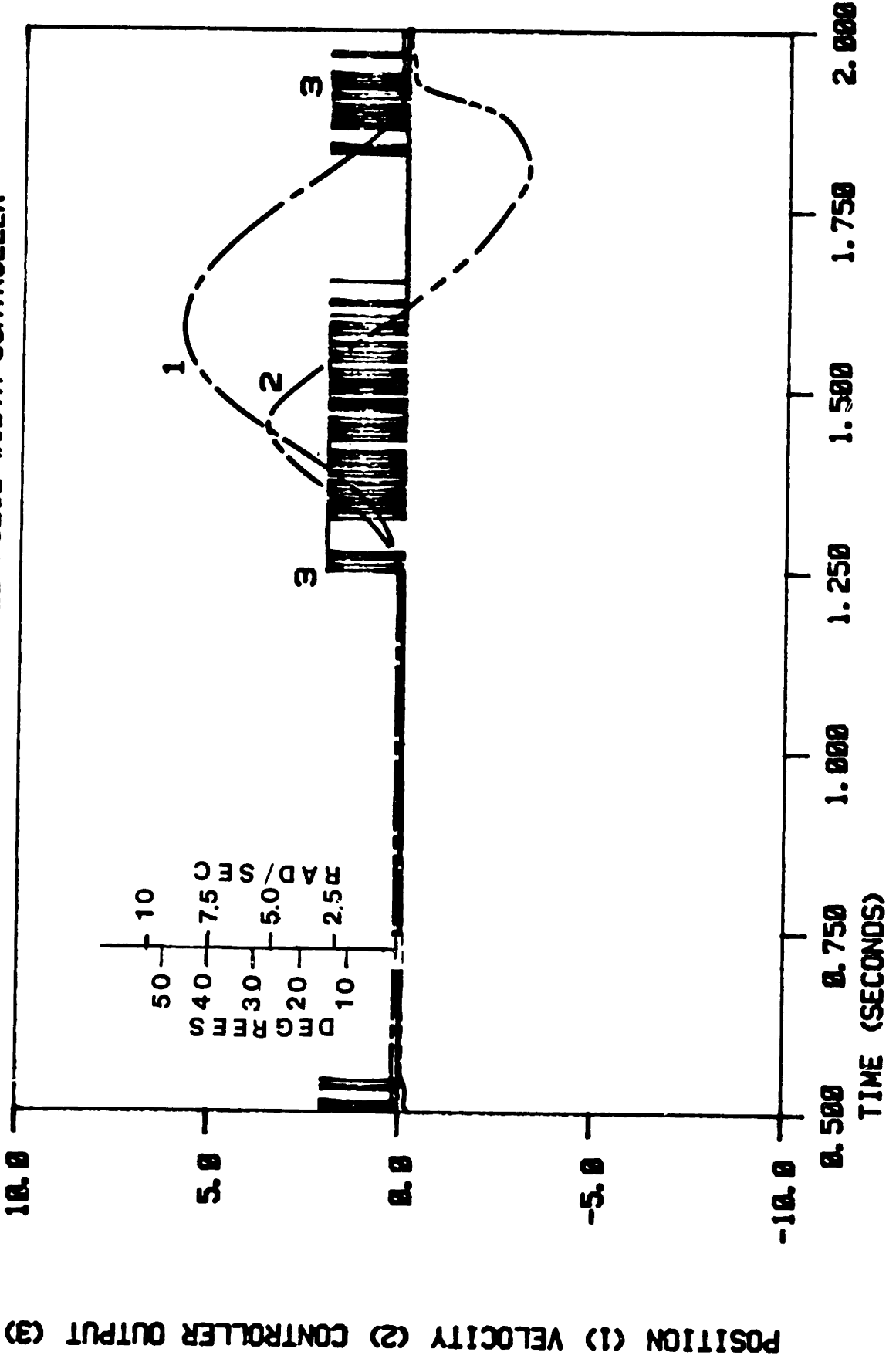


FIGURE 36. SUBJECT 2 MODULATED PULSE WIDTH CONTROLLER



POSITION (1) VELOCITY (2) CONTROLLER OUTPUT (3)

FIGURE 37. SUBJECT 3 MODULATED PULSE WIDTH CONTROLLER

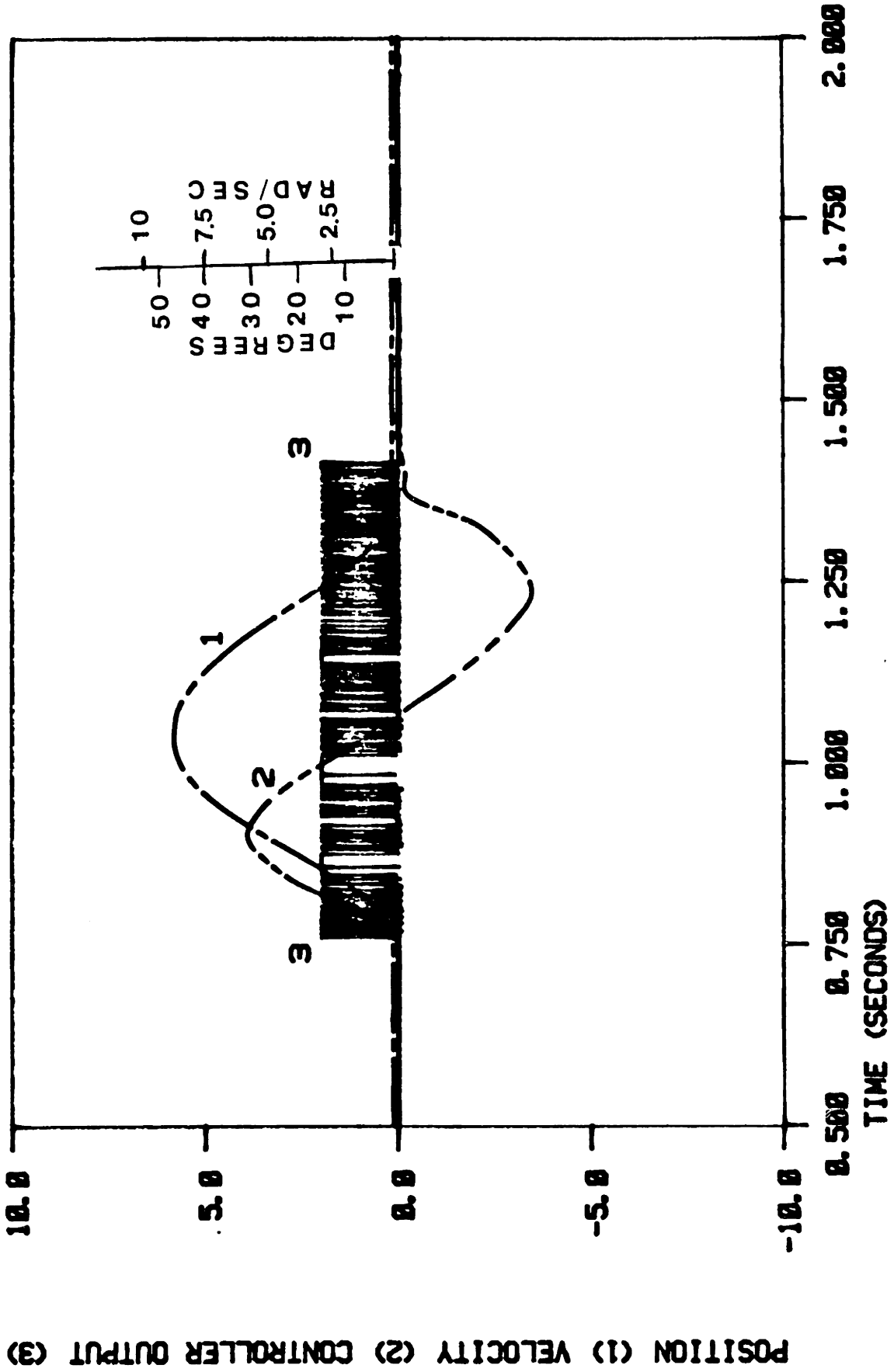
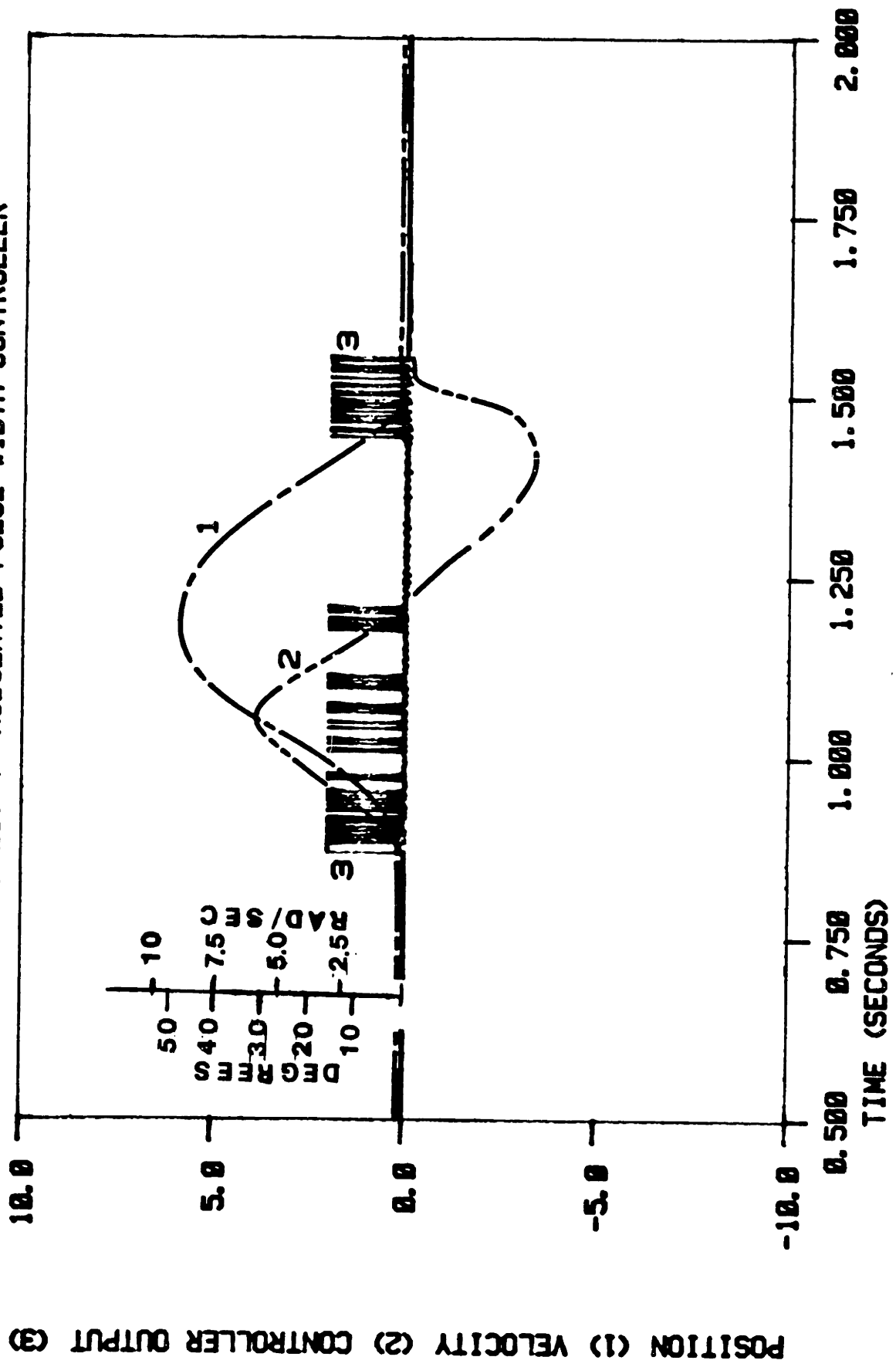
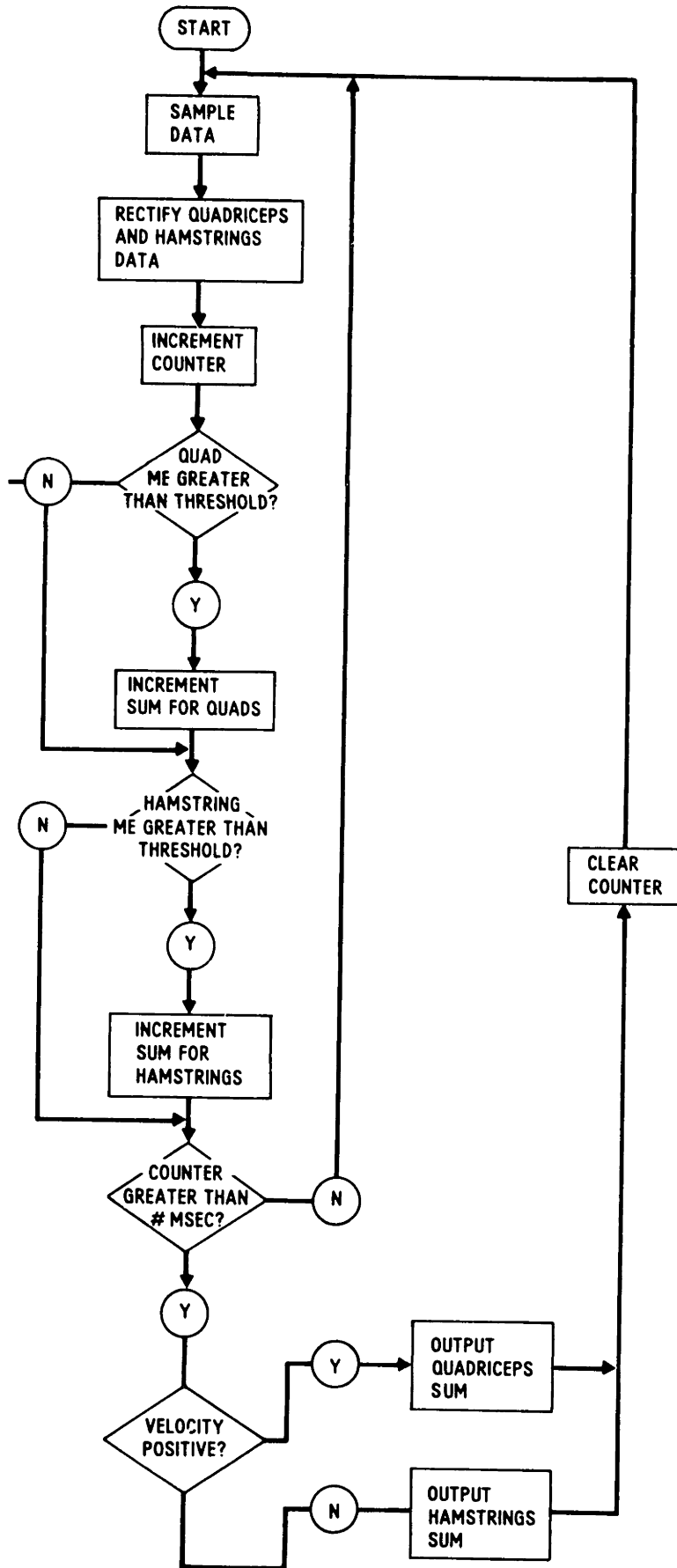


FIGURE 38. SUBJECT 4 MODULATED PULSE WIDTH CONTROLLER



POSITION (1) VELOCITY (2) CONTROLLER OUTPUT (3)



FLOW DIAGRAM FOR THRESHOLD COUNTING

FIGURE 39

FIGURE 40. SUBJECT 1. THRESHOLD COUNTING CONTROLLER

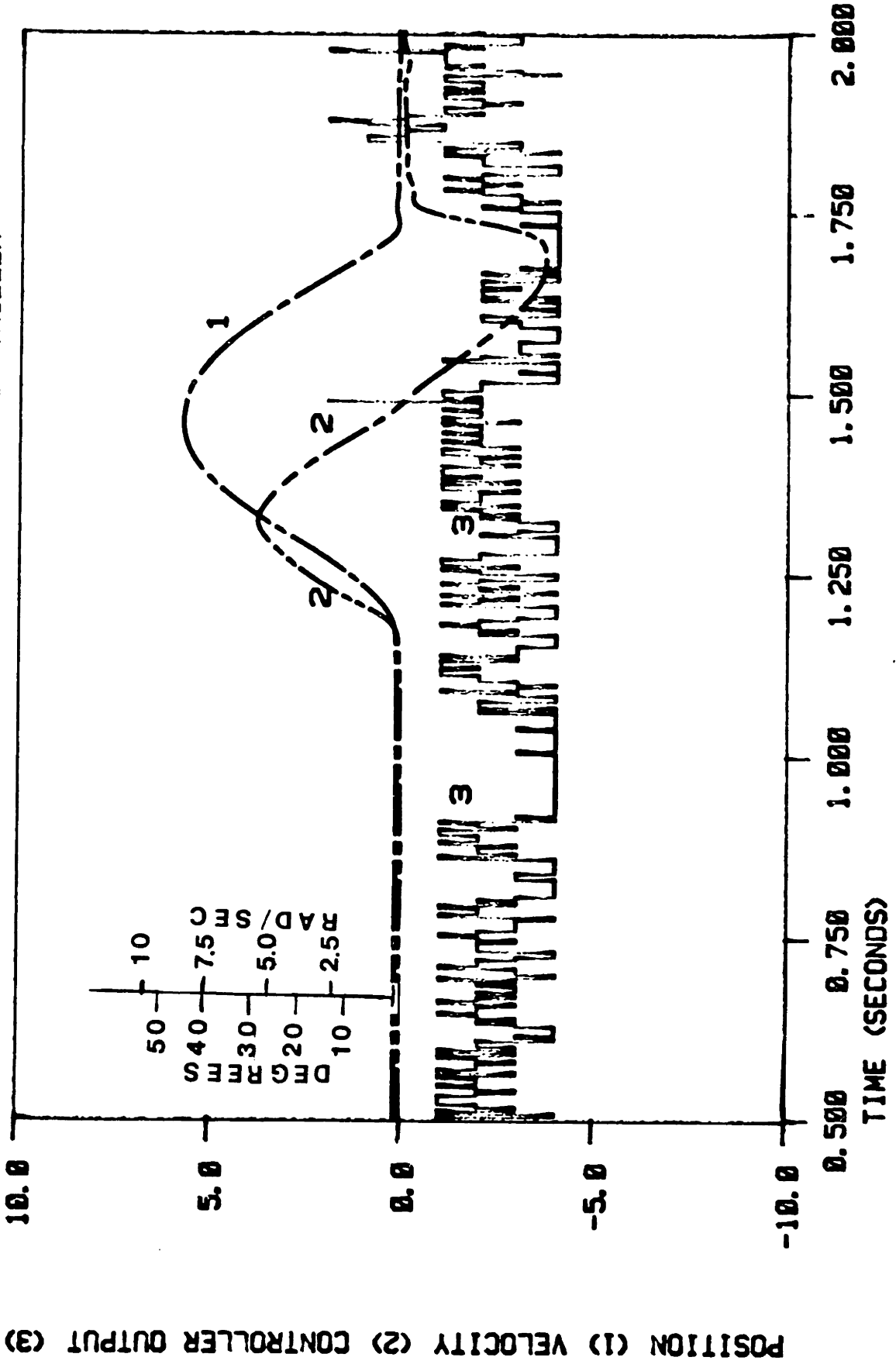
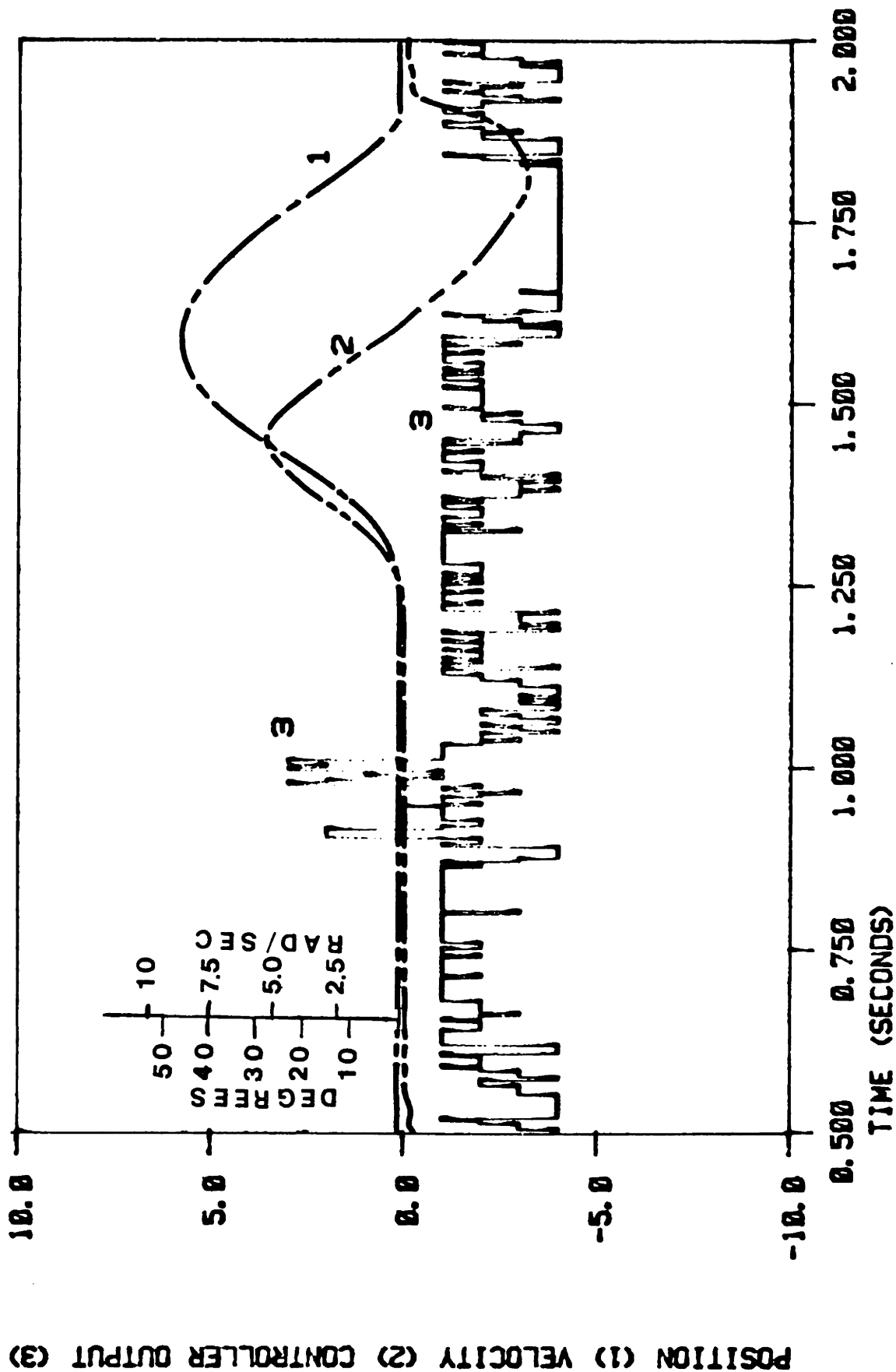


FIGURE 41. SUBJECT 2 THRESHOLD COUNTING CONTROLLER



POSITION (1) VELOCITY (2) CONTROLLER OUTPUT (3)

FIGURE 42. SUBJECT 3 THRESHOLD COUNTING CONTROLLER

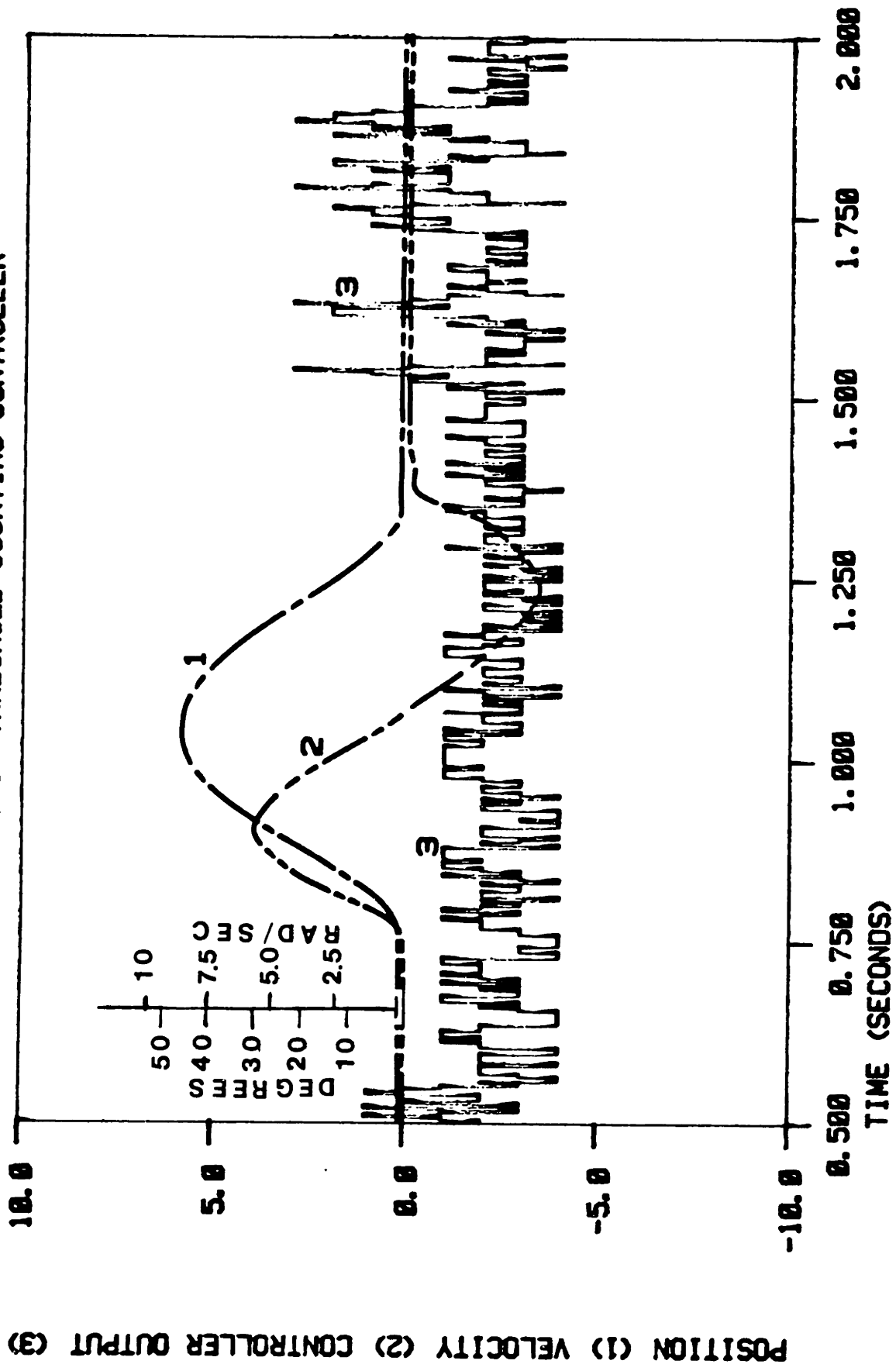
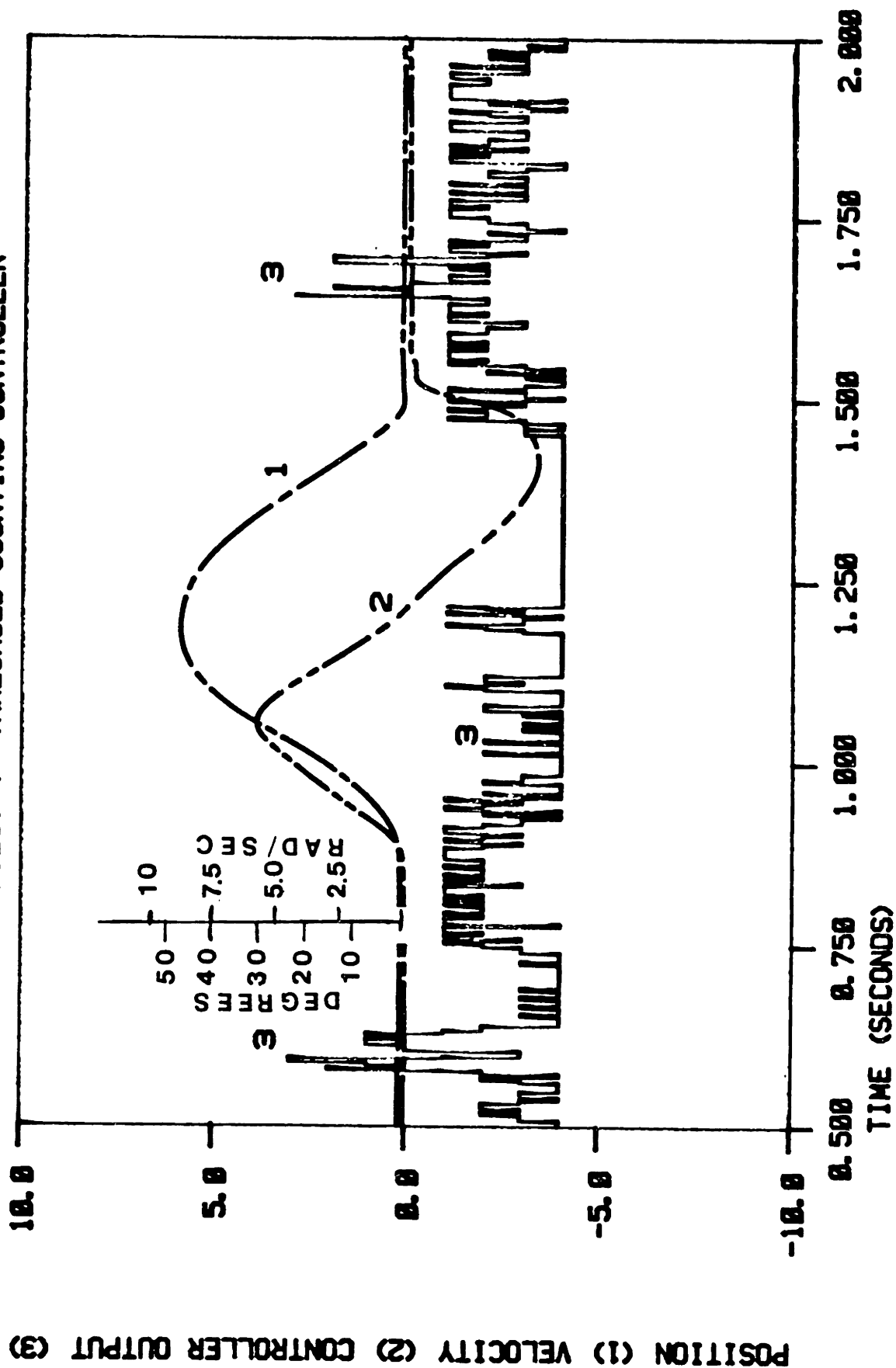


FIGURE 43. SUBJECT 4 THRESHOLD COUNTING CONTROLLER



CHAPTER 5 INITIAL SUBJECT TESTING

5.1 INTRODUCTION

During this phase of the project, the controllers discussed in Chapter 4 were tried in walking trials with the subjects used in previous work. Practical and people problems as well as time constraints allowed testing of all three controllers on subject 1 only. The controllers were not tested on subject 4 and two of them were tested with the remaining subjects. It must be stressed that the controllers were not developed to the authors satisfaction. However, the preliminary results are encouraging. The following sections include procedural details, observations and results.

5.2 Procedure

The procedure followed during this part of the investigation was the same as that for the friction simulations for logistical details such as electrode mounting. During a particular session, friction and hydraulic simulations were tried along with the ME controllers. The simulations of conventional prosthesis were run for comparison purposes. Eight thousand samples were taken and stored of position, velocity, quadriceps and hamstrings data during each walking trial. One walking trial was accomplished for each control scheme. The

subjects were accustomed to the given controller before any data was sampled.

5.3 Observations

The subjects were asked to comment about the controllers during the experimental session. All subjects seemed to feel that the hydraulic simulation was better than the friction simulation. This is not surprising since, in this control mode, the simulator most closely emulates the conventional prosthesis of three subjects. However, most of the subjects were very positive about one or more of the ME controllers. The author noticed that gait cosmesis seemed good for the ME controllers except for a tendency for the simulator shank to impact against the hyperextension stops. It was not extremely difficult to establish appropriate gains for the ME controllers.

5.4 Results

Although eight thousand samples were taken for each walking trial, a limited subset will be presented in the following results. This will enable better comparison of the kinematics resulting from each of the controllers. The results are presented in order from subject 1 through subject 4.

5.4.1 Subject 1 Results

Subject 1 was experiencing some soreness during the day of the final session but consented to try the controllers anyway. Figure 44 shows results from a friction simulation at a comfortable level, Figure 45 shows the results from a hydraulic simulation. Notice the shape of the velocity profile in both of these simulations. Figure 46 shows the results from the rectifying controller, Figure 47 the modulated pulse width controller and Figure 48 shows the threshold counting controller. The myoelectric data has been processed with the conventional method mentioned previously. Compare the kinematics of these controllers to the conventional controllers. It can immediately be seen that although the velocity trace is smoother, heel rise and hyperextension impact are greater for the myoelectric controller. An important point to notice is the similarity of the kinematics resulting from all of the ME controllers.

5.4.2 Subject 2 Results

Figure 49 shows the results from a friction simulation at a comfortable level for subject 2. The characteristic velocity profile shape can be seen at a glance. Also to be noted is that this trace is smoother than that for subject 1. Figure 50 shows the results from a

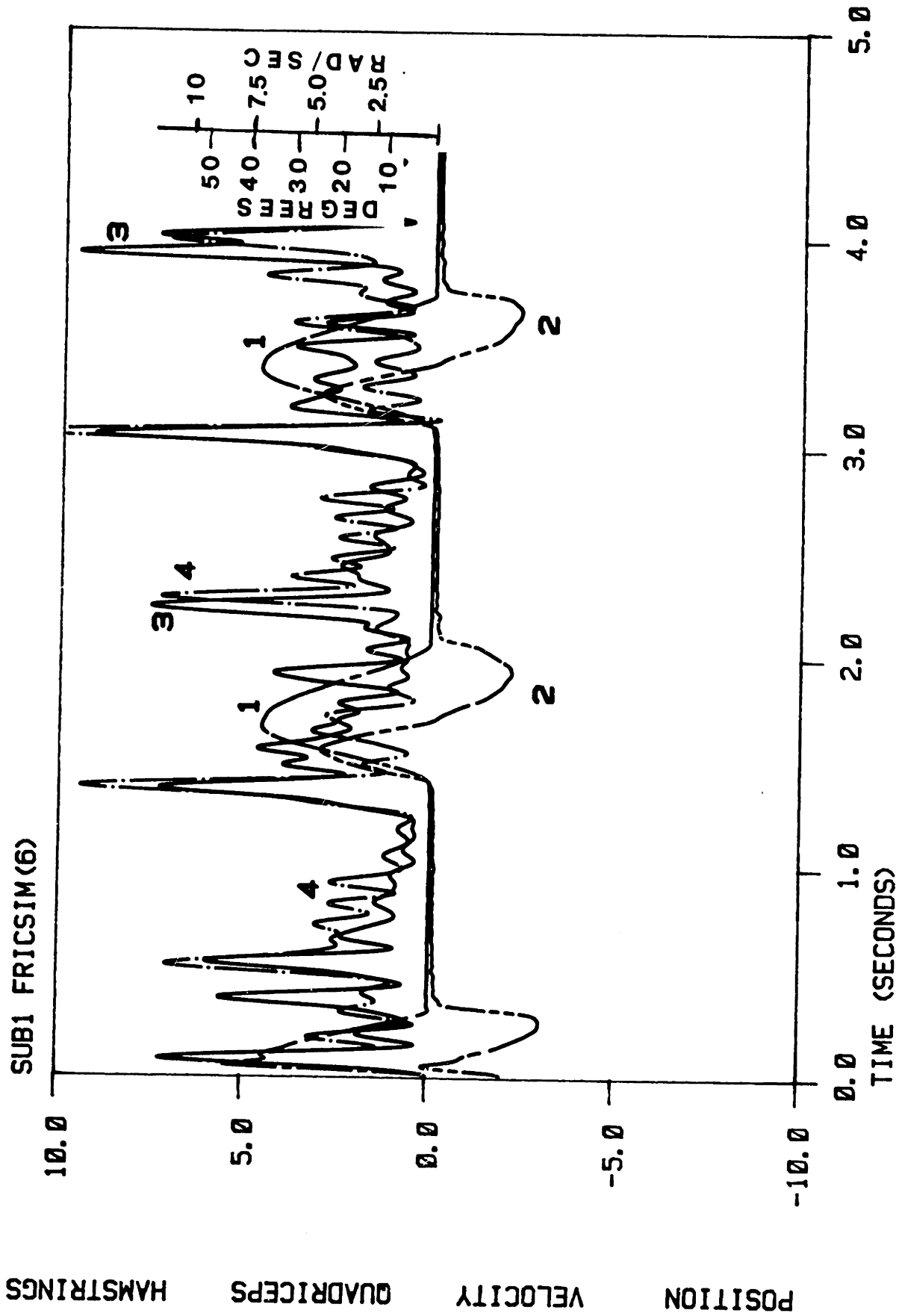


Figure 44. Subject 1: Comfortable Friction Simulation

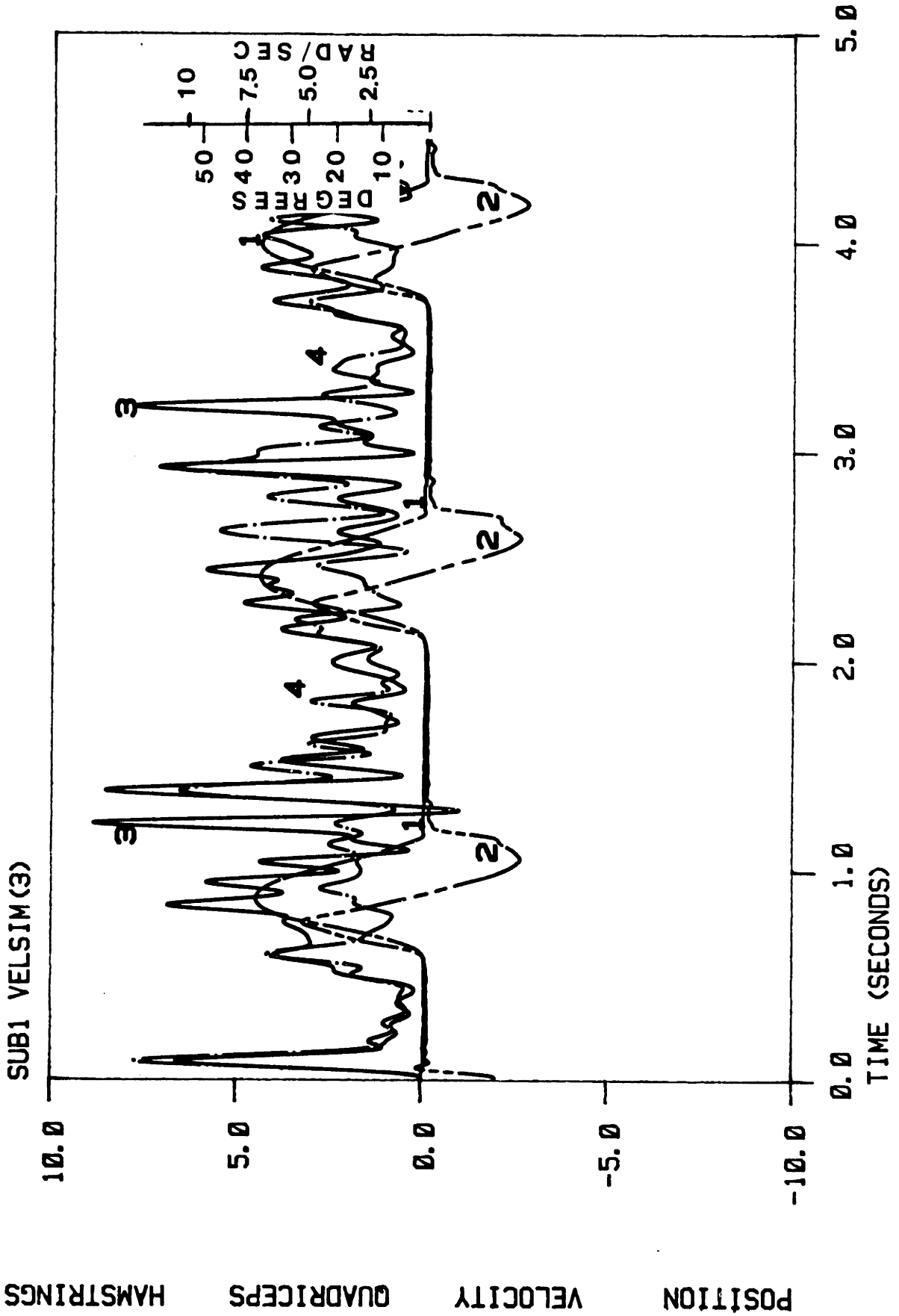


Figure 45: Subject 1: Comfortable Hydraulic Simulation

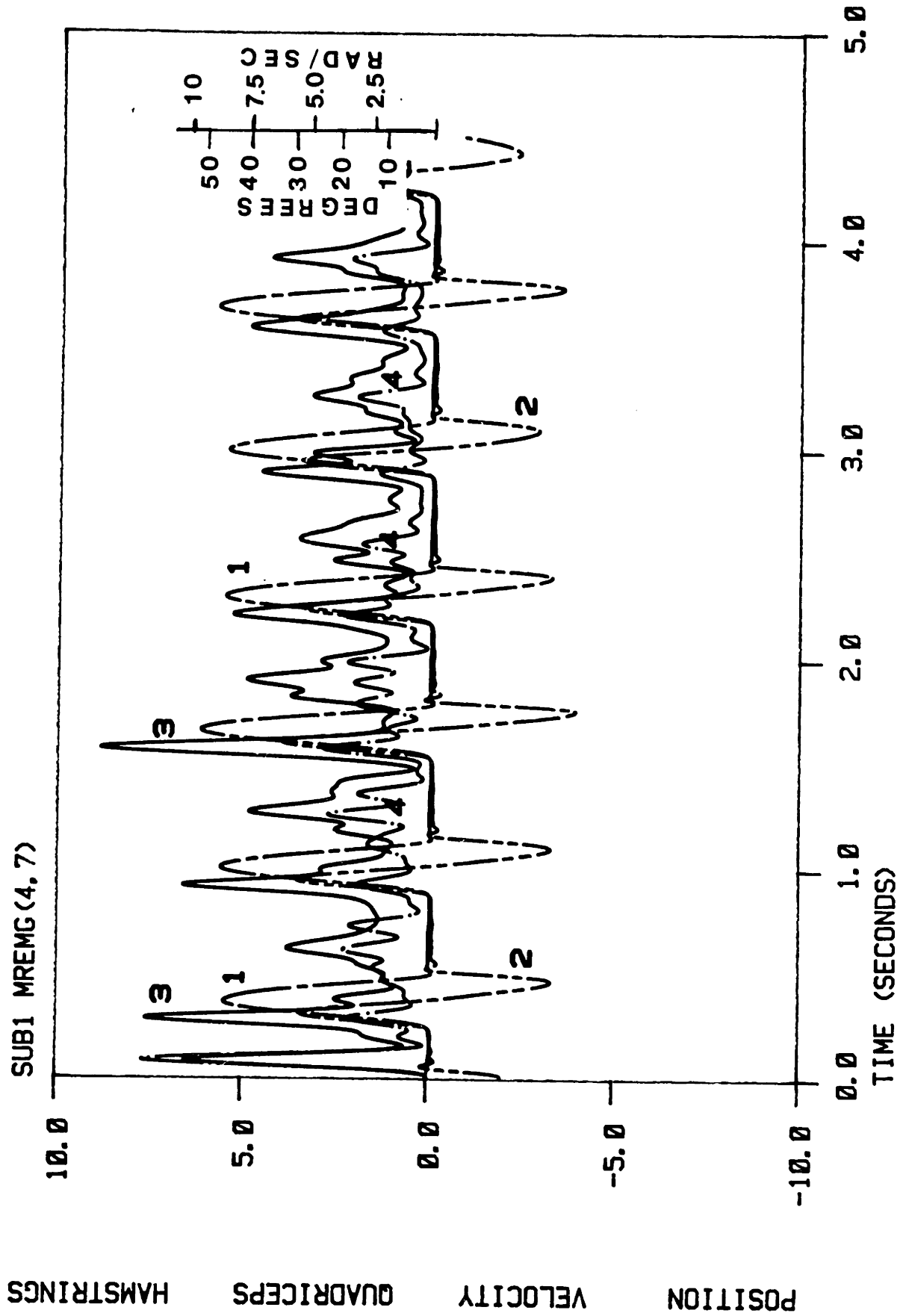


Figure 46. Subject 1: Simple Rectifying Controller

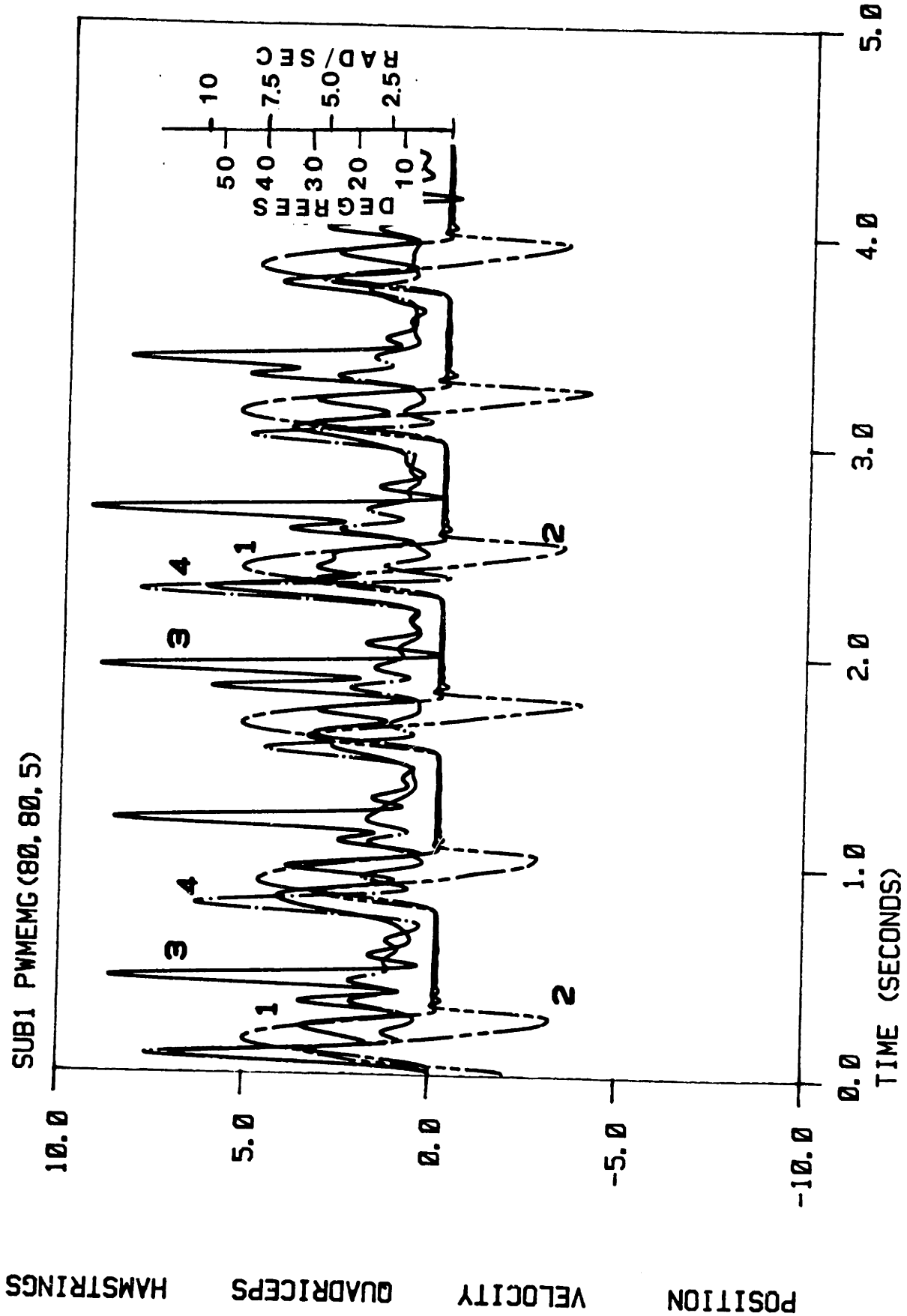


Figure 47. Subject 1: Modulated Pulse Width Controller

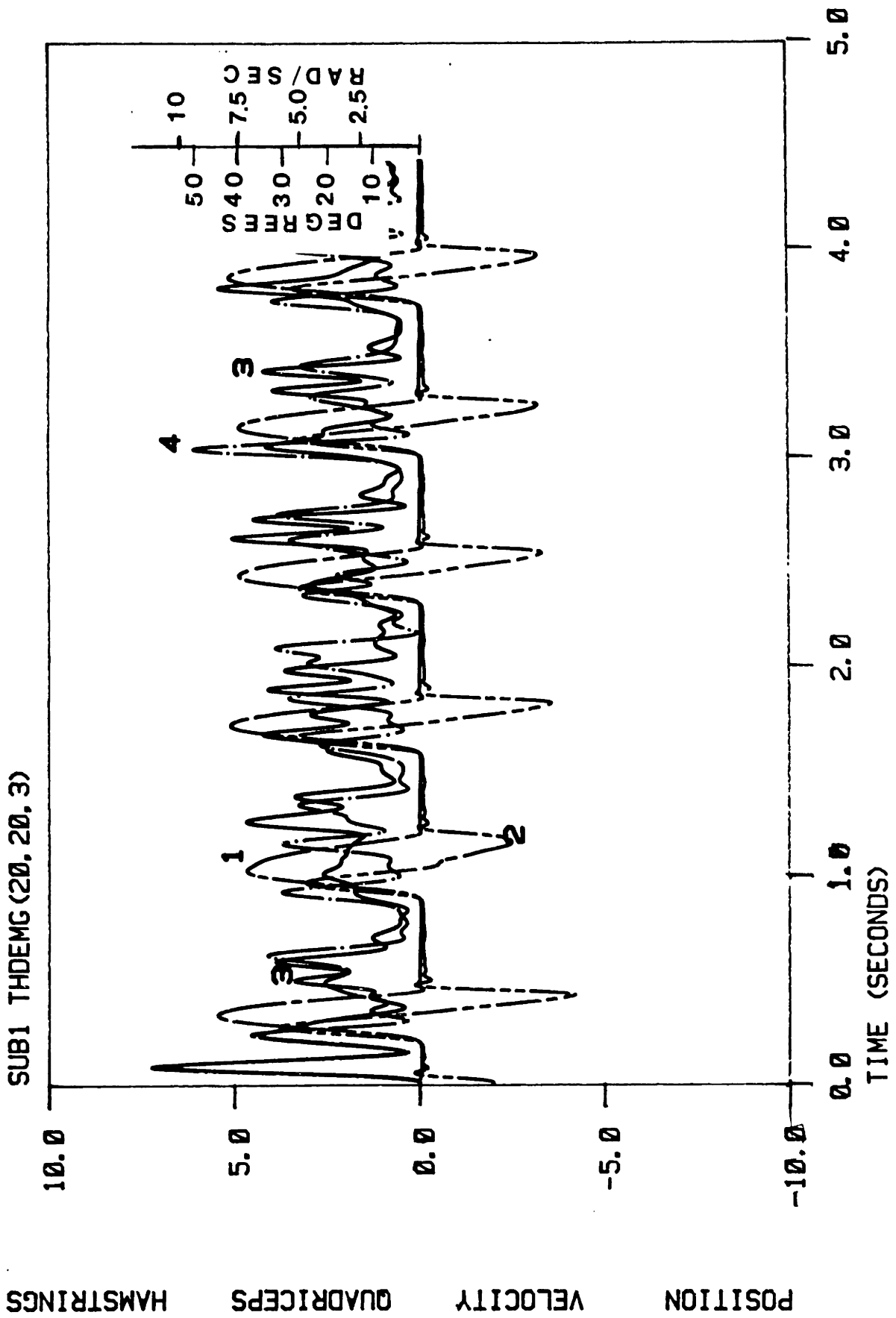
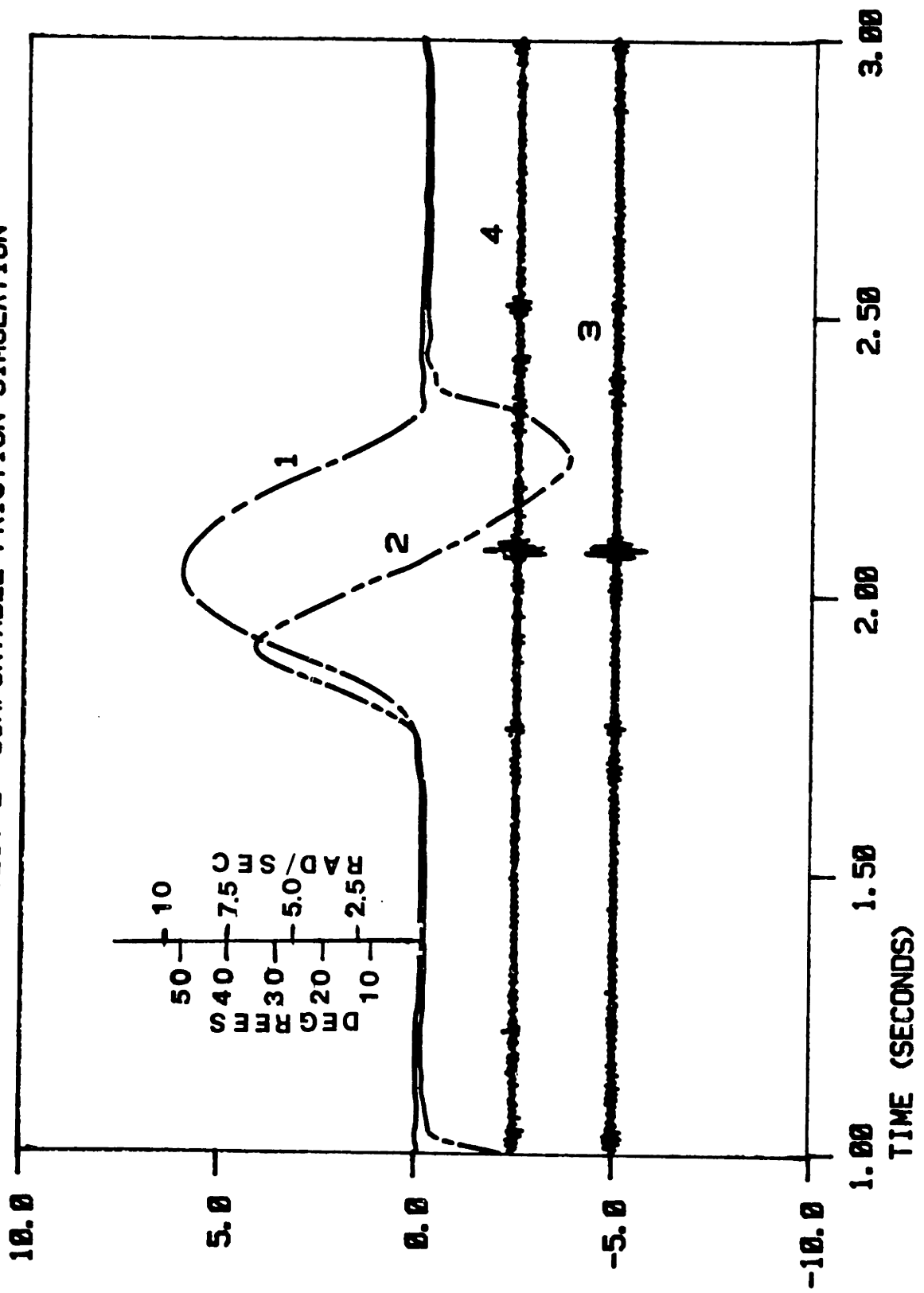


Figure 48. Subject 1: Threshold Counting Controller

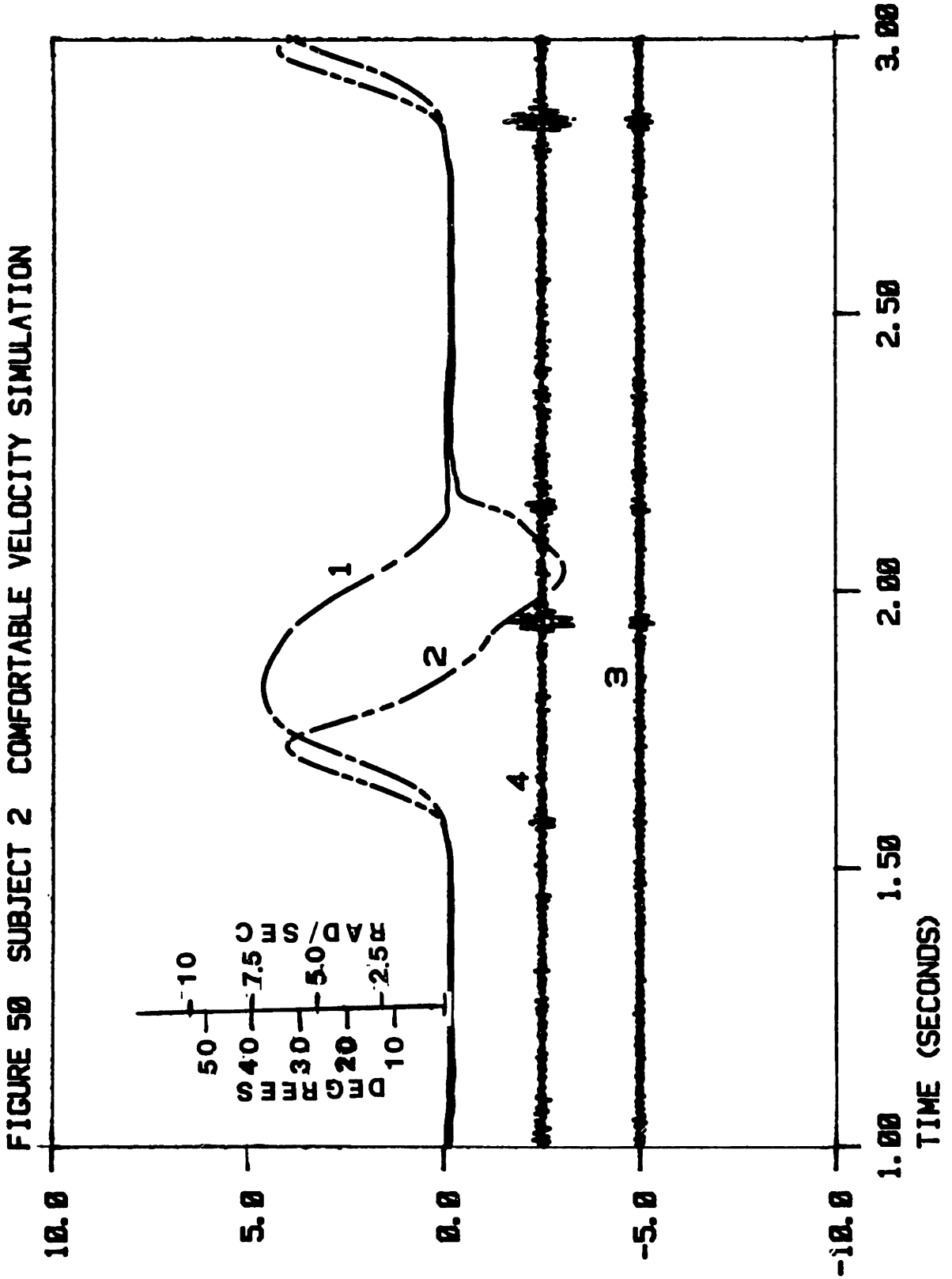
POSITION (1) VELOCITY (2) QUADRICEPS (3) HAMSTRINGS (4)

15 19 41 01-JAN-62

FIGURE 49. SUBJECT 2 COMFORTABLE FRICTION SIMULATION



POSITION (1) VELOCITY (2) QUADRICEPS (3) HAMSTRINGS (4)



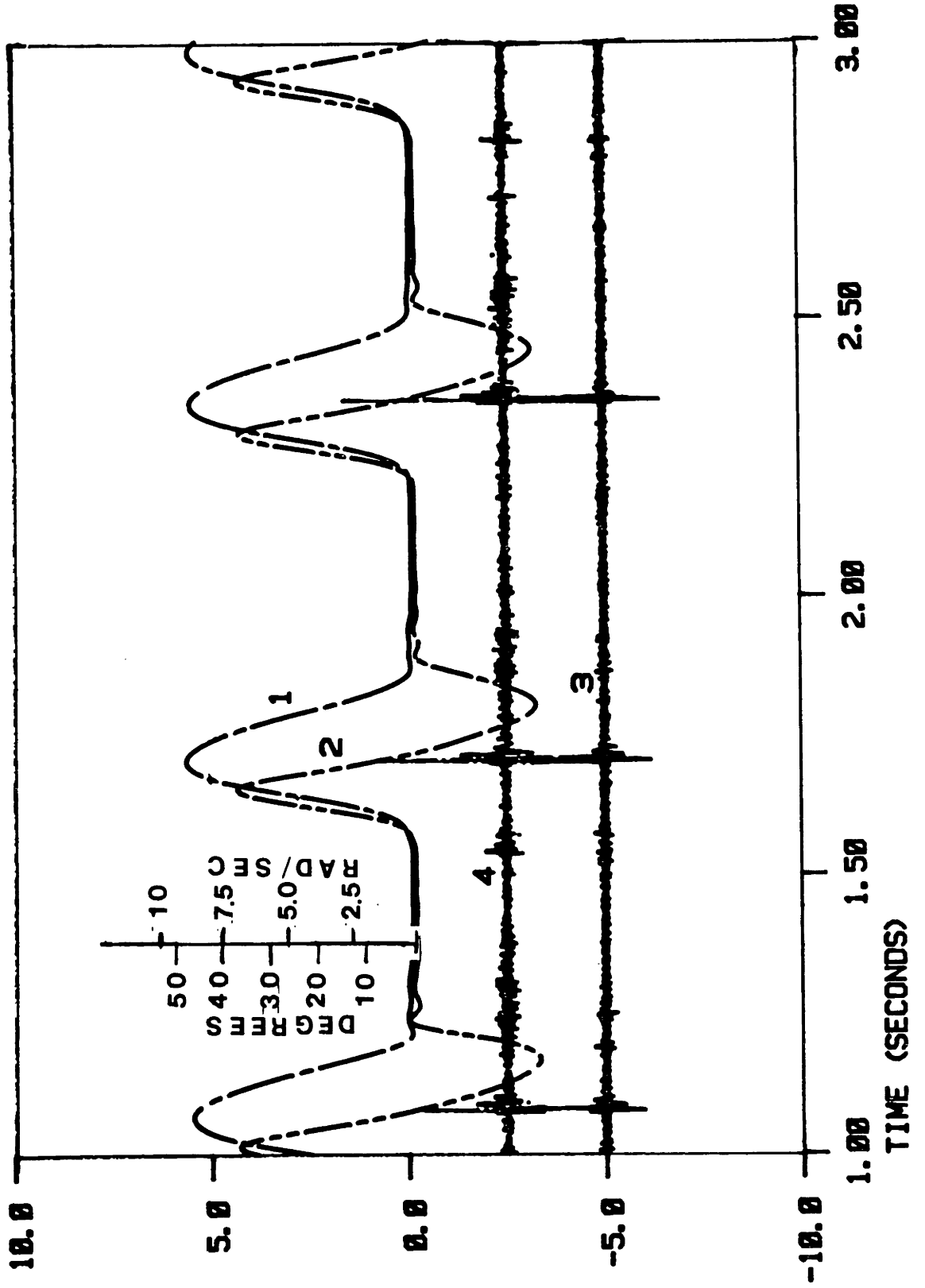
hydraulic prosthesis simulation. The shape of the velocity profile seems consistent with the shape of that for subject 1. Note also that heel rise is inhibited with this controller. Figure 51 shows results from the modulated pulse width controller. Note that heel rise is not as great as the friction controller implying better gate cosmesis. However, hyperextension impact is still a problem for this subject. Figure 52 shows results from the threshold counting controller. Heel rise for this controller was approximately the same as for the modulated pulse width controller. Similarly, the two ME controllers behaved much the same at full extension. The myoelectric data for these figures and those following has been high pass filtered at a break frequency of 70 Hz.

5.4.3 Subject 3 Results

As with subject 2, this subject only tested two of the ME controllers. Figure 53 shows the results from the friction simulation. Figure 54 shows results from the hydraulic simulation. Similar comments about the velocity profile apply for this subject. Figure 55 shows data taken during the trial of the modulated pulse width controller. Heel rise for this controller was approximately the same as for the conventional controllers depicted in the two preceding figures. Again, note the abrupt hyperextension impact at the end of swing phase. Figure 56 shows results

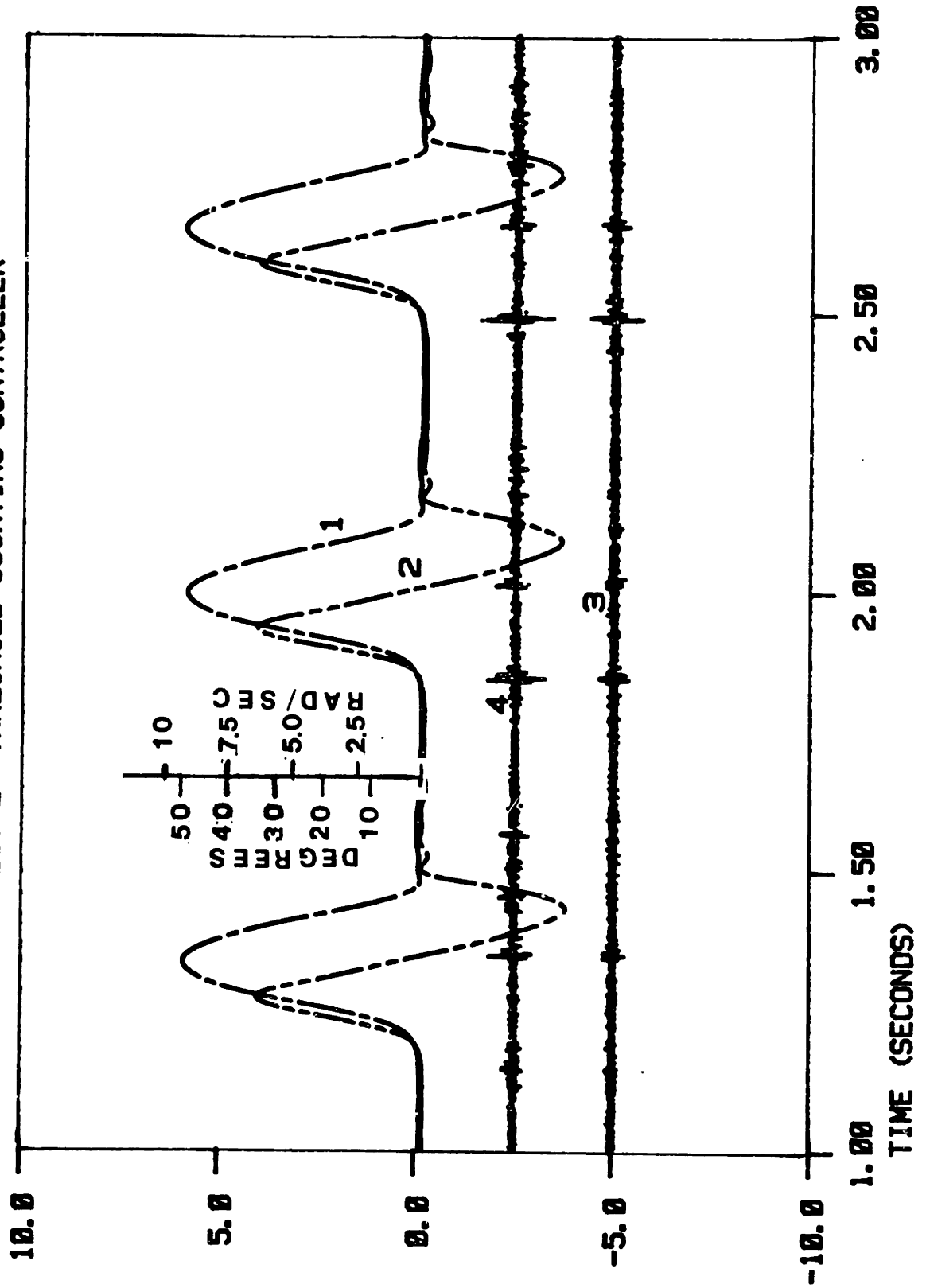
from the threshold counting controller. The performance of this controller is similar to the modulated pulse width controller.

FIGURE 51. SUBJECT 2 MODULATED PULSE WIDTH CONTROLLER



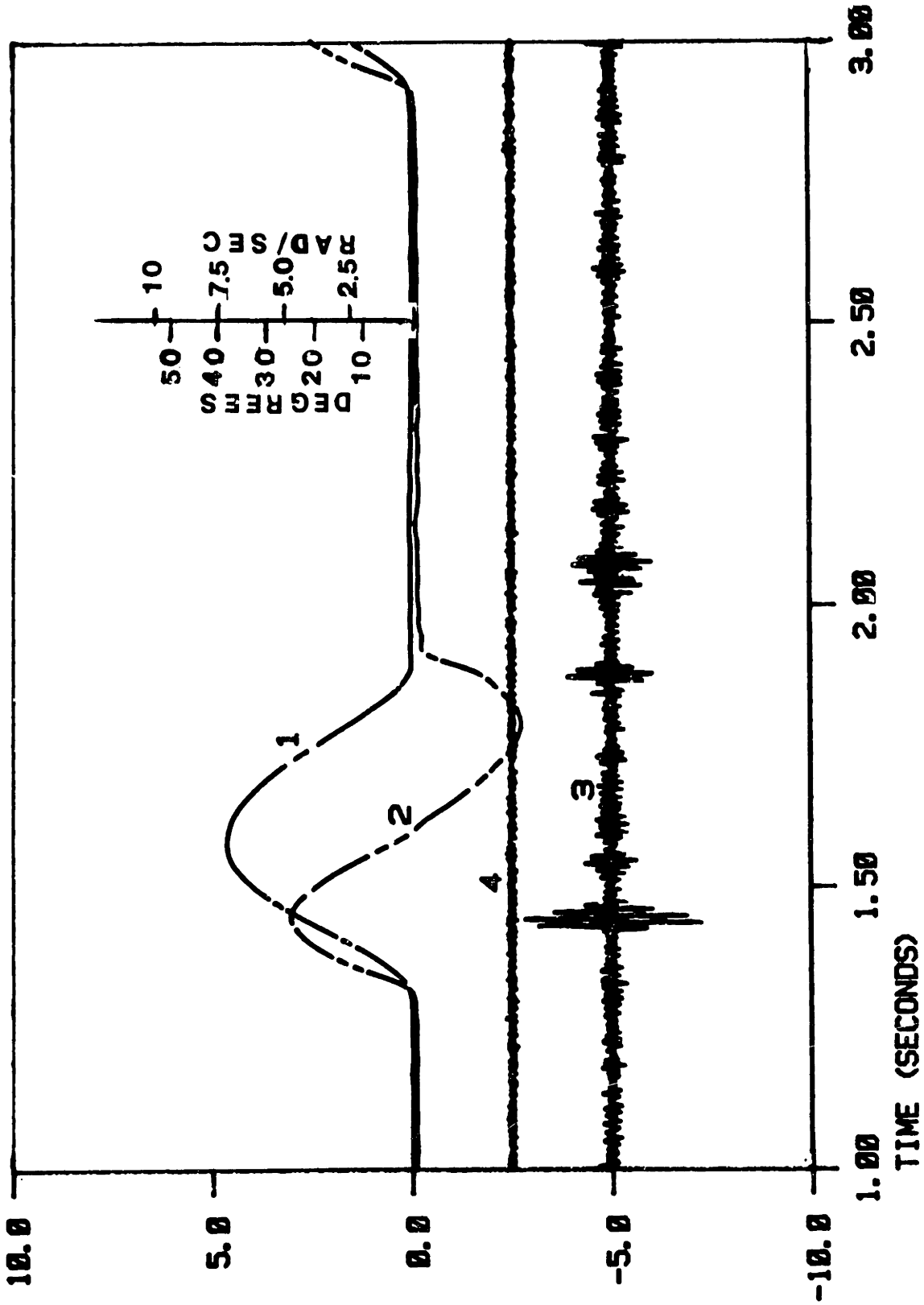
POSITION (1) VELOCITY (2) QUADRICEPS (3) HAMSTRINGS (4)

FIGURE 52. SUBJECT 2 THRESHOLD COUNTING CONTROLLER



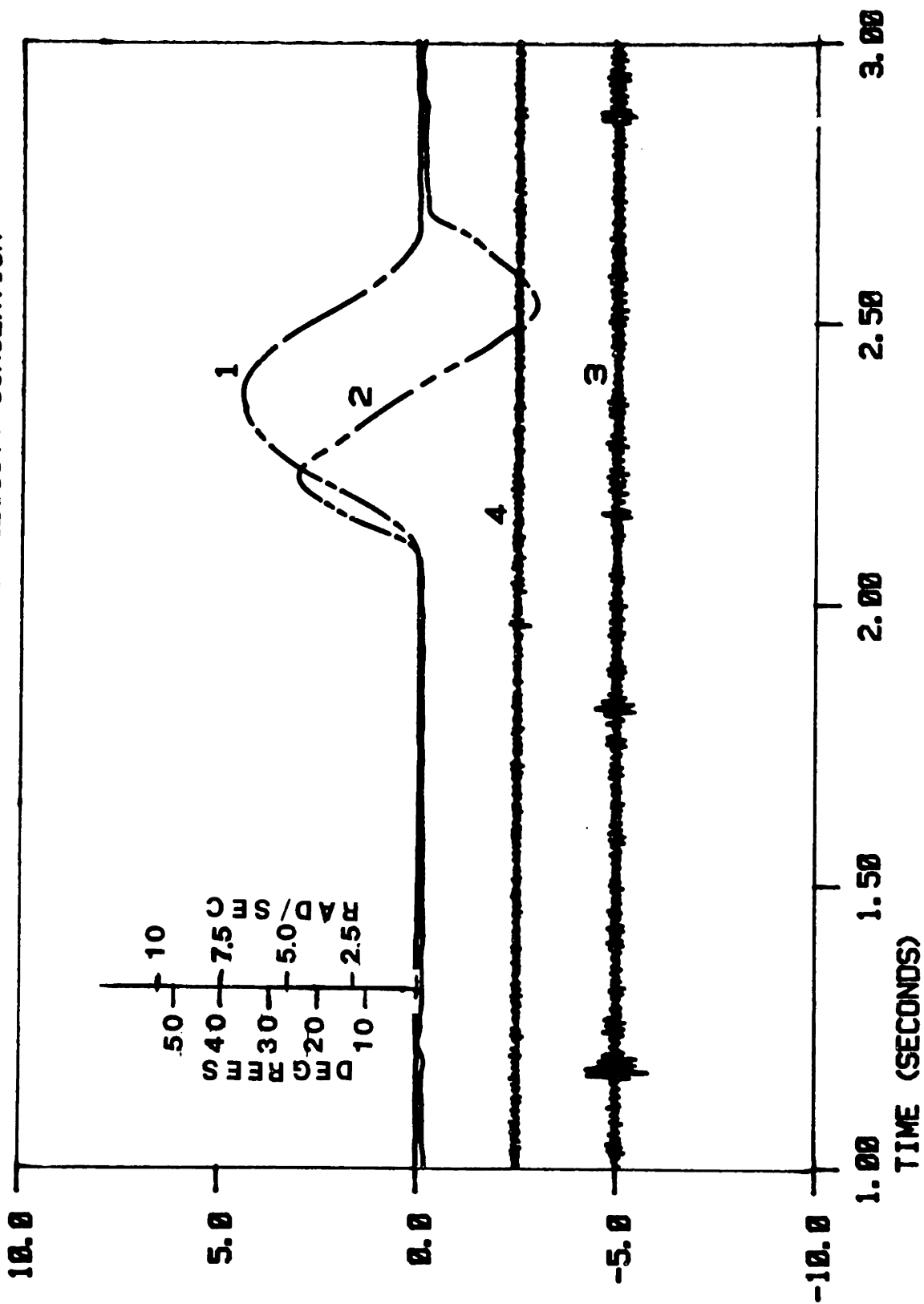
POSITION (1) VELOCITY (2) QUADRICEPS (3) HAMSTRINGS (4)

FIGURE 53. SUBJECT 3 COMFORTABLE FRICTION SIMULATION



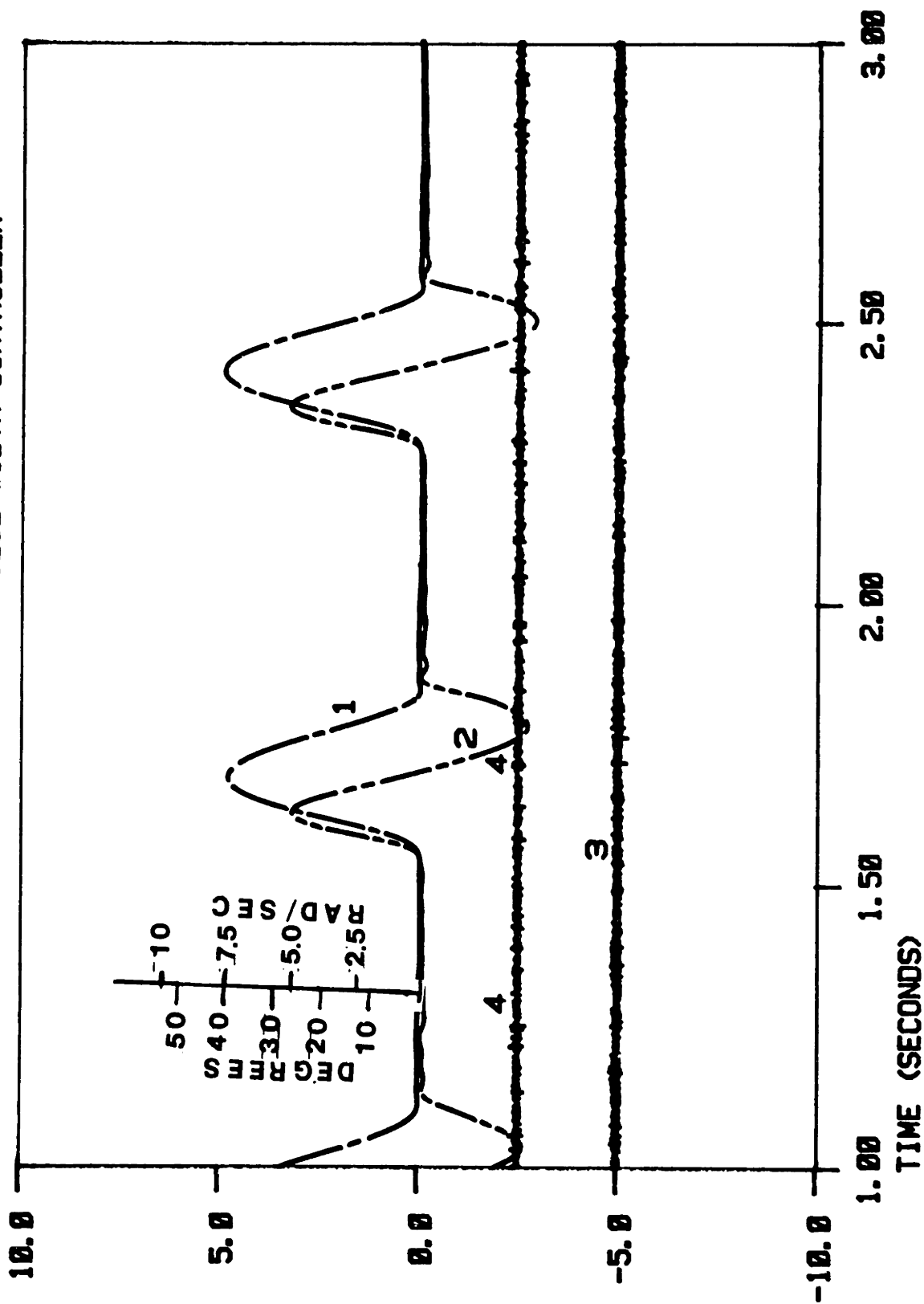
POSITION (1) VELOCITY (2) QUADRICEPS (3) HAMSTRINGS (4)

FIGURE 54. SUBJECT 3 COMFORTABLE VELOCITY SIMULATION



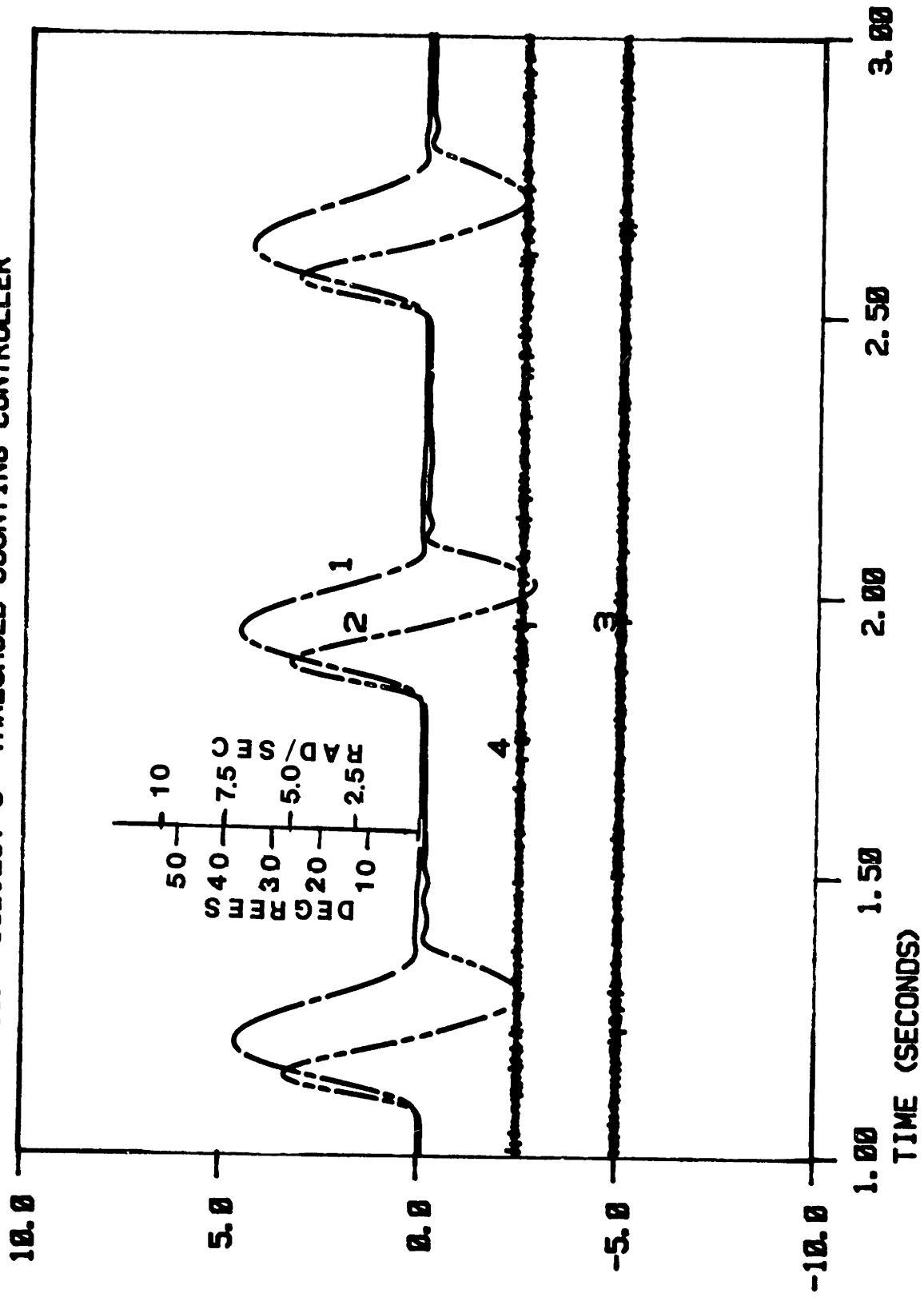
POSITION (1) VELOCITY (2) QUADRICEPS (3) HAMSTRINGS (4)

FIGURE 55. SUBJECT 3 MODULATED PULSE WIDTH CONTROLLER



POSITION (1) VELOCITY (2) QUADRICEPS (3) HAMSTRINGS (4)

FIGURE 56. SUBJECT 3 THRESHOLD COUNTING CONTROLLER



POSITION (1) VELOCITY (2) QUADRICEPS (3) HAMSTRINGS (4)

CHAPTER 6 FINAL REMARKS

6.1 INTRODUCTION

This chapter examines what happened during the course of the investigation and tries to draw reasonable conclusions. Furthermore, recommendations for further research are included. In short, the author feels that the findings of this work are encouraging enough to warrant further investigation.

6.2 Discussion and Conclusions

Some readers may object to the extreme break frequencies of the digital filters used in the ME control schemes. The fact that a lot of information was lost in this process is granted. However, due to the nature of the control task, a simple on-off indication of muscle activity may be quite sufficient input to the control logic. This is verified by the relative success of the modulated pulse width controller as compared to the other ME control schemes which used more of the information contained in the signal.

The fact that all of the ME controllers produced similar results indicates that further refinement of the controllers is necessary before selection of the optimum can be accomplished. Also, better performance criteria need to be established. Comments solicited from the subjects are

not extremely useful due to the lack of good afferent information flow. At best, these comments can provide gross indications of the success of a particular controller. Subjective clinical observations are probably better, when made by a experienced physician but such observations do not lend themselves easily to quantification. Due to the lack of data correlating normal gait patterns to basic physical quantities such as height, weight, sex, and/or segment length; kinematic data must be used with caution. In essence, for good gait cosmesis, this data should yield smooth curves without excessive heel rise and a smooth transition into stance phase. A possible indicator is the energy dissipated in the magnetic particle break of the simulator. This approach is valid because the simulator is approximately conservative with exception of this component. However, this indicator must be tempered with some indication of the gait cosmesis since the minimum energy criterion for the simulator is met by the free swinging or zero friction mode of operation.

In an absolute sense, this research was not successful in that it did not verify the author's hypothesis that ME activity of remnant stump muscles could be used to control prosthesis in a manner that produced an acceptable compromise between energy consumption and good gait cosmesis. However, the work was certainly a worthwhile

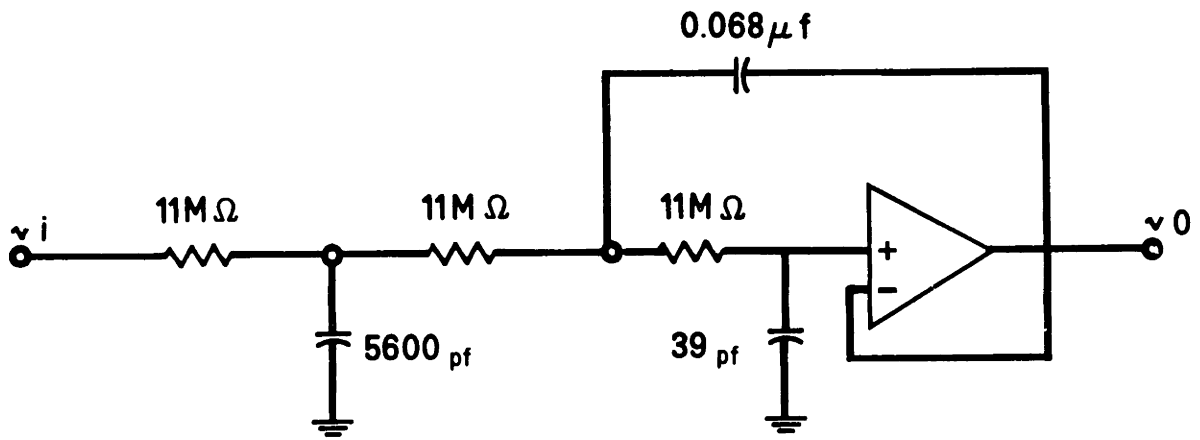
endeavor for the following reasons. This investigation has contributed to the data describing ME activity of a particular subset of the muscles active in above-knee amputee gait. Furthermore, the work has shown that current technology allows acquisition of good ME data from the above-knee stump. The work indicates that ME control can be used effectively to control a passive prosthesis in a manner symbiotic with the amputees intent. Still, further development is necessary. Velocity modulation of the agonist-antagonist pair used in this research proved to be a very good way to control a passive device. Finally, the project was successful as an educational experience.

6.3 Recommendations for Further Research

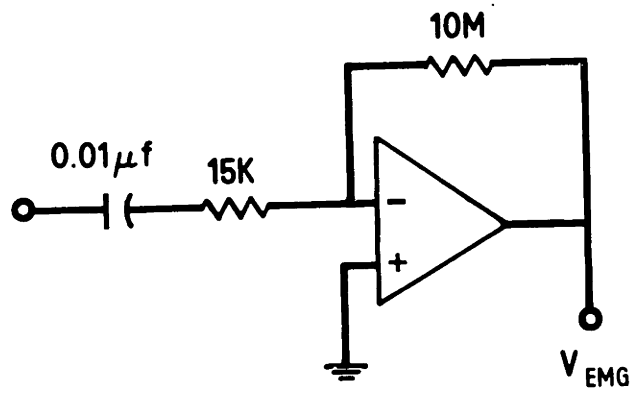
The controllers developed in this research are in need of further refinement. Such refinement could encompass many details. The efficiency of the software embodying the controllers could be improved. Also, perhaps a controller based upon the modulated pulse width controller could be devised which looked at a couple of threshold levels. Further experimentation with the controllers discussed above is necessary to improve their efficacy as measured by gait cosmesis. It would be interesting to plot the energy input into the simulator magnetic particle brake along with the kinematics during experimental sessions to learn more about the trade off involved between energy consumption and gait

cosmesis. Some thought should be given to automating the optimization of the ME controllers for individuals. Ultimately, such algorithms should be compatible with microcomputer limitations. In another area, research of normal gait patterns to find correlations of the type discussed above could help describe "good gait" for an individual. Other work could be done using the data acquired and stored during this project to examine the feasibility of controllers for an active prosthesis.

APPENDIX 1: Selected Circuit Diagrams

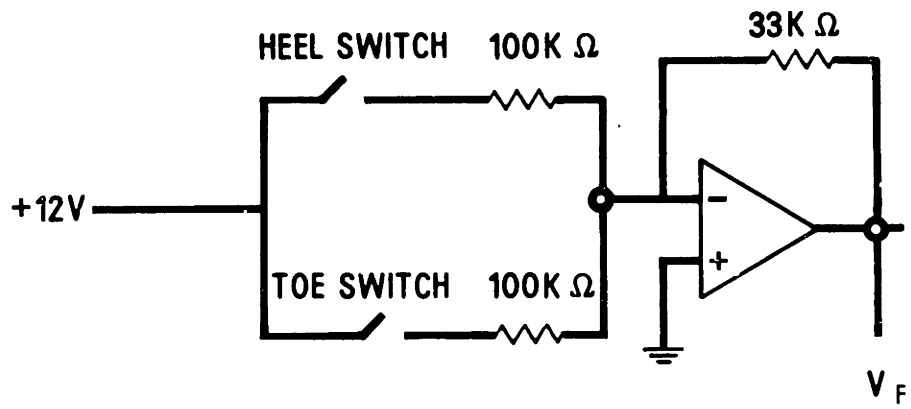


INTERFACE FILTERS
FIGURE 57

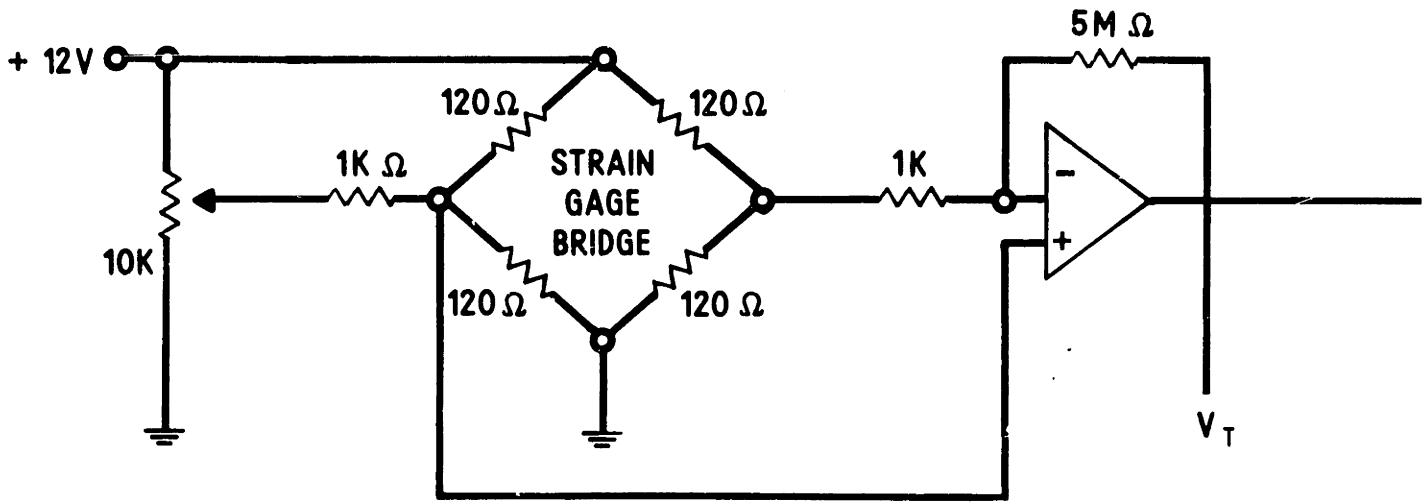


MYO-AMPS

FIGURE 58

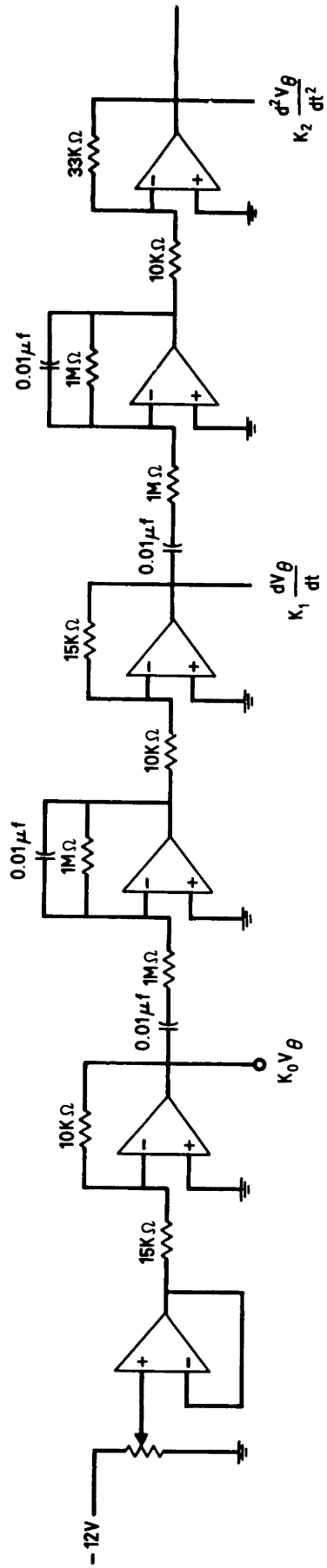


FOOT SWITCH INSTRUMENTATION
FIGURE 59



TORQUE INSTRUMENTATION

FIGURE 60



MOTION INSTRUMENTATION

FIGURE 61

APPENDIX 2: Selected Source Listings

PROGRAM EXPER: Real Time Experimentation

PROGRAM EXPER

AUTHOR:

Ronny Galloway 15/OCT/81

Program to run Lampe Prothesis Simulator.

```
VIRTUAL NDATA(32000)
DIMENSION AA(3),E(3),C(3)
DIMENSION HA(3),HF(3),HC(3)
```

Initialize ANDS5400.

```
CALL ANINIT(IEP)
IF (IEP.NE.0) IYPE *, 'INITIALIZATION ERROR '
CALL ALINIT
CALL ADSTAT
```

Input parameters

```
IEP=1
NSAM=8000
NCHAN=4
TYPE *, 'DEFAULTS ARE NSAM:8000,NCHAN:4,IEP:1,ENTER 0 TO CHANGE.'
ACCEPT *, ICHANG
IF (ICHANG.NE.2) GO TO 102
TYPE *, 'DO YOU WISH TO SET NUMBER OF SAMPLES?(IEP=2048) 1=YES 0=NO '
ACCEPT *, NS
IF (NS.NE.1) GO TO 10
TYPE *, 'ENTER NUMBER OF SAMPLES. (MULTIPLE OF 2) '
ACCEPT *, NSAM
TYPE *, 'SET SIMULATION GAIN. '
ACCEPT *, GAIN
IEP=0
TYPE *, 'ENTER THE NUMBER OF CHANNELS TO SAMPLE.'
ACCEPT *, NCHAN
TYPE *, 'WHAT IS THE CLOCK PERIOD( $\mu$ secs)? '
ACCEPT *, IEP
```

Check for virtual array overflow.

```
102 ICHK=NCHAN*NSAM
IF (ICHK.LE.32000) GO TO 102
TYPE *, 'TOO MANY SAMPLES FOR AMOUNT OF CHANNELS SPECIFIED.'
GO TO 5
```

SET UP FILTER COEFFICIENTS FOR EMG CONTROL

```
102 T=FLOAT(IEP)/1000.
CALL LPCCF(10.,1,3,IA,LE,LC)
CALL HPCCF(20.,1,3,EA,EF,EC)
```

Select the simulation you wish

THE ORIGINAL PRINT ON THE FOLLOWING PAGES IS ILLEGIBLE

C

```

TYPE *, ' SELECT FROM THE FOLLOWING SIMULATIONS: '
TYPE *, '          FRICION ----- ENTER 1 '
TYPE *, '          VELOCITY ----- ENTER 2 '
TYPE *, '          THERSHOLD EMG - ENTER 3 '
TYPE *, '          PULSE WIDTH EMG ENTER 4 '
TYPE *, '          MEAN EMG ----- ENTER 5 '
ACCEPT *, ISIM
IF (ISIM.EQ.1) CALL FRCSIM(NDATA,NSAM,NCHAN,IPEP)
IF (ISIM.EQ.2) CALL VELSIM(NDATA,NSAM,NCHAN,IPEP)
IF (ISIM.EQ.3) CALL THPEMG(NDATA,NSAM,NCHAN,HA,HP,HC,IPEP)
IF (ISIM.EQ.4) CALL PWMEMG(NDATA,NSAM,NCHAN,HA,HP,HC,IPEP)
IF (ISIM.EQ.5) CALL MPEMG(NDATA,NSAM,NCHAN,HA,HP,HC,LA,LP,LC,IPEP)

```

C
C
C

PROCESS THE DATA

```

TYPE *, ' ENTER 1 TO SAVE THE DATA. '
ACCEPT *, IPEEP
IF (IPEEP.NE.1) GO TO 999
DO 132 J=1,ICHEK
WRITE (1,*) NDATA(J)
CONTINUE

```

132
C
C
C

Close data file.

CALL CLOSE(1)

C
999

```

TYPE *, ' ENTER 1 TO TAKE MORE DATA ON THIS RUN '
ACCEPT *, ICONT
IF (ICONT.EQ.1) GO TO 102
STOP
END

```

C
C
C
C
C

SUBROUTINE FRCSIM(NDATA,NSAM,NCHAN,IPEP)

Routine to give constant current to MPE.

12
22

```

VIRTUAL NDATA(32022)
TYPE *, ' ENTER GAIN FOR FRICTION SIMULATION '
ACCEPT *, IGAIN
IDATA=IGAIN*8
IFSAM=2
CALL DTCA(1,IDATA,IER)
CALL ADSTAT
DO 22 I=1,NCHAN+1
CALL ADQUIK(IDAT1)
CONTINUE
IF (IDAT1.LT.12222) GO TO 12
IF (IFSAM.EQ.1) GO TO 50
IFSAM=1
K=0
DO 40 I=1,NSAM
CALL CLKTIK(IPEP)
CALL ADSTAT
DO 30 J=1,NCHAN
CALL ADQUIK(IDAT1)
K=K+1

```

```
30 NDATA(K)=IDAT1
25 CONTINUE
CALL CLKPD(IPONE)
IF (IDONE.EQ.0) GO TO 25
40 CONTINUE
TYPE *, ' SAMPLING COMPLETE '
GO TO 10
50 RETURN
END
```

```
C
C
SUBROUTINE IPCOEF(CF,T,NS,IA,IB,LC)
DIMENSION LA(NS),IF(NS),LC(NS)
PI=3.1415926536
WCF=SIN(CF*PI*T)/COS(CF*PI*T)
DO 10 K=1,NS
CS=COS(FLOAT(2*(K+NS)-1)*PI/FLOAT(4*NS))
X=1./(1.+WCF*WCF-2.*WCF*CS)
IA(K)=WCF*WCF*X
IB(K)=2.*(WCF*WCF-1.)*X
LC(K)=(1.+WCF*WCF+2.*WCF*CS)*X
10 CONTINUE
RETURN
END
```

```
C
C
SUBROUTINE VELSIN(NDATA,NSAM,NCHAN,IPER)
C
C ROUTINE TO SIMULATE A HYDRAULIC PROSTHESIS
C
VIRTUAL NDATA(32200)
TYPE *, ' SET GAIN FOR VELOCITY SQUARED SIMULATION '
ACCEPT *, IGAIN
IFSAM=0
K=0
10 CALL ADSTAT
DO 20 I=1,NCHAN+1
CALL ADQUIK(IDAT1)
IF (I.EQ.2) IVEL=IDAT1-410 12 VOLT OFFSET
20 CONTINUE
IVEL=IVEL/100
IDATA=IVEL**2*IGAIN
CALL DTOA(1,IDATA,IPER)
IF (IDAT1.IT.1000) GO TO 10
IF (IFSAM.EQ.1) GO TO 999
IFSAM=1
DO 40 I=1,NSAM
CALL CLKTIK(IPER)
CALL ADSTAT
DO 30 J=1,NCHAN
CALL ADQUIK(IDAT1)
K=K+1
NDATA(K)=IDAT1
IF (J.EQ.2) IVEL=IDAT1-410
30 CONTINUE
IVEL=IVEL/100
IDATA=IVEL**2*IGAIN
CALL DTOA(1,IDATA,IPER)
```

```

25 CALL CLKFI(IPONE)
IF (IDONE.EQ.0) GO TO 25
40 CONTINUE
TYPE *, ' SAMPLING COMPLETE '
GO TO 10
999 RETURN
END

```

```

C
C
SUBROUTINE THDEMG (NDATA, NSAM, NCHAN, HA, HB, HC, IPER)
C
C ROUTINE TO DO THRESHOLD COUNTING CONTROL OF THE SIMULATOR
C

```

```

VIRTUAL NDATA(32000)
DIMENSION HA(3), HB(3), HC(3)
TYPE *, ' ENTER THE THRESHOLD FOR QUADRICEPS: '
ACCEPT *, MQUAD
TYPE *, ' ENTER THE THRESHOLD FOR HAMSTRINGS: '
ACCEPT *, MHAM
TYPE *, ' ENTER QUADRICEPS GAIN FOR THRESHOLD COUNTING CONTROL: '
ACCEPT *, IGAINQ
TYPE *, ' ENTER HAMSTRINGS GAIN: '
ACCEPT *, IGAINH
IFSAM=0
M=2
10 NHSUM=0
NCSUM=0
IDATA=ISUM*4
CALL DTOA(1, IDATA, IER)
ISUM=0
DO 30 K=1,4 !UPDATE EACH 4 CYCLES
CALL ADSTAT
DO 20 I=1, NCHAN+1
CALL ACQUIK(IDAT1)
IF (I.EQ.2) IVEL=IDAT1
IF (I.EQ.3) IQUAD=IDAT1
IF (I.EQ.4) IHAM=IDAT1
20 CONTINUE
CALL FILTER (IQUAD, HA, HB, HC, -1.)
CALL FILTER (IHAM, HA, HB, HC, -1.)
IF (IAES(IQUAD).GT.MQUAD) NCSUM =NCSUM+1
IF (IAES(IHAM).GT.MHAM) NHSUM=NHSUM+1
30 CONTINUE
IF (IVEL.LT.300) NCSUM=0
IF (IVEL.GT.440) NHSUM=0
ISUM=NCSUM*IGAINQ+NHSUM*IGAINH
IF (IDAT1.LT.1000) GO TO 10
IF (IFSAM.EQ.1) GO TO 999
ITEMP=NSAM/4
IFSAM=1
DO 70 I=1, ITEMP
CALL CLKTIK(1)
NHSUM=0
NCSUM=0
IDATA=ISUM*4
CALL DTOA(1, IDATA, IER)
ISUM = 0
DO 60 K=1,4

```

```

CALL CIKTIK(IPER)
CALL ADSTAT
DC 50 J=1,NCHAN
M=M+1
CALL ADQUIK(IDAT1)
NDATA(M)=IDAT1
IF (J.EQ.2) IVEL=IDAT1
IF (J.EQ.3) IQUAD=IDAT1
IF (J.EQ.4) IHAM=IDAT1
50 CONTINUE
CALL FILTER (IQUAD,HA,HB,HC,-1.)
CALL FILTER (IHAM,HA,HB,HC,-1.)
IF (IABS(IQUAD).GT.MQUAD) NQSUM =NQSUM+1
IF (IABS(IHAM).GT.MHAM) NHSUM=NHSUM+1
60 CCONTINUE
IF (IVEL.IT.362) NQSUM=0
IF (IVEL.IT.448) NHSUM=0
ISUM=NQSUM*IGAINQ+NHSUM*IGAINH
65 CALL CLKRD(IDONE)
IF (IDONE.EQ.0) GO TO 65
70 CONTINUE
TYPE *, ' SAMPLING COMPLETE '
GO TO 10
999 RETURN
END

```

```

C
C
SUBROUTINE FILTER(ISIG,AA,P,C,SIGN)
DIMENSION FIN(4,3),AA(3),B(3),C(3)
DC 1 N=1,4
DO 1 M=1,2
1 FIN(N,M)=2.
FIN(1,3)=FILCAT(ISIG)/205.
DO 2 N=1,3
TEMP=AA(N)*(FIN(N,3)+SIGN*2.*FIN(N,2)+FIN(N,1))
2 FIN(N+1,3)=TEMP-B(N)*FIN(N+1,2)-C(N)*FIN(N+1,1)
DO 3 N=1,4
DO 3 MM=1,2
3 FIN(N,MM)=FIN(N,MM+1)
4 ISIG=INT(FIN(4,3))*205
RETURN
END

```

```

C
C
SUBROUTINE PULPING(NDATA,NSAM,NCHAN,HA,HB,HC,IPEP)
C
C ROUTINE TO DO PULSE WIDTH CONTROL OF THE SIMULATOR
C

```

```

VIRTUAL NDATA(72222)
DIMENSION HA(3),HB(3),HC(3)
TYPE *, ' ENTER THE THRESHOLD FOR QUADRICEPS: '
ACCEPT *,MQUAD
TYPE *, ' ENTER THE THRESHOLD FOR HAMSTRINGS: '
ACCEPT *,MHAM
TYPE *, ' ENTER QUADRICEPS GAIN FOR PULSE WIDTH MODULATION CONTROL: '
ACCEPT *,IGAINQ
TYPE *, ' ENTER HAMSTRINGS GAIN: '
ACCEPT *,IGAINH

```

```
IFSAM=0
M=0
10 NRSUM=0
   NQSUM=0
   IDATA=ISUM*10
   CALL DTOA(1, IDATA, IER)
   ISUM=0
   CALL ADSTAT
   DO 20 I=1, NCHAN+1
   CALL ADQUK(IDAT1)
   IF (I.EQ.2) IVEL=IDAT1
   IF (I.EQ.3) ICUAD=IDAT1
   IF (I.EQ.4) IHAM=IDAT1
20 CONTINUE
   CALL FILTER (IQUAD, HA, HF, HC, -1.)
   CALL FILTER (IHAM, HA, HF, HC, -1.)
   IF (IAES(ICUAD).GT.MQUAD) NQSUM =1
   IF (IAES(IHAM).GT.MHAM) NRSUM=1
   IF (IVEL.LT.380) NQSUM=0
   IF (IVEL.GT.440) NRSUM=0
   ISUM=NQSUM*IGAINQ+NRSUM*IGAINH
   IF (IDAT1.LT.1000) GO TO 10
   IF (IFSAM.EQ.1) GO TO 999
   IFSAM=1
   DO 70 I=1, NSAM
   CALL CLKTK(IPER)
   NRSUM=0
   NQSUM=0
   IDATA=ISUM*10
   CALL ETOA(1, IDATA, IER)
   ISUM = 0
   CALL ADSTAT
   DO 50 J=1, NCHAN
   M=M+1
   CALL ADQUK(IDAT1)
   NDATA(M)=IDAT1
   IF (J.EQ.2) IVEL=IDAT1
   IF (J.EQ.3) IQUAD=IDAT1
   IF (J.EQ.4) IHAM=IDAT1
50 CONTINUE
   CALL FILTER (IQUAD, HA, HF, HC, -1.)
   CALL FILTER (IHAM, HA, HF, HC, -1.)
   IF (IAES(IQUAD).GT.MQUAD) NQSUM =1
   IF (IAES(IHAM).GT.MHAM) NRSUM=1
   IF (IVEL.LT.380) NQSUM=0
   IF (IVEL.GT.440) NRSUM=0
   ISUM=NQSUM*IGAINQ+NRSUM*IGAINH
   CALL CLKRT(IDONE)
   IF (IDONE.EQ.0) GO TO 60
70 CONTINUE
   TYPE *, ' SAMPLING COMPLETE '
   GO TO 10
999 RETURN
   ENI
C
C
C SUPERCUTINE MREMG(NDATA, NSAM, NCHAN, HA, HF, HC, IA, IB, IC, IPER)
```

```
C      ROUTINE TO DC PROPORTIONAL CONTROL OF THE SIMULATOR
C
VIRTUAL NDATA(32000)
DIMENSION EA(3),HF(3),HC(3),LA(3),LP(3),LC(3)
TYPE *, 'ENTER QUADFICEPS GAIN FOR PROPORTIONAL EMG CONTROL: '
ACCEPT *,IGAINQ
TYPE *, 'ENTER GAIN FOR HAMSTRINGS.'
ACCEPT *,IGAINH
IFSAM=0
M=0
10  IDATA=ISUM*10
    CALL DTCA(1, IDATA, IER)
    ISUM=0
    CALL ADSTAT
    DC 20 I=1, NCHAN+1
    CALL ADQUIK(IDAT1)
    IF (I.EQ.2) IVF1=IDAT1
    IF (I.EQ.3) ICUAD=IDAT1
    IF (I.EQ.4) IFAM=IDAT1
20  CONTINUE
    CALL FILTER (ICUAD,EA,EB,HC,-1.)
    CALL FILTER (IFAM,EA,EB,HC,-1.)
    ICUAD=IAFS(ICUAD)
    IFAM=IAFS(IFAM)
    IF (IVEL.LT.380) ICUAD=0
    IF (IVEL.GT.440) IFAM=0
    ISUM=ICUAD*IGAINQ+IFAM*IGAINH
    IF (IDAT1.LI.1000) GO TO 10
    IF (IFSAM.EQ.1) GO TO 999
    IFSAM=1
    DC 70 I=1, NSAM
    CALL CLKTK(IPER)
    IDATA=ISUM*10
    CALL DTCA(1, IDATA, IER)
    ISUM = 0
    CALL ADSTAT
    DC 50 J=1, NCHAN
    M=M+1
    CALL ADQUIK(IDAT1)
    NDATA(M)=IDAT1
    IF (J.EQ.2) IVF1=IDAT1
    IF (J.EQ.3) ICUAD=IDAT1
    IF (J.EQ.4) IFAM=IDAT1
50  CONTINUE
    CALL FILTER (ICUAD,EA,EB,HC,-1.)
    CALL FILTER (IFAM,EA,EB,HC,-1.)
    ICUAD=IAFS(ICUAD)
    IFAM=IAFS(IFAM)
    IF (IVEL.LT.380) ICUAD=0
    IF (IVEL.GT.440) IFAM=0
    ISUM=ICUAD*IGAINQ+IFAM*IGAINH
60  CALL CLKRD(IDONE)
    IF (IDONE.EQ.0) GO TO 60
70  CONTINUE
    TYPE *, ' SAMPLING COMPLETE '
    GO TO 10
999  RETURN
    END
```

! 2VCLT OFFSET

C
C
C
C
C
C
C

SUBROUTINE HPCOEF(FC,T,NS,HA,HE,HC)
DIMENSION HA(NS),HE(NS),HC(NS)

ROUTINE TO CALCULATE COEFFICIENTS FOR DIGITAL
HIPASS FILTER.

FOR APPLICATION, SEE STEARNS "DIGITAL SIGNAL ANALYSIS",
APPENDIX C.

PI=3.1415926536
WCF=SIN(FC*PI*T)/COS(FC*PI*T)
DO 120 K=1,NS
CS=COS(PI*(2*(K+NS)-1)/4*NS)
HA(K)=1./(1.+WCF*WCF-2.*WCF*CS)
HE(K)=2.*(WCF*WCF-1.)*HA(K)
HC(K)=(1.+WCF*WCF+2.*WCF*CS)*HA(K)
RETURN
END

120

PROGRAM DPROG: Off-Line Data Manipulation

PROGRAM DPROG

PROGRAM TO PROCESS DATA OFFLINE

DIMENSION ARRAYS

DIMENSION AA(3),B(3),C(3),GR(2,10)
VIRTUAL A(4,4500)

READ INPUT PARAMETERS

NSAM: NUMBER OF SAMPLES IN RECORD

NCHAN: NUMBER OF CHANNELS SAMPLED

IITEST: THE RECORD LENGTH OF THE SORTED STEP, INITIAL VALUE IS NSAM.

AVGNUM: THE NUMBER OF SORTED STEPS TO AVERAGE

IRUN: 0 FOR THE FIRST RUN AT A GIVEN LEVEL

IIPROS: DESCRIBES HOW THE EMG IS TO BE PROCESSED 0 FOR RECTIFYING
CONTROLLER, 1 FOR THRESHOLD COUNTING CONTROLLER, AND 2 FOR MODULATED
PULSE WIDTH CONTROLLER, 3 FOR RAW EMG, 4 FOR HIGHPASS FILTER.

QT: THE VALUE OF THE QUADRICEPS THRESHOLD FOR IIPROS = 1 OR 2

HT: THE VALUE OF THE HAMSTRINGS THRESHOLD FOR IIPROS = 1 OR 2

KMSEC: THE NUMBER OF TIME STEPS TO CONSIDER FOR THRESHOLD COUNTING

NOTE---THIS MUST BE AN EVEN FACTOR OF NSAM!!

READ (3,*) NSAM,NCHAN,IITEST,AVGNUM,IRUN,IIPROS,QT,HT,KMSEC
TYPE *, 'NUMBER OF SAMPLES AND CHANNELS:',NSAM,NCHAN

GET DATA FROM UNIT 1

DO 30 N=1,NSAM

DO 20 J=1,NCHAN

READ (1,*) IDAT

A(J,N)=FLOAT(IDAT)*11./2248.

CONTINUE

CONTINUE

PROCESS POSITION DATA

CALL LFCOEF(22.,.221,3,AA,B,C,GR)

CALL FILTER(A,NSAM,AA,B,C,1,1.)

PROCESS VELOCITY DATA

CALL FILTER(A,NSAM,AA,B,C,2,1.)

DO 141 I=1,NSAM

A(3,I)=A(2,I)-2.

PROCESS EMG DATA

IF (IIPROS.EQ.1) CALL FCIMG(A,NSAM,QT,HT,KMSEC)

IF (IIPROS.EQ.2) CALL FMCD(A,NSAM,QT,HT)

IF (IIPROS.EQ.0) CALL MREMG(A,NSAM)

IF (IIPROS.EQ.3) CALL RAWEMG(A,NSAM)

IF (IIPROS.EQ.4) CALL FILEMG(A,NSAM)

IF AVERAGING, SORT THE DATA

IF (AVGNUM.GT.1.) CALL SOFT(A,NSAM,ILUM,ITEST,NCHAN)

ADD TO THE DATA IN UNIT 2 FOR LATER PROCESSING.

```
IF (IDUM.IT.ITEST) ITEST=ILUM
IF (AVGNUM.EQ.1.) ITEST=NSAM
IF (IRUN.EQ.2) GO TO 220
DO 212 I=1,ITEST
DO 202 J=1,NCHAN
READ (2,*) DATA
A(J, )=DATA+A(J,I)
202 CONTINUE
212 CONTINUE
CLOSE (UNIT=2)
DO 240 I=1,ITEST
DO 232 J=1,NCHAN
WRITE (2,*) A(J,I)
232 CONTINUE
240 CONTINUE
CLOSE (UNIT=3)
IF (AVGNUM.NE.1.) IRUN=1
WRITE (3,*) NSAM,NCHAN,ITEST,AVGNUM,IRUN,IPROC,QT,ET,KMSEC
```

STOP
END

```
SUBROUTINE FILTER(A,NSAM,AA,P,C,ICHAN,SIGN)
VIRTUAL A(4,4500)
DIMENSION FIN(4,3),AA(3),B(3),C(3)
DO 1 N=1,4
DO 1 M=1,2
1 FIN(N,M)=0.
DO 4 M=1,NSAM
FIN(1,3)=A(ICHAN,M)
DO 2 N=1,3
2 TEMP=AA(N)*(FIN(N,3)+SIGN*2.*FIN(N,2)+FIN(N,1))
FIN(N+1,3)=TEMP-B(N)*FIN(N+1,2)-C(N)*FIN(N+1,1)
DO 3 N=1,4
DO 3 MM=1,2
3 FIN(N,MM)=FIN(N,MM+1)
4 A(ICHAN,M)=FIN(4,3)
RETURN
END
```

```
SUBROUTINE MRMG(A,NSAM)
DIMENSION AA(3),B(3),C(3),GR(2,10)
VIRTUAL A(4,4500)
TYPE *, ' ENTER THE GAIN FOR QUADRICEPS ACTIVITY: '
ACCEPT *,GAINC
TYPE *, ' ENTER THE GAIN FOR HAMSTRINGS ACTIVITY: '
ACCEPT *,GAINH
CALL HPCCEF(70.,.001,3,AA,B,C,GR)
```

```

LO 20 M=3,4
CALL FILTER(A,NSAM,AA,E,C,M,-1.)
CONTINUE
LO 10 I=1,NSAM
IF (A(2,I).GT..01) A(4,I)=0.
IF (A(2,I).LT.-.01) A(3,I)=0.
A(3,I)=ABS(A(3,I)*GAINQ)+ABS(A(4,I)*GAINH)
CONTINUE
RETURN
END

```

C-----
C-----

```

SUBROUTINE FNCD(A,NSAM,QT,HT)
DIMENSION AA(3),F(3),C(3),GR(2,10),HC(2)
VIRTUAL A(4,4500)
HC(1)=QT
HC(2)=HT
CALL HPCDEF(72.,.721,3,AA,F,C,GR)
DO 20 M=3,4
CALL FILTER(A,NSAM,AA,E,C,M,-1.)
CONTINUE
DO 10 I=1,NSAM
DO 10 M=3,4
IF (ABS(A(M,I)).GT.HC(M-2)) A(M,I)=2.
DO 100 I=1,NSAM
IF (A(2,I).LT.0.1) A(3,I)=2.
IF (A(2,I).GT.-0.1) A(4,I)=2.
A(3,I)=A(3,I)+A(4,I)
RETURN
END

```

C-----
C-----

```

SUBROUTINE FCMSG(A,NSAM,QT,HI,NMSEC)
DIMENSION AA(3),E(3),C(3),GR(2,10),HO(2)
VIRTUAL A(4,4500)

CHECK IF NSAM/NMSEC IS AN EVEN QUOTIENT.

NHCID=NSAM/NMSEC
HOLD=FLOAT(NSAM)/FLOAT(NMSEC)
CHECK=HOLD-FLOAT(NHCID)
IF (CHECK.NE.0.) TYPE *, ' NSAM/NMSEC IS NOT AN EVEN QUOTIENT. '
TYPE *, ' NUMBER OF MILLISECONDS:',NMSEC
CALL HPCDEF(72.,.721,3,AA,E,C,GR)
HO(1)=QT
HO(2)=HT
DO 50 M=3,4
CALL FILTER(A,NSAM,AA,F,C,M,-1.)
CONTINUE
DO 20 M=3,4
DO 20 I=1,NSAM,NMSEC
A(M,I)=SUM
SUM=0.
N=I+NMSEC-1
ICOUNT=I
DO 10 J=ICOUNT,N
IF (ABS(A(M,J)).GT.HO(M-2)) SUM=SUM+1.
IF (J.NE.ICOUNT) A(M,J)=A(M,I)

```

```

10 CONTINUE
20 CONTINUE
   DO 30 I=1,NSAM
   IF (A(2,I).GT.2.21) A(4,I)=2.
   IF (A(2,I).LT.-2.21) A(3,I)=2.
30  A(3,I)=A(3,I)+A(4,I)-5.
   RETURN
   END

```

```

C-----
C
SUBROUTINE SORT(A,NSAM,ITEST,IDUM,NCHAN)
  FIND STEP FROM POSITION DATA
C

```

```

  VIRTUAL A(4,4500)
  DO 100 I=1,NSAM
100 IF (A(1,I).LE.2.2) GO TO 110
  TYPE *, 'END OF RECORD DURING SORT'
110  ISTART=I
  DO 120 J=I,NSAM
120  IF (A(1,J).GT.1.) GO TO 130
  TYPE *, 'END OF RECORD DURING SORT'
130  DO 140 K=J,NSAM
140  IF (A(1,K).LE.2.2) GO TO 150
  TYPE *, 'END OF RECORD DURING SORT'
150  NSTEPS=K-ISTART
  TYPE *, 'NUMBER OF SAMPLES IN STEP:',NSTEPS
  TYPE *, 'NUMBER OF FIRST SAMPLE IN SORTED STEP:',ISTART
  SHIFT DATA INTO THE STANDARD STEP
C

```

```

  IDUM=NSAM-ISTART
  DO 160 I=1,IDUM
  DO 160 J=1,NCHAN
  A(J,I)=A(J,ISTART+I)
160 CONTINUE
170 CONTINUE
C

```

```

  FILL THE REST WITH ZERGES
C
  DO 175 I=IDUM,NSAM
  DO 175 J=1,NCHAN
175  A(J, )=0.
  RETURN
  END

```

```

C-----
C
SUBROUTINE RAWMG(A,NSAM)
  VIRTUAL A(4,4500)
  DIMENSION AA(3),B(3),C(3)
  DO 100 I=1,NSAM
100  A(4,I)=2.5 + A(4,I)
  CONTINUE
  RETURN
  END

```

```

C-----
C
SUBROUTINE FILEMG(A,NSAM)
  VIRTUAL A(4,4500)
  DIMENSION AA(3),B(3),C(3),CR(2,10)

```

```
CALL HPCCEF(70.,0.001,3,AA,E,C,GR)
IC 10 M=3,4
10 CALL FILTER(A,NSAM,AA,E,C,M,-1.)
DC 20 I=1,NSAM
A(3,I)=A(3,I)-5.
20 A(4,I)=A(4,I)-2.5
RETURN
END
```

PROGRAM THFIND: Threshold Identification

```

C   PROGRAM TO FIND THE THRESHOLD IN EMG DATA
    VIRTUAL NDATA(4,8000)
    DIMENSION AA(3),B(3),C(3),GR(2,10)
    NSAM=2048
    NCHAN=4

C
C   CALL HPCOEF(70...001,3,AA,B,C,GR)

C
    DO 20 I=1,NSAM
    DO 10 J=1,NCHAN
    READ (1,*) IDATA
    NDATA(J,I)=IAES(IDATA)
10  CONTINUE
20  CONTINUE
C
    DO 22 M=3,4
    CALL FILTER(NDATA,NSAM,AA,B,C,M,-1.)
22  CONTINUE
C
C
C   FIND THE THRESHOLDS.
C
    I25=NSAM/4
    I50=NSAM/2
    I75=3*NSAM/4
    DO 25 K=1,2048
    M=0
    DO 15 I=1,NSAM
    IF (NDATA(3,I).LE.K) M=M+1
    IF (M.EQ.I25) GO TO 30
15  CONTINUE
25  CONTINUE
30  TYPE *, ' QUADRICEPS 25% THRESHOLD: ',K
    WRITE (2,*) K
    DO 40 K=1,2048
    M=0
    DO 40 I=1,NSAM
    IF (NDATA(3,I).LE.K) M=M+1
    IF (M.EQ.I50) GO TO 50
40  CONTINUE
50  TYPE *, ' QUADRICEPS 50% THRESHOLD: ',K
    WRITE (2,*) K
    DO 60 K=1,2048
    M=0
    DO 60 I=1,NSAM
    IF (NDATA(3,I).LE.K) M=M+1
    IF (M.EQ.I75) GO TO 70
60  CONTINUE
72  TYPE *, ' QUADRICEPS 75% THRESHOLD: ',K
    WRITE (2,*) K
    DO 80 K=1,2048
    M=0
    DO 80 I=1,NSAM
    IF (NDATA(4,I).LE.K) M=M+1
    IF (M.EQ.I25) GO TO 90
80  CONTINUE
90  TYPE *, ' HAMSTRINGS 25% THRESHOLD: ',K
    WRITE (2,*) K
    DO 100 K=1,2048

```



```

M=0
120 DC 100 I=1,NSAM
110 IF (NDATA(4,I).LE.K) M=M+1
IF (M.EQ.150) GO TO 110
CONTINUE
TYPE *, 'HAMSTRINGS 50% THRESHOLD:',K
WRITE (2,*) K
DO 120 K=1,2040
M=2
DO 120 I=1,NSAM
IF (NDATA(4,I).LE.K) M=M+1
IF (M.EQ.175) GO TO 130
120 CONTINUE
130 TYPE *, 'HAMSTRINGS 75% THRESHOLD:',K
WRITE (2,*) K
STOP
END

```

```

C-----
SUBROUTINE FILTER(NDATA,NSAM,AA,B,C,ICHAN,SIGN)
VIRTUAL NDATA(4,2000)
DIMENSION FIN(4,3),AA(3),B(3),C(3)
DO 1 N=1,4
DO 1 M=1,2
1 FIN(N,M)=0.
DO 4 M=1,NSAM
FIN(1,3)=FLCAT(NDATA(ICHAN,M))/204.8
DO 2 N=1,3
2 TEMP=AA(N)*(FIN(N,3)+SIGN*2.*FIN(N,2)+FIN(N,1))
FIN(N+1,3)=TEMP-B(N)*FIN(N+1,2)-C(N)*FIN(N+1,1)
DO 3 N=1,4
DO 3 MM=1,2
3 FIN(N,MM)=FIN(N,MM+1)
4 NDATA(ICHAN,M)=INT(FIN(4,3)*204.8)
RETURN
END
C-----

```

Selected Machine Language Routines

ROUTINES FOR KW11-K DUAL REAL TIME PROGRAMMABLE CLOCK.

AUTHOR:

RONNY GALLOWAY 18/OCT/81

.SBTTL - CLKTIK KW11-K CLOCK ROUTINE

ROUTINE:

CLKTIK

CALLING SEQUENCE:

CALL CLKTIK(IMIL)

INPUT:

IMIL - NUMBER OF MILLISECONDS UNTIL OVERFLOW

CLKTIK::

CLR ASTAT
MOV @IMIL(R5),ABUFF ; LOAD BUFFER
NEG ABUFF
BIS #411,ASTAT ; ENABLE CLOCK A
RTS PC

.SBTTL - CLKRD READ OVERFLOW

ROUTINE:

CLKRD

CALLING SEQUENCE:

CALL CLKRD(IDONE)

OUTPUTS:

IDONE - IF IDONE IS 0, THE CLOCK HAS NOT OVERFLOWED.
IF IDONE IS 1, THE CLOCK HAS OVERFLOWED.

CLKRD::

BIT #200,ASTAT
BNE DONE
MOV #0,@IDONE(R5)
BR RE
DONE: MOV #1,@IDONE(R5)
RE: RTS PC

.SBTTL ADINIT - ATOD INITIALIZATION

ROUTINE:

ADINIT

CALLING SEQUENCE:

CALL ADINIT

FUNCTION:

INITIALIZES ANDS5400.

ADINIT::

MOV #170000,Q#DROUT

;CLEAR

CALL WAITGO

MOV #170000,Q#DROUT

;CLEAR

CALL WAITGO

MOV #40000,Q#DROUT

;SET RANGE TO SINGLE EN

CALL WAITGO

MOV #60000,Q#DROUT

;RESET STATUS BITS

CALL WAITGO

RTS PC

.SBTTL ADSTAT - SET RANGE AND STATUS

ROUTINE:

ADSTAT

FUNCTION:

SETS STATUS AND LOADS ADDRESS FOR ATOD CONVERSION.

ADSTAT::

MOV #60000,Q#DROUT

MOV #50000,Q#DROUT

MOV #0,Q#DROUT

BIS #60016,Q#DROUT

RTS PC

.SBTTL ADQUIK - ATOD CONVERSION ROUTINE

ROUTINE:

ADQUIK(IDAT1)

FUNCTION:

PERFORMS ATOD CONVERSION ON CURRENTLY ADDRESSED CHANNEL.

ADQUIK::

```
MOV R1,-(SP)
MOV #70000,G#DROUT
TEST: BIT #200,G#DRCSR
      BEQ TEST
      MOV G#DRIN,R1
      .REPT 4
      ASR R1
      .ENDM
      MOV R1,GIDAT1(R5)
      MOV (SP)+,R1
      RTS PC
```

BIBLIOGRAPHY

1. Veterans Administration, "Selection and Application of Knee Mechanism." Bulletin of Prosthetics Research BPR 10-18, 1972.
2. Dyck, W. R., "A Voluntarily Controlled Electrohydraulic Above-Knee Prosthesis." Bulletin of Prosthetics Research Spring 1975.
3. Horn, G. W., "Electro-Control: AM EMG-Controlled A/K Prosthesis." Medical and Biological Engineering, Vol. 10, p. 61-71.
4. Saxena, S. C. and Mukhopadhyay, P., " E. M. G. Operated Electronic Artificial-Leg Controller," Medical and Biological Engineering, 1977, Vol. 15, p. 553-557.
5. Kato, I., "An Above-Knee Prosthesis with Myoelectric Controller," Proceedings of the 5th International Symposium on External Control of Human Extremities, 1975, p. 313-322.
6. Donath, M. "Proportional EMG Control or Above Knee Prosthesis," S. M. and Mech E. Thesis, Dept. of Mech. Eng. M.I.T..

7. Hogan, N. J., "Myoelectric Prosthesis Control: Optimal Estimation Applied to EMG and the Cybernetic Considerations for its use in a Man Machine Interface,": Ph. D. Thesis, Dept. of Mech. Eng., M.I.T., 1976.
8. Hogan, N. J., "Memorandum on EMG Processing," 1973.
9. Childress, D. S., "An Approach to Powered Grip," Proceedings of the Fourth International Symposium on External Control of Human Extremities, Belgrade 1972.
10. Close, J. R., "Motor Unit Action Potential Counts: Their Significance in Isometric and Isotonic Contractions."
11. Myers, D. R. and Moskowitz, G. D., "Development of Myoelectric Knee Control for A/K Prosthesis," 1978.
12. Grimes, D. L. "On Active Multi-Mode Above-Knee Prosthesis Controller," Ph. D. Thesis, Dept. of Mech. Eng. M.I.T., 1979.
13. Chow, C. K. and Jacobsen, D. H., "Studies of Human Locomotion via Optimal Programming," Mach Biosciences, 10, p. 239-306, 1979.
14. Brandell, B. R. and William, K., "Interrelationship of Lower Limb Movements and Muscle Contractions in Normal

Human Locomotion."

15. Carlsoo, S., "How Man Moves: Kinesiological Methods and Studies," Crane, Russak and Co., Inc., 1972
16. Lampe, D. R., "Design of a Magnetic Particle Brake Above-Knee Prosthesis Simulator System," M.S. Thesis, Dept. Mech. Eng. M.I.T., 1973.
17. Antonsson, E. K., Ph. D. Thesis in Progress, Dept. of Mech. Eng. M.I.T., 1981.
18. Stearns, S. D., "Digital Signal Processing," Hayden Book Company, Inc., 1975
19. Stout, D. F., "Handbook of Operational Amplifier Circuit Design," McGraw Hill, 1976
20. Kreysig, E., "Advanced Engineering Mathematics," Fourth Edition, John Wiley and Sons, 1979
21. Gray, H. "Anatomy of the Human Body," 29th American Edition, Lea and Febiger